SANDIA REPORT
SAND2020-13925
Printed September 2020

Sandia National Laboratories

FY20 Improvements to the New CTH Code Verification & Validation Test Suite

Gabrielle C. Duncan-Reynolds, Christopher T. Key

Prepared by
Sandia National Laboratories
Albuquerque, New Mexico 87185
Livermore, California 94550

Issued by Sandia National Laboratories, operated for the United States Department of Energy by National Technology & Engineering Solutions of Sandia, LLC.

Available to DOE and DOE contractors from

U.S. Department of Energy
Office of Scientific and Technical Information
P.O. Box 62
Oak Ridge, TN 37831

Telephone: (865) 576-8401
Facsimile: (865) 576-5728
E-Mail: reports@osti.gov
Online ordering: http://www.osti.gov/scitech

Available to the public from

U.S. Department of Commerce
National Technical Information Service
5301 Shawnee Road
Alexandria, VA 22312

Telephone: (800) 553-6847
Facsimile: (703) 605-6900
E-Mail: orders@ntis.gov
Online order: https://classic.ntis.gov/help/order-methods

ABSTRACT

The CTH multiphysics hydrocode, which is used for a wide range of important calculations, has undertaken in recent years to overhaul its software quality and testing processes. A key part of this effort entailed building a new, robust V&V test suite made up of traditional hydrocode verification problems, such as those listed in the ASC Tri-Lab Test Suite [3] and the Enhanced Tri-Lab Test Suite [15], as well as validation problems for some of CTH's most frequently used equations of state, materials models, and other key capabilities. Substantial progress towards this goal was made in FY19 (see [6]). In FY20, this test suite has been expanded to include verification and validation tests of the Sesame and JWL equation of state models as well as the Mader verification problem from the Tri-Lab Test Suite and the Blake verification problem - a linear elastic analog to the Hunter problem from the Enhanced Tri-Lab Test Suite [14].

This report documents CTH performance on the new test suite problems. Verification test results are compared to analytic solutions and, for most tests, convergence results are presented. Validation test results are compared to experimental data and mesh refinement studies are included.

CTH performs well overall on the new test problems. Convergence rates for the Blake and Mader problems are comparable to those for similar ASC codes. The JWL and Sesame verification tests show good agreement with analytic solutions. Likewise, CTH simulation results show good agreement with experimental validation data for the Sesame and JWL equations of state for the materials tested. Future V&V work will focus on adding tests for other key capabilities like fracture and high explosive models.

ACKNOWLEDGMENT

The authors would like to thank Kim Mish and the ASC Integrated Codes program for supporting this work. We would also like to acknowledge the valuable resources published by Los Alamos National Laboratory, such as the code verification tool ExactPack [27], which was used in this work to calculate and plot analytic solutions, and the Standardized Definitions for Code Verification Problems, which was helpful in implementing the ASC Tri-Lab Test Suite and Enhanced Tri-Lab Test Suite problems.

CONTENTS

LIST OF FIGURES

LIST OF TABLES

ACRONYMS & DEFINITIONS

Abbreviation	Definition
ASC	Advanced Simulation and Computing
EOS	Equation of State
EPPVM	Von Mises Elastic Perfectly Plastic
HE	High Explosive
JWL	Jones-Wilkins-Lee
SES	Sesame (Table)
V&V	Verification and Validation

1. INTRODUCTION

Starting in FY18, the CTH multiphysics hydrocode [21], began overhauling its software quality and testing processes. One key element of this effort has been to introduce rigorous verification and validation (V&V) testing. Documenting these efforts is essential in establishing code credibility for the many programs and critical applications for which CTH is used. Over the last couple years, CTH has carefully compiled new verification and validation test suites. The individual tests have been selected so as to address test coverage gaps involving the most frequently used capabilities first. In FY19, substantial progress was made and many new problems were added to the test suites (see [6]), covering multiple material strength models and several traditional hydrocode verification problems from the Tri-Lab Test Suite [3] and the Enhanced Tri-Lab Test Suite [15]. In FY20, new V&V test problems have been added, including verification and validation tests of the JWL and Sesame equation of state models as well as the Mader verification problem from the Tri-Lab Test Suite and the Blake verification problem - a linear elastic analog to the Hunter problem from the Enhanced Tri-Lab Test Suite [14].

The current V&V test suite, including the FY20 additions, is shown in Figure 1-1. Several of the tests in this list are detailed in [6]. The radiation transport related tests in Figure 1-1 come from verification work previously published in [11] and will not be discussed here. In addition to the tests listed in Figure 1-1, there are a large number of verification tests that check whether material is being inserted correctly into the mesh (Diatom testing). These tests will be documented in an upcoming report, expected sometime around the end of the calendar year.

Code verification and validation are essential for ensuring (and demonstrating) accuracy and credibility of simulation results. V&V efforts demonstrate both that the physics models have been correctly implemented in the code and that those models are sufficient approximations to the real world for the intended application. For example, in this report, there are both verification and validation tests for the Sesame equation of state (EOS) model. The verification tests compare simulation results to a known solution, providing evidence that the model was coded correctly. The validation tests compare simulated flyer plate impact results using the Sesame EOS to experimental data from actual flyer plate impact tests. This provides evidence that the Sesame EOS model sufficiently approximates real-world behavior for the materials under consideration.

The verification test suite (VERTS) is designed to test whether a given feature performs as intended by the developer - in other words, that the feature was implemented/coded correctly. To test features involving core physics, problems with known/analytic solutions are compared with simulation results and convergence studies are performed to ensure that simulation results are in fact approaching the true solution as the mesh is refined.

In FY20, verification tests have been added for the JWL and Sesame equations of state as well as two traditional hydrocode verification problems: the Blake problem [2] and the Mader problem (see [8]). The JWL equation of state is verified against the closed form solution for the Riemann shock tube problem for two different types of high explosive (HE) materials under different initial conditions. The implementation of the SESAME tabular form for the equation of state is verified using both an independent code (BCAT) which accesses the tables through an independent interface and also through the development and implementation of a hypothetical analytical

Test Problem	Gas Dynamics	Material Response	Radiation Transport	High Explosives
Verification Test Suite				
Blake		•		
Einfeldt	•			
EPPVM Verification: Uniaxial Strain		•		
Johnson-Cook Verification: Uniaxial Strain Loading		•		
JWL Verification: 1D Riemann	•	•		•
LeBlanc	•			
Mader	•			•
Noh	•			
Rad. Diff. Through Slab	•		•	
Rad. Diff. from Hot Bubble Source	•		•	
Rad. Cooling of Isothermal Sphere	•		•	
Sedov	•			
SES Verification: CTH vs. BCAT		•		
SES Verification: Custom EOS Table		•		
Shock-Contact-Shock	•			
Slow Shock	•			
Sod	•			
Stationary Contact	•			
Validation Test Suite				
AVAVE (Strength) Validation: Pressure-Shear Plate Impact		•		
AVAVE (Strength) Validation: Taylor Rod Impact		•		
EPPVM (Strength) Validation: Taylor Rod Impact		•		
Johnson-Cook (Strength) Validation: Taylor Rod Impact		•		
Johnson-Cook (Strength) Validation: Alumina Sphere Impact		•		
JWL (EOS) Validation: Cylindrical Expansion		•		•
JWL (EOS) Validation: Hemispherical Expansion		•		•
Mie-Grüneisen (EOS) Validation: Aluminum Flyer Plate Impact		•		
Mie-Grüneisen (EOS) Validation: Plexiglass Flyer Plate Impact		•		
SES (EOS) Validation: Symmetric Flyer Plate Impact		•		
SES (EOS) Validation: Flyer Plate Impact		•		

Figure 1-1 New CTH V&V Test Suite

equation of state surface in the form of a Sesame table. The Blake problem is a test of a code's ability to calculate elastic wave propagation in the absence of boundary reflections [4]. It is used here as a test of the EPPVM (Von Mises elastic perfectly-plastic) model. The Mader problem tests whether a code is able to accurately capture the Chapman-Jouget state at the detonation front and the rarefaction behind the burn front for a detonation through a compressible gas [4]. It is used here as a test of the HEBURN (High Explosive Burn) model.

The purpose of a validation test suite (VALTS) is to test whether a given feature approximates real-world behavior within an acceptable margin of error - in other words, that the physics model and simplifications used are sufficient to capture key physical phenomena for the given materials and conditions. To test features involving core physics, simulation results are compared to experimental test data and mesh refinement studies are performed to ensure that simulation results are in fact approaching a solution as the mesh is refined.

In FY20, validation tests have been added for the Jones-Wilkins-Lee (JWL) and Sesame (SES) equations of state. The JWL EOS is validated using experimental data from conventional cylinder and hemisphere expansion tests. The cylinder expansion experimental test data is taken from [17]

where validation simulations are performed for the following high explosives: HMX, TNT, PBX-9404 and Nitromethane (NM). This validation test compares the radius of the copper cylinder versus time (i.e. radial expansion velocity) during the detonation process. The second validation test is based on the experimental work of Lee et al. [19] and consists of a radial expanding aluminum hemispherical shell which encases a hemisphere of high explosive. These spherical expansion tests were performed using CompB-GradeA, PBX-9404 and LX-04-1 high explosives. These two sets of validation test data were chosen for this report as they provide conventional validation data for energetic equation of states and they also exercise the JWL EOS within CTH for multiple energetic materials.

For the Sesame EOS, several Sesame tables are validated against various experimental flyer plate testing and data. Specifically, the first validation problem involves various experiments by Nellis et al. [22] which incorporate multiple combinations of aluminum, copper, and tantalum in configurations which probe both on- and off-Hugoniot states of each of the three materials. The second set of validation problems considers the time history of particle velocity from flyer plate impact data for lithium fluoride (LIF) from Rigg et al. [24]. These experimental flyer plates tests were chosen as they provide validation for the LIF polymer and also allow for comparison of the entire wave profile rather than just the final shock states as with the first validation problem.

In this report, we present each of the new test suite problems. Basic problem theory as well as parameters and problem setup are described. Simulation results are compared to analytic solutions (in the case of verification problems) or experimental data (for validation problems) and convergence results or mesh refinement studies are presented. Finally, we discuss CTH's overall performance on the new test problems as well as V&V priorities for FY21.

2. VERIFICATION TEST SUITE: BLAKE PROBLEM

2.1. Problem Description

The Blake verification problem [2] is based on the analytic solution to the problem of a uniform infinite elastic medium with a spherical cavity centered at the origin [5]. A time-dependent pressure is applied to the inner boundary of the cavity, causing it to expand and a wave to propagate through the elastic material. When the pressure in the cavity is a simple step function, as is the case in the version of the problem implemented here, the Blake problem approximates the scenario of an embedded explosive source [4].

The Blake problem is one of the few dynamic strength of materials problems that has a closed-form solution, and as such it is a traditional hydrocode verification problem [5]. It tests small strain linear elasticity [14]. Specifically, it tests the code's ability to simulate wave propagation for outgoing, spherically divergent elastic waves [4]. It is used here as a test of the Von Mises elastic perfectly-plastic model (EPPVM) model.

The problem is initialized as a stationary, unstressed isotropic linear-elastic material, with the domain selected such that the elastic wave front will not reach the edge of the domain before t_{final} [4]. At time $t = 0$, a uniform pressure p_0 is applied to the inside of the cavity wall. To ensure that no plastic strain is accumulated, the elastic material is given an unattainably high yield strength [14]. The material filling the cavity is identical to the elastic medium, except that it has zero strength.

2.2. Analytic Results

We present only a summary of the solution to the Blake problem here. The reader is referred to [27] for the full derivation.

For the driving pressure $p(t) = p_0\,\mathcal{H}(t)$, where $\mathcal{H}$ represents the Heaviside function, the displacement potential ϕ is given by

$$\phi(r,t) = -\frac{a}{\rho}\,\frac{p_0\,\mathcal{H}(t)}{(\alpha^2+\beta^2)\,r}\left[1-\mathrm{e}^{-\alpha t}\left\{\cos(\beta t)+\frac{\alpha}{\beta}\sin(\beta t)\right\}\right] \tag{1}$$

In the above, α and β are given by

$$\alpha = \frac{2c_T^2}{a\,c_L}, \quad \beta^2 = \alpha^2\left(\frac{c_L^2}{c_T^2}-1\right), \quad c_L^2 = \frac{\lambda+2\mu}{\rho_0}, \quad c_T^2 = \frac{\mu}{\rho_0} \tag{2}$$

where c_L and c_T are the longitudinal and shear wave speeds, respectively, ρ_0 is the initial mass density, and λ and μ are the (constant) Lamé moduli. Note that Poisson's ratio ν is given by

$$\nu = \frac{\lambda}{2(\lambda+\mu)} \tag{3}$$

The parameter values for ρ_0, p_0, μ, and ν are given in Table 2-1. It is this case that is implemented in the ExactPack solver [27].

2.3. Parameters

Parameter values for the Blake problem, matching those used in [4] are given in Table 2-1. The problem domain was 100 cm, one-dimensional spherical (1DS) geometry. The mesh was divided into 50 zones and then refined by halving the cell size at each refinement, as shown in Table 2-2.

Final time	Cavity radius	Reference density	Driving pressure	Shear modulus	Poisson's ratio	Elastic wave speed
t_{final}	r_{cav}	ρ_0	p_0	μ	ν	c_e
[s]	[cm]	[g/cm^3]	[dyn/cm^2]	[dyn/cm^2]		[cm/s]
1.6×10^{-4}	10	3.0	1.0×10^7	2.5×10^{11}	0.25	5.0×10^5

Table 2-1 Blake Problem Parameters

Number of Cells:	50	100	200	400	800
Cell Size [cm]:	2.0	1.0	0.5	0.25	0.125

Table 2-2 Mesh Resolution

2.4. Results

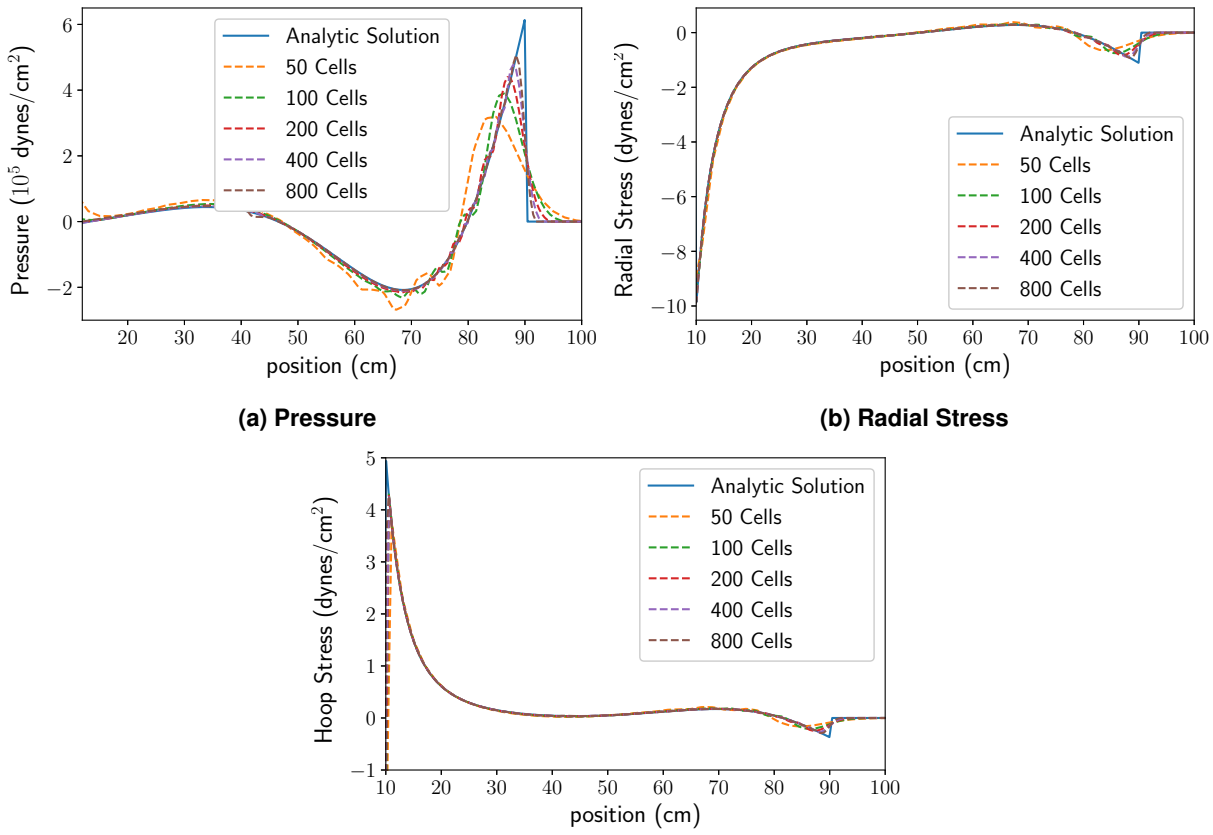

(a) Pressure

(b) Radial Stress

(c) Hoop Stress

Figure 2-1 Comparison of solution at $t_{\text{final}} = 1.6 \times 10^{-4}$ s for various mesh resolutions. Note that we are only considering the solution in the domain outside the cavity ($r >$ 10 cm)

A comparison of 1-D simulation results for various mesh resolutions is shown in Figure 2-1. Following the example of [5], we consider the results for pressure, radial stress, and hoop stress.

All CTH results were computed using CTH version 12.1. The input deck for the Blake problem is included in Appendix A. Visual inspection shows agreement with the analytic solution, though coarser mesh fails to resolve the sharp corners in the solution. Convergence results are discussed further in Section 2.5.

2.5. Convergence Study

Following the convention of similar codes [5], we compute convergence rates over the domain outside the cavity radius, rather than including the discontinuity which occurs at the cavity boundary. Specifically, we consider the domain $r > 11$ cm.

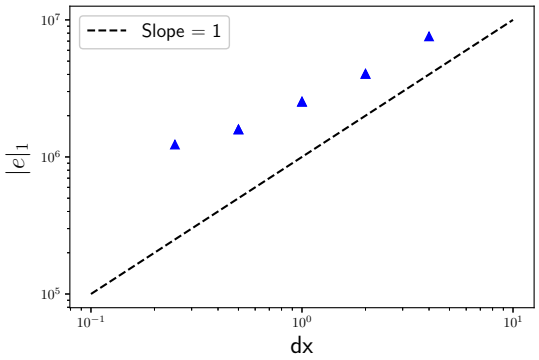

(a) pressure

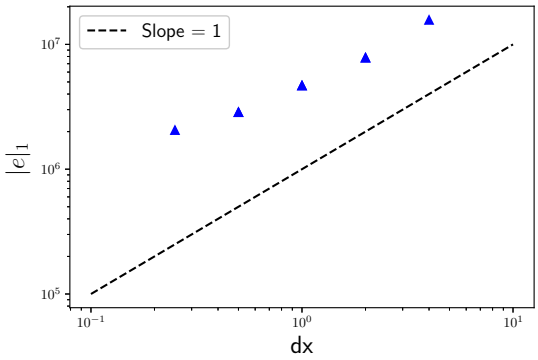

(b) radial stress

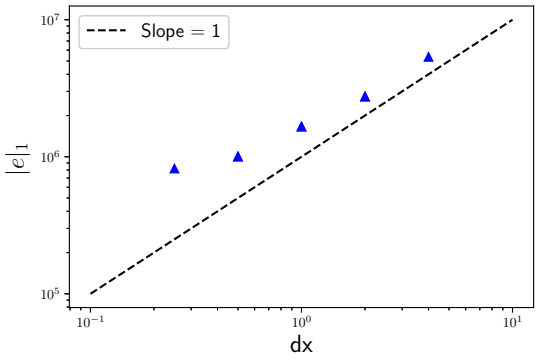

(c) hoop stress

Figure 2-2 L_1 norm of error for Blake problem

Number of Cells	h	$\|e\|_1$	rate
50	2.0	7.573792	-
100	1.0	4.035666	0.90820883
200	0.5	2.526428	0.67570774
400	0.25	1.587075	0.67072896
800	0.125	1.230351	0.36730086

Table 2-3 Blake Pressure (10^6 dynes/cm^2) Convergence Rates

Number of Cells	h	$\|e\|_1$	rate
50	2.0	1.571262e+07	-
100	1.0	7.825823e+06	1.0056091
200	0.5	4.682394e+06	0.74099607
400	0.25	2.862376e+06	0.71003343
800	0.125	2.057544e+06	0.47628973

Table 2-4 Blake Radial Stress Convergence Rates

CTH uses a second order van Leer scheme. As such, we expect spatial convergence rates of less than 2. For a problem with a discontinuity, such as this one, a convergence rate of approximately 1 is expected. Similar codes exhibit approximately half-order convergence for the Blake problem in general, but closer to first-order convergence when the domain is restricted to exclude the regions near the cavity wall and the elastic wave front (see, for example, [5]).

As in the case of other codes, the largest errors for CTH are observed near the cavity wall and near the elastic wave front. Considering only the region outside the cavity, $r > 11$ cm, Tables 2-3 - 2-5, list spatial convergence rates for the Blake problem. For mesh resolutions between $h = 2.0$ and $h = 0.125$, CTH is exhibiting convergence rates of approximately 0.66 for pressure, 0.73 for radial stress, and 0.68 for hoop stress. Overall, convergence is 2/3-order for the Blake problem.

If, following the example of [5], we restrict the domain of consideration still further to 15 cm $< r <$ 85 cm, convergence rates are roughly linear. Specifically, for mesh resolutions between $h = 2.0$ and $h = 0.125$, CTH exhibits convergence rates of approximately 0.93 for pressure, 1.0 for radial stress, and 0.87 for hoop stress. Refer to Tables 2-6 - 2-8.

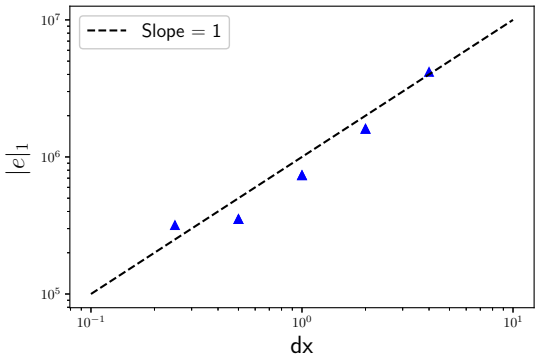

(a) pressure

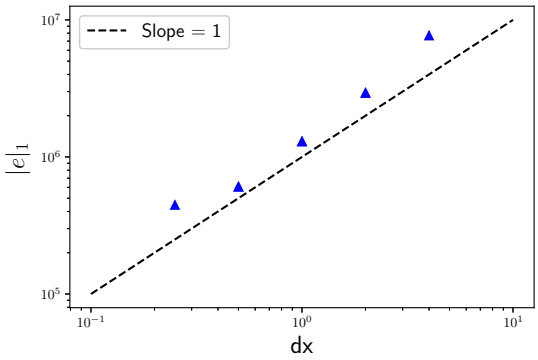

(b) radial stress

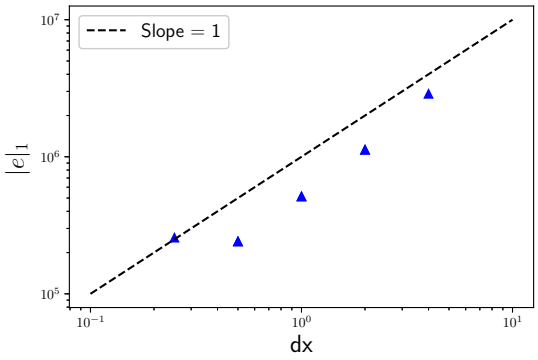

(c) hoop stress

Figure 2-3 L_1 norm of error for Blake problem on the domain 15 cm $< r <$ 85 cm

Number of Cells	h	$\|e\|_1$	rate
50	2.0	5.357582e+06	-
100	1.0	2.748910e+06	0.96272234
200	0.5	1.660282e+06	0.72743161
400	0.25	1.003646e+06	0.72617707
800	0.125	8.202698e+05	0.2910805

Table 2-5 Blake Hoop Stress Convergence Rates

Number of Cells	h	$\|e\|_1$	rate
50	2.0	4.170981	-
100	1.0	1.601967	1.380542
200	0.5	0.7345407	1.124930
400	0.25	0.3517275	1.062384
800	0.125	0.3177769	1.464442

Table 2-6 Blake Pressure (10^6 dynes/cm^2) Convergence Rates (15 cm $< r <$ 85 cm)

Number of Cells	h	$\|e\|_1$	rate
50	2.0	7.686800	-
100	1.0	2.933936	1.389546
200	0.5	1.297397	1.177217
400	0.25	0.6065950	1.096815
800	0.125	0.4466288	0.4416573

Table 2-7 Blake Radial Stress (10^6 dynes/cm^2) Convergence Rates (15 cm $< r <$ 85 cm)

Number of Cells	h	$\|e\|_1$	rate
50	2.0	2.879360	-
100	1.0	1.124793	1.356089
200	0.5	5.133356	1.131685
400	0.25	2.410503	1.090568
800	0.125	2.568687	-0.09169696

Table 2-8 Blake Hoop Stress (10^6 dynes/cm^2) Convergence Rates (15 cm $< r <$ 85 cm)

3. VERIFICATION TEST SUITE: JWL RIEMANN PROBLEMS

3.1. Description of the Problems

These verification tests solve the classic one-dimensional Riemann shock tube problem, but using the JWL EOS rather than the ideal gas EOS. The problem consists of two gases separated by a massless interface. Each of the gases has an initial condition that describes the pressure, density, and velocity for each gas on the left and right side of the interface. The velocity for both gases are taken to be zero. At time $t = 0$, the interface is instantaneously removed from the problem which results in the formulation of shock, contact, and rarefaction waves. For the two problems considered here, the gases to the left and right side of the interface are considered detonation products and the JWL EOS is used to solve the equations in order to verify the implementation of the model in CTH. The analytical solution for each problem was solved using the ExactPack [27] software from Los Alamos National Laboratory.

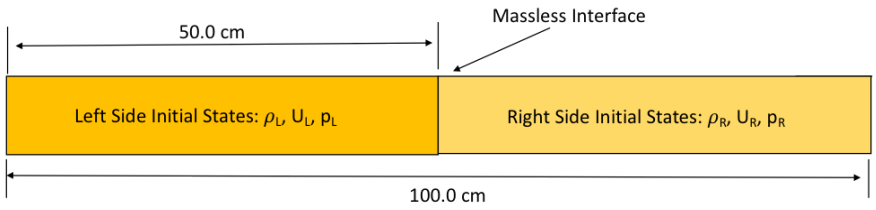

Figure 3-1 Schematic of the Riemann Shock Tube Geometrical Configuration.

The first case is taken from the work of Shyue et al. [26] who solved a simple shock tube problem using a JWL EOS for TNT. The second problem considered is similar to the Riemann problem from Lee et al. [18], where the problem was solved analytically using the JWL EOS for LX-17. The shock tube configuration is shown in Figure 3-1 and the initial conditions for each of the two verification cases considered are provided in Table 3-1.

	Problem #1 - TNT	Problem #2 – LX-17
ρ_L (g/cm^3)	1.7	0.9525
U_L (cm/s)	0.0	0.0
p_L (dynes/cm^2)	1.0E+13	1.0E+12
ρ_R (g/cm^3)	1.0	3.7
U_R (cm/s)	0.0	0.0
p_R (dynes/cm^2)	5.0E+11	2.0E+12

Table 3-1 JWL Riemann Problem Initial Conditions.

3.2. Analytic Solution

The JWL equation of state model provides empirical relationships for the pressure and energy of both explosive detonation products and unreacted explosives [19], [10] when used with the CTH HEBURN option. The JWL EOS model is an extension of early work by Jones and Miller [13]

and Wilkins [33]. Using this work, Lee developed the final set of relationships for pressure and energy as given below:

$$P(\rho,T) = A\,\mathrm{e}^{-R_1\nu} + B\,\mathrm{e}^{-R_2\nu} + \omega\rho C_v T \tag{4}$$

$$E(\rho,T) = \frac{1}{\rho_0}\left(\frac{A}{R_1}\,\mathrm{e}^{-R_1\nu} + \frac{B}{R_2}\,\mathrm{e}^{-R_2\nu} - \varepsilon_0\right) + C_v T \tag{5}$$

$$\nu = \frac{\rho_0}{\rho} \tag{6}$$

In Equation (6), ρ_0 is the initial density of the unreacted explosive. In Equations (4) and (5), the variables A, B, R_1, R_2, ω, and ε_0 are material constants. These material constants are typically determined using either cylinder expansion tests, similar to those used in Section 6.1 for validation purposes, or with thermochemical code calculations. The JWL EOS is commonly used with the programmed burn (HEBURN) option within CTH, which assumes that the same EOS will be used for the unreacted explosive and the detonation products of the explosive. For the unreacted explosive, Equations (4) and (5) are modified such that the initial pressure and energy of the unreacted explosive are zero. These modification results in the following equations for the unreacted explosives.

$$P_{\mathrm{UR}}(\rho,T) = P_{\mathrm{R}}(\rho,T) - P_{\mathrm{R}}(\rho_0,T_0)\,(1-\chi)^2 \tag{7}$$

$$E_{\mathrm{UR}}(\rho,T) = E_{\mathrm{R}}(\rho,T) - E_{\mathrm{R}}(\rho_0,T_0)\,(1-\chi)^2 - P_{\mathrm{R}}(\rho_0,T_0)\left(1-\chi^2\right)(1-\nu)/\rho_0 \tag{8}$$

$$\chi = 3\,\frac{T}{T_0} \tag{9}$$

where the subscripts UR and R denoted unreacted and reacted (i.e. detonation products), respectively.

The analytic solution to the Riemann problem is computed similarly to the traditional 1D Riemann problems, but using the JWL equation of state rather than ideal gas. For accuracy and ease of comparing results with similar codes, the analytic solution for each problem was calculated using the open source code verification software ExactPack [27].

3.3. Parameters

The CTH simulations performed for these two verification tests consisted of one-dimensional (1DR) models that used reflecting boundary conditions at either end of the 1D shock tube representation. The length of the shock tube was meshed with 2000 uniformly sized cells across the 100 cm, which results in a cell size of 0.05 cm. The HE explosive, either TNT or LX-17, was specified using a different package definition for the left (L) and right (R) side of the setup. This allowed the initial conditions of pressure, density and velocity to be set independently for each material within the shock tube. The JWL EOS model parameters for the reacted explosive gases used for the TNT and LX-17 are given below in Table 3-2 and Table 3-3, respectively. For brevity, definitions of the model parameters listed in these tables are not given here. Instead, the reader is referred to the CTH user's manual [25] for a full definition.

EOS	JWL
EOS_Data ID	"TNT"
R0	1.840 (g/cm^3)
AG	8.545E+12 (dynes/cm^2)
BG	2.05E+11 (dynes/cm^2)
R1	4.6
R2	1.35
WG	0.25
E0	1.7E+12 (dynes/cm^2)

Table 3-2 TNT Reaction Products JWL EOS Parameters.

EOS	JWL
EOS_Data ID	"LX-17-0"
R0	1.905 (g/cm^3)
AG	6.321E+14 (dynes/cm^2)
BG	-44.72E+9 (dynes/cm^2)
R1	11.3
R2	1.13
WG	0.8938
E0	9.925972E+10 (dynes/cm^2)

Table 3-3 LX-17 Reaction Products JWL EOS Parameters.

The CTH input file for the Riemann problem using the TNT high explosive is given in Appendix B for reference.

3.4. Results

For the shock tube configuration of Shuye et al. [26], Figure 3-2 through Figure 3-5 provide a comparison of the analytical solutions of the Riemann problem using the JWL EOS from the ExactPack [27] software versus the corresponding CTH simulation results for density, velocity, pressure, and energy, respectively. From each of these images, one can see that the CTH simulations and the analytical solutions are in excellent agreement with one another. The only variation in each of these comparisons is at the shock fronts which are slightly more rounded in the CTH simulations. This is expected as the CTH simulations must introduce artificial viscosity to capture the discontinuous shock front, which results in these minor differences.

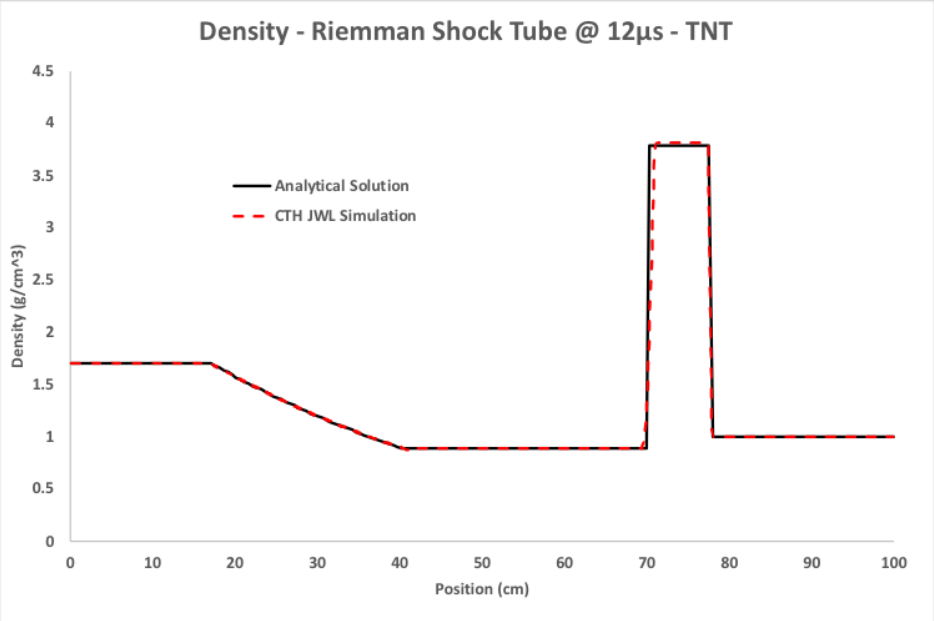

Figure 3-2 TNT Riemann Shock Tube Density Results Comparison.

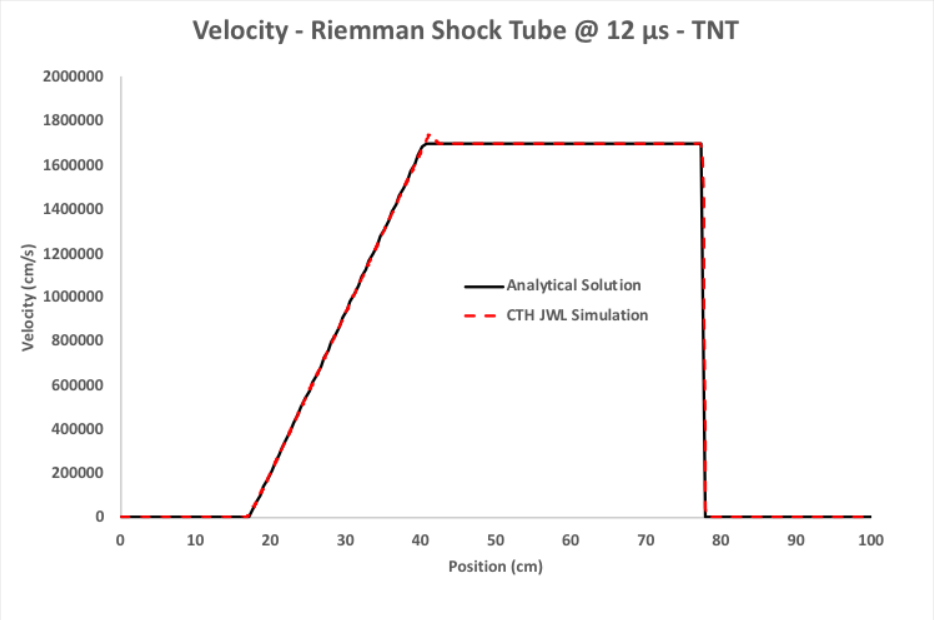

Figure 3-3 TNT Riemann Shock Tube Velocity Results Comparison.

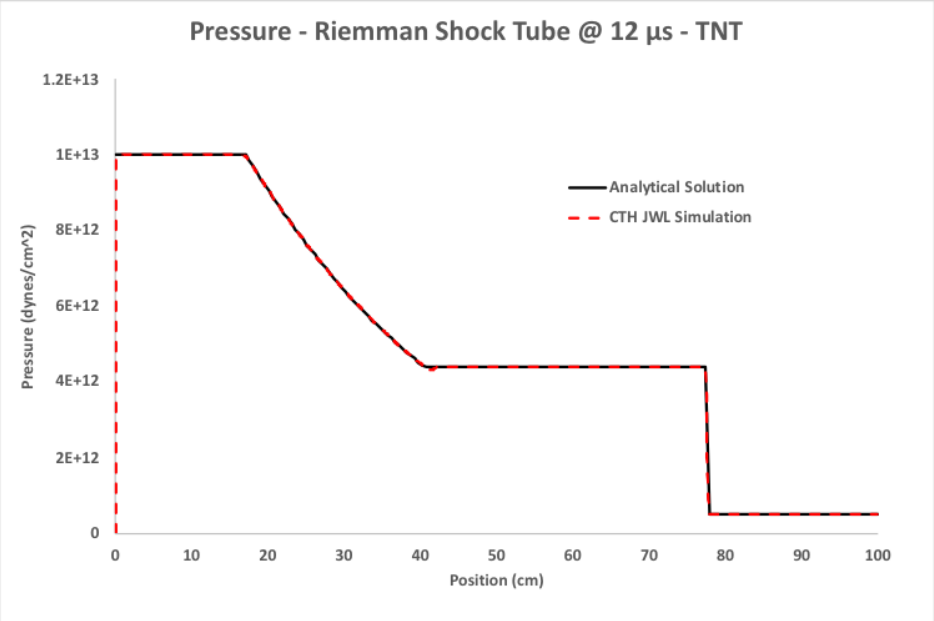

Figure 3-4 TNT Riemann Shock Tube Pressure Results Comparison.

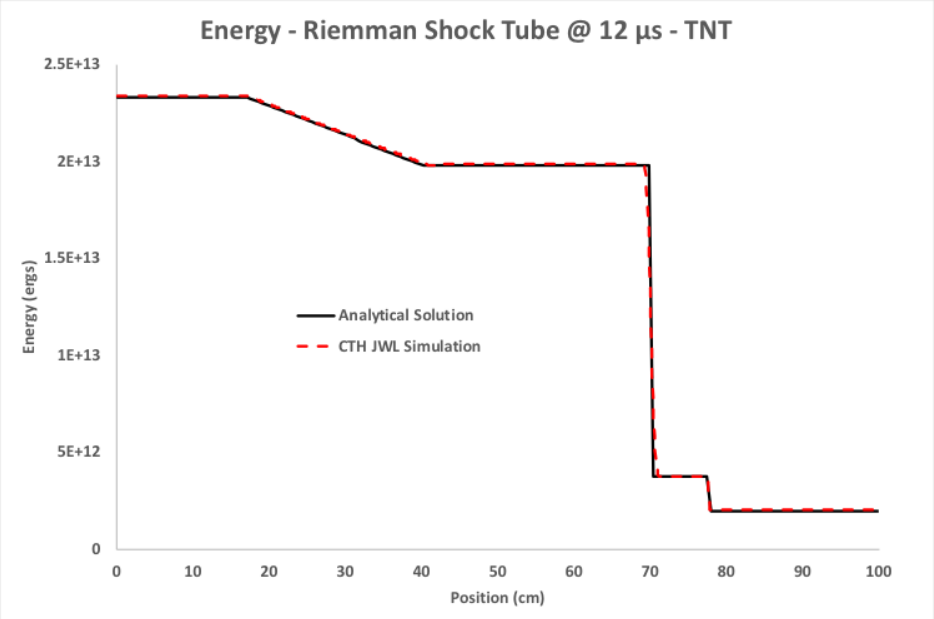

Figure 3-5 TNT Riemann Shock Tube Energy Results Comparison.

For the second shock tube configuration of Lee et al. [18], Figure 3-6 through Figure 3-9 provide a comparison of the analytical solutions of the Riemann problem using the JWL EOS from the ExactPack [27] software versus the corresponding CTH simulation results for density, velocity, pressure and energy, respectively. From each of these images one can again see that the CTH simulations and the analytical solutions are in excellent agreement with one another.

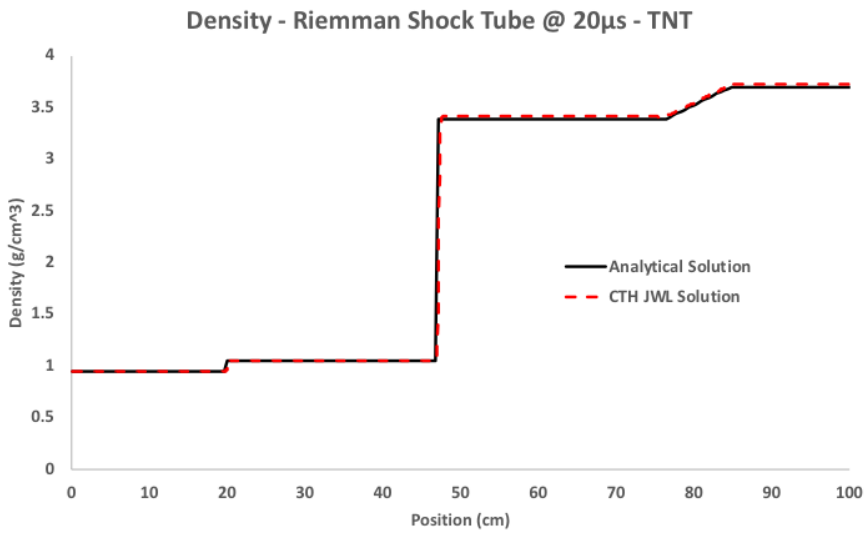

Figure 3-6 LX-17 Riemann Shock Tube Density Results Comparison.

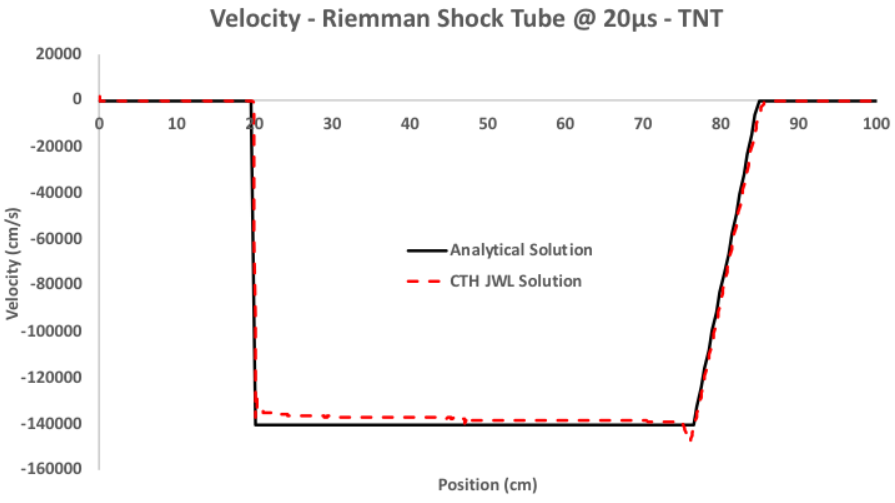

Figure 3-7 LX-17 Riemann Shock Tube Velocity Results Comparison.

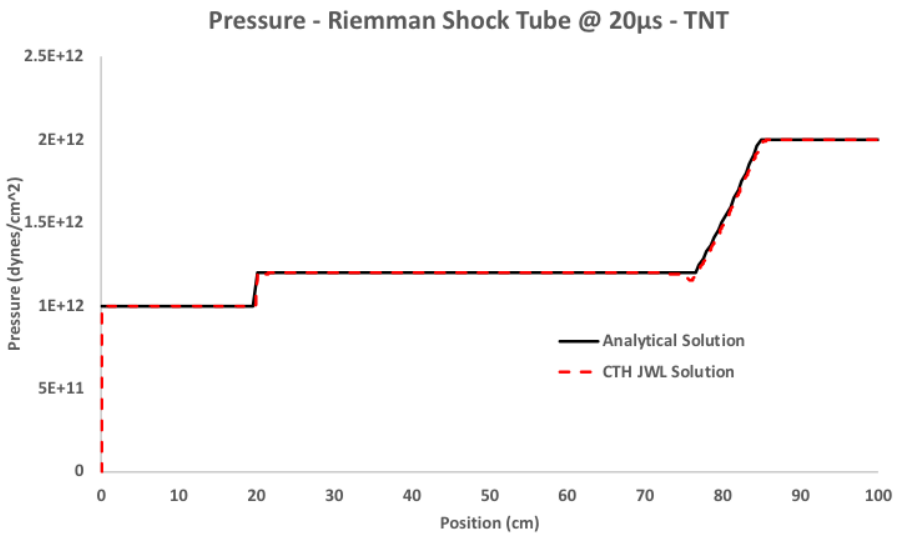

Figure 3-8 LX-17 Riemann Shock Tube Pressure Results Comparison.

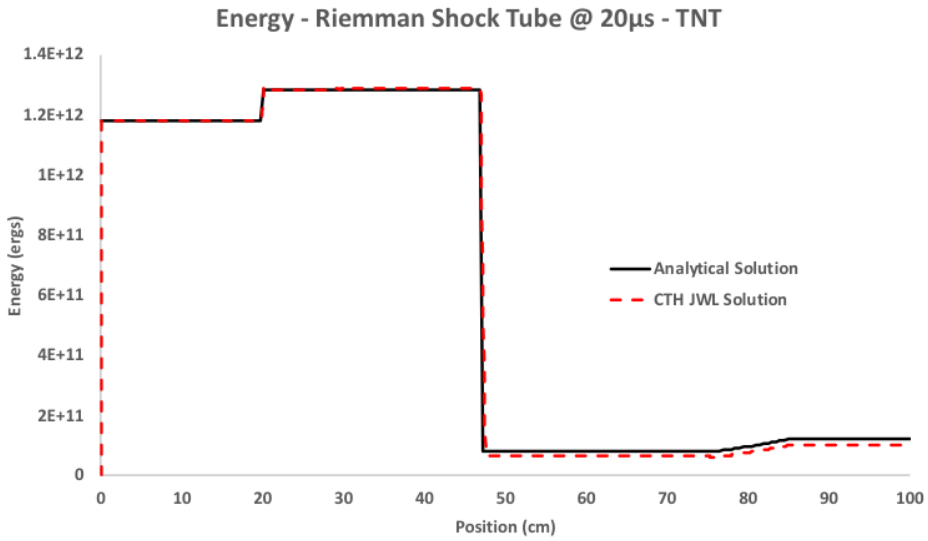

Figure 3-9 LX-17 Riemann Shock Tube Energy Results Comparison.

3.5. Convergence Study

CTH uses a second order van Leer scheme. As such, we expect spatial convergence rates of less than 2. For a problem with a discontinuity, such as this one, a convergence rate of approximately 1 is expected. Though the solution for the JWL 1-D Riemann problem is implemented in the code verification software ExactPack, it is currently unknown what convergence rates similar codes exhibit for this problem. Tables 3-4 - 3-6, list spatial convergence rates for the JWL 1-D Riemann problem. For mesh resolutions between $h = 2.0$ and $h = 0.125$, CTH is exhibiting convergence

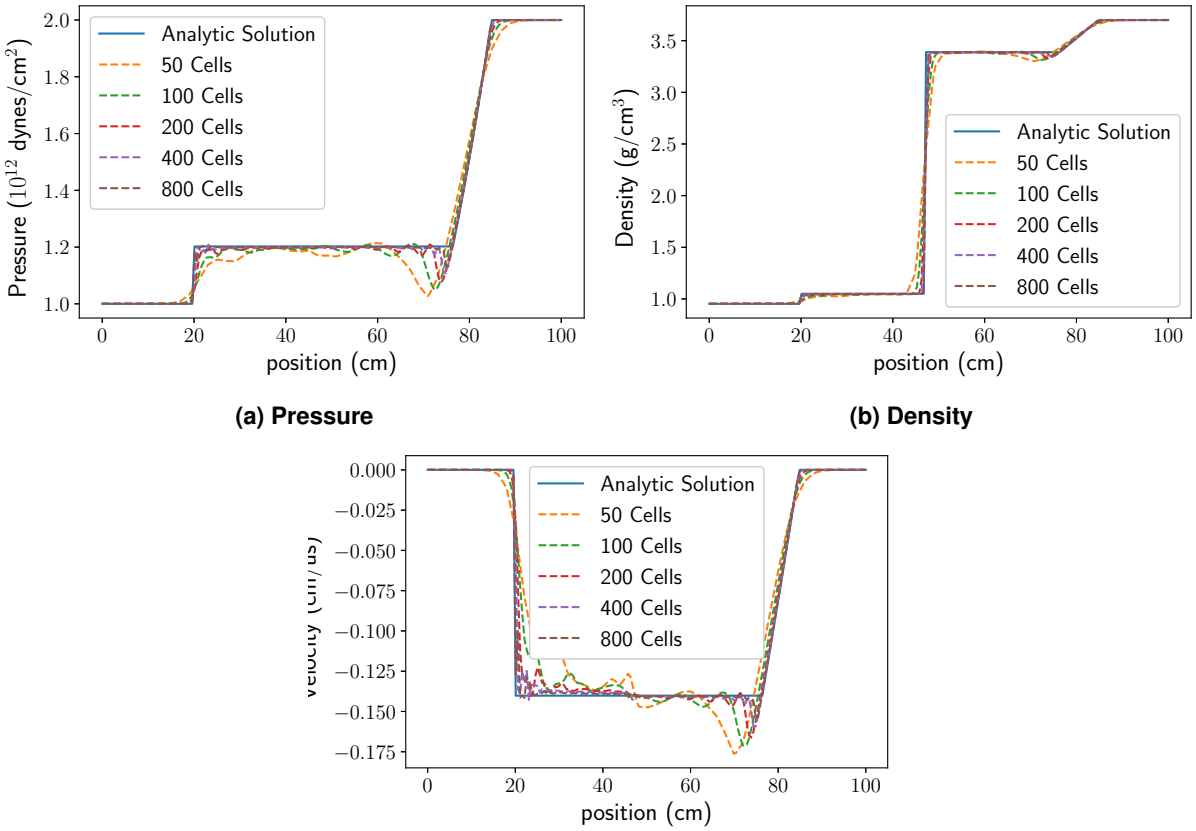

(a) Pressure **(b) Density**

(c) Velocity

Figure 3-10 Comparison of solution at $t_{\text{final}} = 20\ \mu$s for various mesh resolutions.

rates of approximately 0.85 for pressure, 0.78 for density, and 0.83 for velocity. Overall, convergence is a bit less than linear for the JWL 1-D Riemann problem.

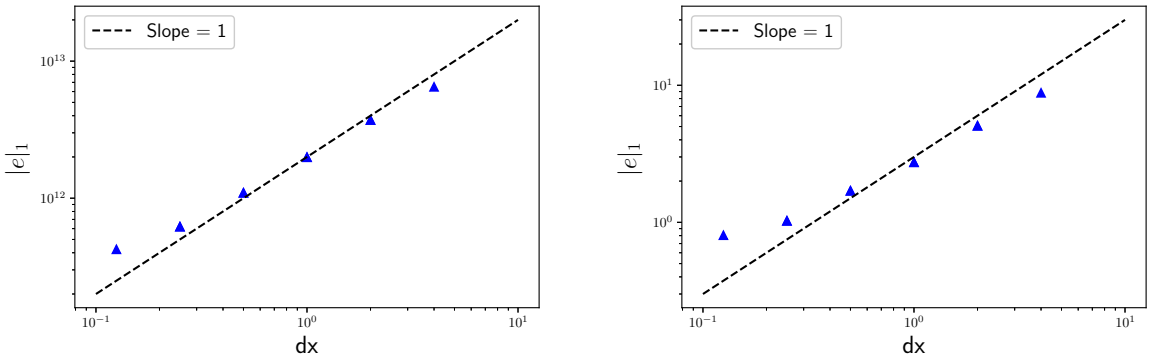

(a) pressure

(b) density

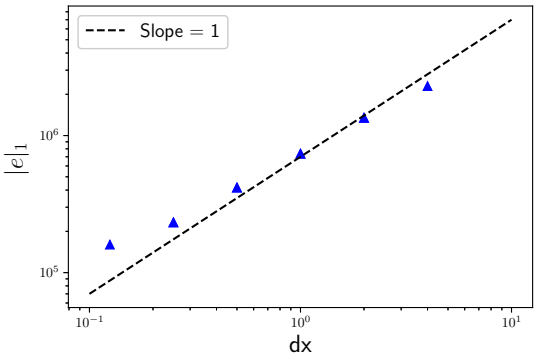

(c) velocity

Figure 3-11 L_1 norm of error for JWL 1-D Riemann problem

Number of Cells	h	$\|e\|_1$	rate
50	2.0	6.495227	-
100	1.0	3.721414	0.8035289
200	0.5	1.990706	0.9025706
400	0.25	1.095238	0.8620359
800	0.125	0.6199672	0.8209808

Table 3-4 JWL 1-D Riemann Pressure (10^{12} dynes/cm^2) Convergence Rates

Number of Cells	h	$\|e\|_1$	rate
50	2.0	8.811454	-
100	1.0	5.065165	0.7987708
200	0.5	2.743037	0.8848354
400	0.25	1.698767	0.6912861
800	0.125	1.025655	0.7279423

Table 3-5 JWL 1-D Riemann Density (g/cm^3) Convergence Rates

Number of Cells	h	$\|e\|_1$	rate
50	2.0	2.296026	-
100	1.0	1.346052	0.7704047
200	0.5	0.7363437	0.8702834
400	0.25	0.4168397	0.8208867
800	0.125	0.2322515	0.8438046

Table 3-6 JWL 1-D Riemann Velocity (cm/μs) Convergence Rates

4. VERIFICATION TEST SUITE: MADER PROBLEM

4.1. Problem Description

The Mader problem is based on the simplest detonation theory, as laid out in Section 2A of Fickett and Davis [8]. It is characterized by a one-dimensional steady detonation front, driven by a piston, followed by a rarefaction wave. The chemical reaction is assumed to instantaneously burn to completion so that the reaction products emerge from the front at equilibrium [27]. From the moment of initiation, the detonation wave travels at constant velocity, generating a self-similar flow between it and the piston [8].

The problem setup is as follows. A piston-driven detonation wave propagates through a 5 cm slab of high explosive (HE), which is modeled as a γ-law gas, with $\gamma = 3$, for both the unreacted explosive and the reaction products. In order to use the HEBURN model, this is implemented by using the JWL equation of state with the parameters *AG* and *BG* set to 0, effectively reducing the JWL EOS to the Ideal Gas EOS. For the Mader problem, the piston is assumed to be stationary. Because of this, the head of the rarefaction stays at the detonation front and the tail is halfway between the front and the piston [31]. The density of the HE is taken to be 1.875 g/cm^3 and the temperature is 0.025 eV. The Chapman-Jouget (CJ) detonation speed is 0.8 cm/μs, so that the detonation reaches the other edge of the HE (at $x = 0$) in 6.25 μs.

The Mader problem provides a test of how well a code captures the CJ state at the detonation front and the rarefaction behind the front [4]. We use it here as a test of the HEBURN (High Explosive Burn) model.

4.2. Analytic Results

The solution to the Mader problem is comprised of three regions: the undisturbed region ahead of the detonation wave, the self-similar flow in the rarefaction fan behind the detonation front, and the (uniform) flow behind the rarefaction fan. The solution given here is summarized from [27] (also [4]).

The Mader problem makes use of the Chapman–Jouguet approximation. The reaction zone is assumed to be infinitesimally thin and the reaction products are assumed to emerge from the detonation front at equilibrium. With these assumptions, the flow can be calculated from the (given) CJ detonation speed, reaction enthalpy, and initial conditions in the undisturbed region (see Table 4-1).

The medium is assumed to be a γ-law gas, so that the equation of state is given by

$$p = (\gamma - 1)\,\rho\, e \tag{10}$$

At $t_{\text{final}} = 6.25\mu$s, the detonation front has reached 5 cm and the terminal point of the rarefaction is at 2.5 cm. The CJ state - the state of the reaction products at the detonation front - is determined

from the Hugoniot and Rayleigh line, giving

$$p_{\mathrm{CJ}} = \frac{\rho_0 D_{\mathrm{CJ}}}{\gamma+1} \tag{11}$$

$$\rho_{\mathrm{CJ}} = \rho_0 \left(\frac{\gamma+1}{\gamma}\right) \tag{12}$$

$$v_{\mathrm{CJ}} = \frac{D_{\mathrm{CJ}}}{\gamma+1} \tag{13}$$

$$c_{\mathrm{CJ}} = D_{\mathrm{CJ}} \left(\frac{\gamma}{\gamma+1}\right) \tag{14}$$

The specific reaction enthalpy q and the position of the detonation front at time t are given by

$$q = \frac{D_{\mathrm{CJ}}^2}{2\left(\gamma^2-1\right)} \tag{15}$$

$$x_{\mathrm{det}} = D_{\mathrm{CJ}} t \tag{16}$$

The undisturbed region ahead of the detonation wave is described by

$$v = -v_{\mathrm{piston}} \tag{17}$$

$$p = 0.0 \tag{18}$$

$$\rho = 1.875 \tag{19}$$

$$c = 0 \tag{20}$$

in which v_{piston} is the speed of the piston in the lab frame ($v_{\mathrm{piston}} = 0$ for the case implemented here).

The self-similar flow in the rarefaction is determined by the ratio x/t and the characteristics are bounded between $x/t = D_{\mathrm{CJ}}$ and $x/t = D_{\mathrm{CJ}}/2$. The transition point between tail of the rarefaction fan and the final state is then given by $x_{\mathrm{tail}} = (1/2) D_{\mathrm{CJ}} t$, so that the flow is described by

$$v = \frac{2\left(x/t\right) - D_{\mathrm{CJ}}}{\gamma+1} \tag{21}$$

$$p/p_{\mathrm{CJ}} = \left[1 + \frac{(\gamma-1)\left(v - v_{\mathrm{CJ}}\right)}{2 c_{\mathrm{CJ}}}\right]^{2\gamma/(\gamma-1)} \tag{22}$$

$$\rho = \rho_{\mathrm{CJ}} \left(p/p_{\mathrm{CJ}}\right)^{1/\gamma} \tag{23}$$

$$c = c_{\mathrm{CJ}} \left(p/p_{\mathrm{CJ}}\right)^{(\gamma-1)/2\gamma} \tag{24}$$

Finally, the flow in the region behind the rarefaction is equal to the state at the tail of the rarefaction fan, that is

$$v = 0 \tag{25}$$

$$p/p_{\mathrm{CJ}} = \left[1 - \frac{v_{\mathrm{CJ}}\left(\gamma-1\right)}{2 c_{\mathrm{CJ}}}\right]^{2\gamma/(\gamma-1)} \tag{26}$$

$$\rho = \rho_{\mathrm{CJ}} \left(p/p_{\mathrm{CJ}}\right)^{1/\gamma} \tag{27}$$

$$c = c_{\mathrm{CJ}} \left(p/p_{\mathrm{CJ}}\right)^{(\gamma-1)/2\gamma} \tag{28}$$

For a problem in which $v_{\text{piston}} \neq 0$, solutions in the lab frame can be determined by subtracting v_{piston} from the other velocities

$$v \rightarrow \left(v - v_{\text{piston}}\right) \tag{29}$$

4.3. Parameters

Parameter values for the Mader problem, matching those used in [4] are given in Table 4-1. The problem domain was 5 cm, one-dimensional rectangular (1DR) geometry. The mesh was divided into 50 zones and then refined by halving the cell size at each refinement, as shown in Table 4-2.

Final time	Ratio of specific heats	Detonation velocity	Specific reaction enthalpy	Initial velocity	Initial density	Initial pressure	Sound speed
t_{final}	γ	D_{CJ}	q	v_0	ρ_0	p_0	c_0
[μs]		[cm/μs]	[erg/g]	[cm/μs]	[g/cm^3]	[dyn/cm^2]	[cm/μs]
6.25	3	0.8	4.0×10^{10}	$-v_{\text{piston}}$	1.875	0.0	0.0

Table 4-1 Mader Problem Parameters

Number of Cells:	50	100	200	400	800
Cell Size [cm]:	0.1	0.05	0.025	0.0125	0.00625

Table 4-2 Mesh Resolution

4.4. Results

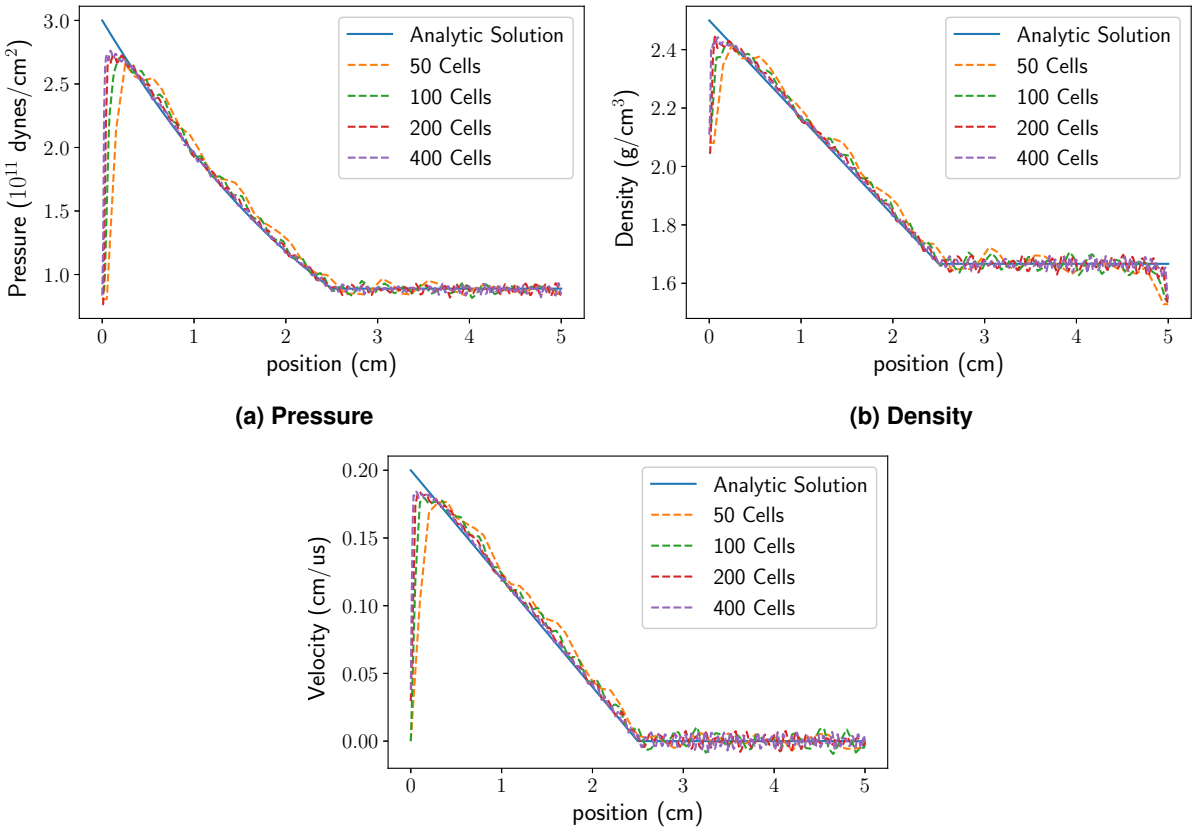

(a) Pressure **(b) Density**

(c) Velocity

Figure 4-1 Comparison of solution at $t_{\text{final}} = 6.25$ μs for various mesh resolutions.

Figure 4-1 shows a comparison of 1-D simulation results for pressure, density, and velocity for various mesh resolutions. In each case, we see the greatest error occurring at the $x = 5$ cm boundary due to the simulated detonation lagging behind the analytic solution.

All CTH results were computed using CTH version 12.1. The input deck for the Mader problem is included in Appendix C. Visual inspection shows rough agreement with the analytic solution, though the simulated position of the detonation front appears to lag behind the true position and the solution exhibits oscillations behind the rarefaction. Convergence results are discussed in Section 4.5.

4.5. Convergence Study

CTH uses a second order van Leer scheme. As such, we expect spatial convergence rates of less than 2. For a problem with a discontinuity, such as this one, a convergence rate of approximately 1 is expected. Similar codes exhibit approximately linear convergence for the Mader problem (see, for example, [30]). Tables 4-3 - 4-5, list spatial convergence rates for the Mader problem.

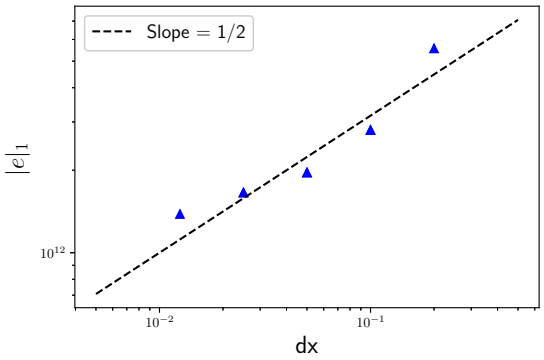

(a) pressure

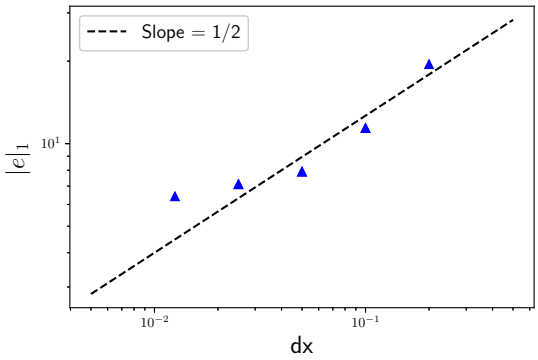

(b) density

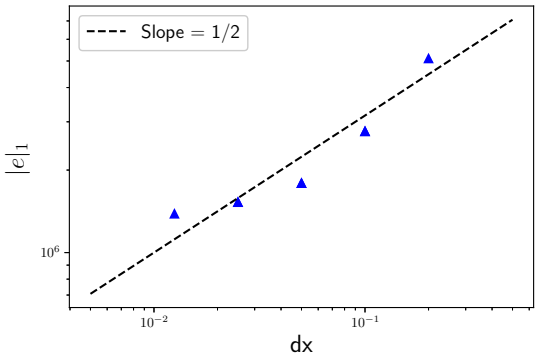

(c) velocity

Figure 4-2 L_1 norm of error for Mader problem

Number of Cells	h	$\|e\|_1$	rate
50	0.1	54.36083	-
100	0.05	31.47490	0.7883657
200	0.025	21.54473	0.5468668
400	0.0125	14.84887	0.5369824
800	0.00625	12.85016	0.2085666

Table 4-3 Mader Pressure (10^{11} dynes/cm^2) Convergence Rates

Number of Cells	h	$\|e\|_1$	rate
50	0.1	19.12468	-
100	0.05	12.15724	0.6536198
200	0.025	8.806630	0.4651541
400	0.0125	6.183115	0.5102561
800	0.00625	5.780946	0.09702828

Table 4-4 Mader Density (g/cm^3) Convergence Rates

Number of Cells	h	$\|e\|_1$	rate
50	0.1	4.938060	-
100	0.05	3.184843	0.6327221
200	0.025	2.052841	0.6336005
400	0.0125	1.647971	0.3169306
800	0.00625	1.447430	0.1871978

Table 4-5 Mader Velocity (cm/μs) Convergence Rates

For mesh resolutions between $h = 0.1$ and $h = 0.00625$, CTH is exhibiting convergence rates of approximately 0.52 for pressure, 0.43 for density, and 0.44 for velocity. Overall, convergence is slightly less than half-order for the Mader problem. This is lower than expected, possibly due to the lag in the position of the detonation wave in the simulations.

5. VERIFICATION TEST SUITE: SESAME

5.1. Model Theory

The Sesame tabular equation of state library from Los Alamos National Laboratory [7] is a computer-based library of tables for the thermodynamic properties of a large collection of materials. The Sesame library contains various tables and data types for each material within the library. Specifically, thermodynamic data exists for pressure and energy as a function of density and temperature which is the primary data used for a CTH simulation. There are also data tables

Table 101	Comments
Table 102	Comments
Table 201	Atomic Number, Atomic Mass, Normal Density
Table 301	Total EOS (304 + 305 + 306)
Table 303	Ion EOS Plus Cold Curve (305 + 306)
Table 304	Electron EOS
Table 305	Ion EOS (Including Zero Point)
Table 306	Cold Curve (No Zero Point)
Table 401	Vaporization Table
Table 411	Solid Melt Table
Table 412	Liquid Melt Table
Table 431	Shear Modulus Table
Table 501	Opacity Grid Boundary: Calculated vs. Interpolated
Table 502	Rosseland Mean Opacity ($cm^2\ g^{-1}$)
Table 503	Electron Conductive Opacity[1] ($cm^2\ g^{-1}$)
Table 504	Mean Ion Charge[1] (free electrons per atom)
Table 505	Planck Mean Opacity ($cm^2\ g^{-1}$)
Table 601	Mean Ion Charge[2] (free electrons per atom)
Table 602	Electrical Conductivity (sec^{-1})
Table 603	Thermal Conductivity ($cm^{-1}\ sec^{-1}$)
Table 604	Thermoelectric Coefficient ($cm^{-1}\ sec^{-1}$)
Table 605	Electron Conductive Opacity[2] ($cm^2\ g^{-1}$)

[1]Opacity Model (Hubbard-Lampe)
[2]Conductivity Model (Ziman)

Figure 5-1 Listing of Available Sesame Tables Types.

for vaporization, melt, shear, opacity and conductivity which are not used by CTH. Figure 5-1

provides a list of each type of table that may be available for a material in the Sesame library taken from [7].

Of the tables show in Figure 5-1, only Table 201 (basic data) and Table 301 (total EOS) are needed by CTH. Further, for Table 201 only the reference density is necessary for CTH.

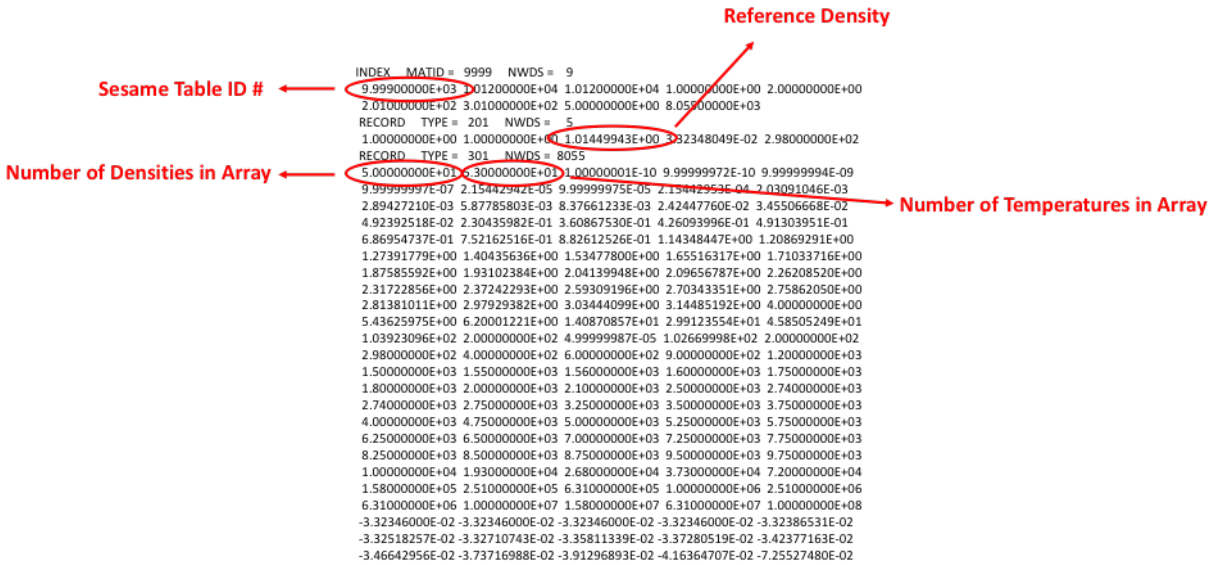

Figure 5-2 Sesame Table Data Structure.

An abbreviated sample of the input structure of a typical 201 and 301 Sesame table are shown in Figure 5-2.

For this example, the Sesame table ID is 9999 and the reference density of the material is 1.0145 g/cm3. Additionally, this table has a data structure (mesh) that is 50 densities x 53 temperatures or a total of 2650 data points. Further details of the Sesame tables and their structure can be found in [7].

5.2. SESAME Verification Problem #1: CTH Symmetric Impact vs. BCAT

5.2.1. Description of the Problem

The first verification test case consists of a symmetric impact condition modeled using CTH to determine the resulting shock (Hugoniot) state of the material using the Sesame table EOS for the materials of interest. These shock or Hugoniot states calculated from CTH are then compared with Hugoniot conditions that are extracted from the Sesame table library using the independent BCAT [16] code. The BCAT code is part of the CTH distribution which combines routines from PANDA [9] and the CTH EOS package and is commonly used for testing and developing EOS models. This comparison procedure was chosen as the initial verification of the Sesame table implementation in CTH as it utilizes the BCAT code which is independent of CTH and hence validates the interface of CTH with the Sesame table libraries.

The particular materials chosen for this verification case were titanium and lead. In separate CTH simulations, each material was impacted at three different levels (impact velocities) in order to probe the Sesame tables EOS of each material at various locations. A schematic and the dimensions of the CTH symmetric impact configurations are shown below in Figure 5-3, where the right-hand target plate was specified to be stationary and the left-hand target had a prescribed impact velocity.

The six different symmetric impact conditions (2 materials x 3 impact velocities) considered for this verification test suite are detailed below in Table 5-1.

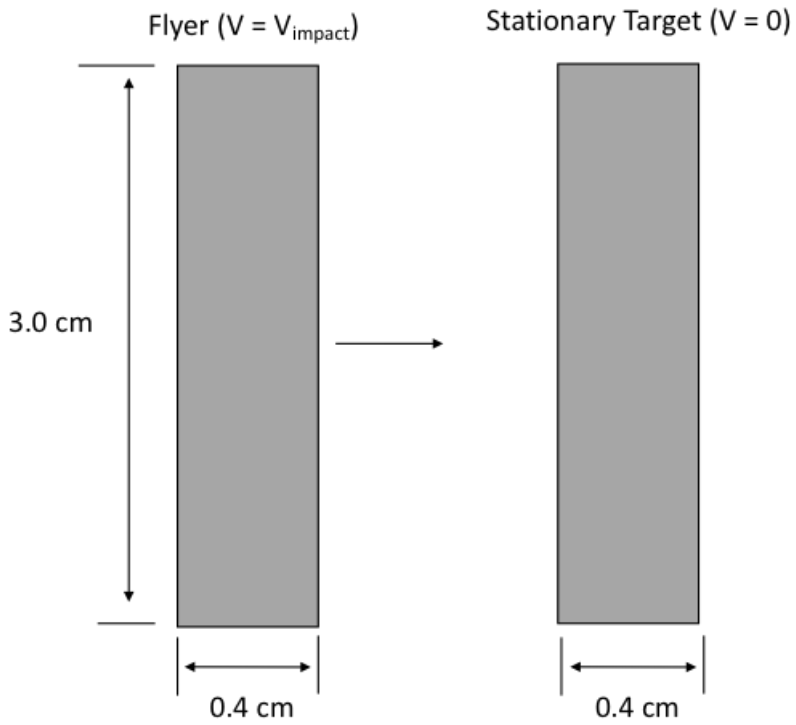

Figure 5-3 Schematic of the CTH Symmetric Impact Configuration for Verification Test #1.

Test_ID	Flyer and Target Material	Flyer Velocity (km/s)
LEAD_1	Lead	0.5
LEAD_2	Lead	1.0
LEAD_3	Lead	0.1
TIT_1	Titanium	1.0
TIT_2	Titanium	0.5
TIT_3	Titanium	1.5

Table 5-1 Experimental Flyer Plate Configurations for Verification Test #1.

5.2.2. Parameters

The CTH simulations for these verification problems consisted of two-dimensional (2DR) models with radial extents designed to capture the nominally plane strain response of the planar impact problem prior to the arrival of boundary waves or other three-dimensional effects. Specifically, a rectangular mesh size of 0.001 cm x 0.02 cm was used for each of these simulations which results in 400 cells through the thickness of both the impactor and target panel. For this verification problem both the lead and titanium materials considered were assumed hydrodynamic (no strength component) and utilized the corresponding Sesame table equation of state as show below in Table 5-2.

EOS	SES
LEAD_#	"LEAD"
TITANIUM_#	"TITANIUM"

Table 5-2 EOS Parameters for Verification #1.

The CTH input file for the configuration LEAD_1 is given in Appendix D for reference. Likewise, the input file and the BCAT results output for the same configuration are given in Appendix E .

5.2.3. Results

The resulting shock state (density, pressure, temperature, and energy) predicted in each of the symmetric impact simulations along with the corresponding state extracted from the Sesame tables using the BCAT program is given below in Table 5-3. Table 5-3 shows that the material shock state from the CTH simulations which utilize the Sesame table EOS are nearly identical to the extracted Sesame table shock states from the BCAT program. Specifically, the largest percentage error between the CTH simulations and the BCAT extractions from the Sesame tables is 0.0282%.

It is noted that when probing the Sesame EOS using the BCAT program, the user must specify the density and temperature of the shocked state and BCAT will then determine the resulting pressure and energy states. Therefore, the primary variables of comparison from Table 5-3 are the pressure

and energy. The specified density and temperature values will always in identical agreement given that they were specified in BCAT.

Test ID		Density (g/cm^3)	Temperature (eV)	Pressure ($dynes/cm^2$)	Energy (erg/g)
LEAD_1	CTH	12.6883	0.03616	6.70634E+10	6.7498E+08
	BCAT	12.6883	0.03616	6.70659E+10	6.7505E+08
	% Error	0.0%	0.0%	0.0037%	0.0104%
LEAD_2	CTH	13.8749	0.05829	1.5572E+11	1.5921E+09
	BCAT	13.8749	0.05829	1.5572E+11	1.5922E+09
	% Error	0.0%	0.0%	0.0%	0.0063%
LEAD_3	CTH	11.6286	0.02741	1.16923E+10	3.7755E+08
	BCAT	11.6286	0.02741	1.16956E+10	3.7760E+08
	% Error	0.0%	0.0%	0.0282%	0.0132%
TIT_1	CTH	4.9935	0.02923	1.1559E+11	2.9084E+09
	BCAT	4.9934	0.02923	1.15587E+11	2.9086E+09
	% Error	0.0%	0.0%	0.0026%	0.0069%
TIT_2	CTH	4.7293	0.02723	5.84786E+10	1.8551E+09
	BCAT	4.7293	0.02723	5.84791E+10	1.8554E+09
	% Error	0.0%	0.0%	0.0009%	0.0162%
TIT_3	CTH	5.2264	0.03338	1.82645E+11	4.3397E+09
	BCAT	5.2264	0.03338	1.82646E+11	4.3401E+09
	% Error	0.0%	0.0%	0.0005%	0.0092%

Table 5-3 Symmetric Impact Results Comparison for Verification Test #1.

5.3. SESAME Verification Problem #2: User Defined SESAME Table

5.3.1. Description of the Problem

The second verification test case considers a symmetric impact problem similar to the first verification test. However, for this verification test a user defined Sesame table was generated from assumed thermodynamic relationships between density, temperature, pressure, and energy. This verification problem allowed for verification of the CTH implementation of the Sesame tables through comparison of the symmetric impact simulations against the known analytical shock (Hugoniot) states that were used to develop the Sesame table.

A schematic of the CTH symmetric impact problem, which is similar to the previous validation problem, is shown below in Figure 5-4. As was the case for the first verification problem, the right hand target plate is stationary while the left hand target plate has a specified impact velocity which varies for each of the test cases. Two impact velocities were simulated for this verification problem, the details of which are provided in Table 5-4.

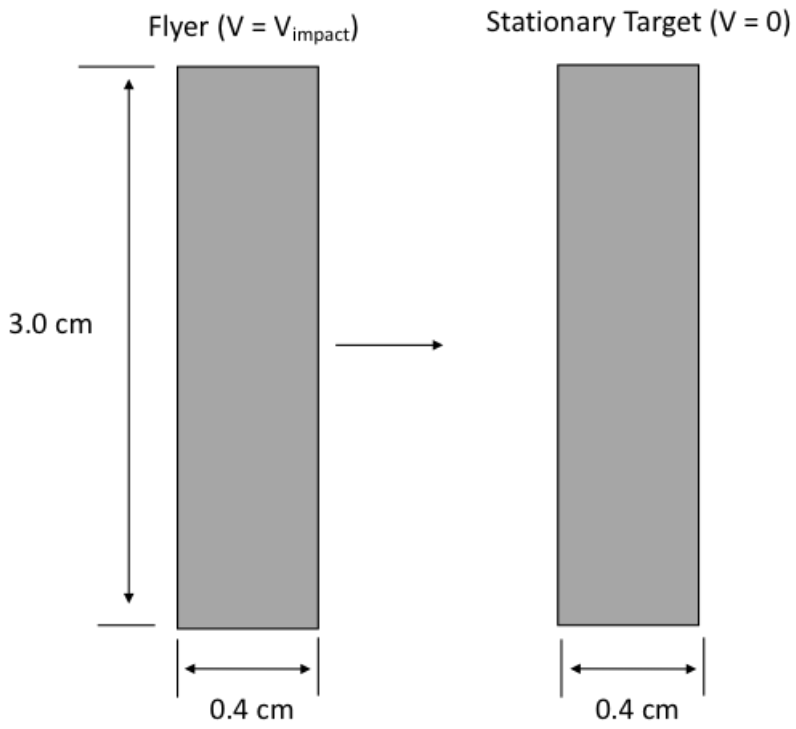

Figure 5-4 Schematic of the CTH Symmetric Impact Configuration for Verification Test #2.

Test_ID	Flyer and Target Material	Flyer Velocity (km/s)
UD_1	User_Defined	2.0
UD_2	User_Defined	0.5

Table 5-4 Experimental Flyer Plate Configurations for Verification Test #2.

5.3.2. Parameters

The CTH simulations performed for these verification tests consisted of two-dimensional (2DR) models with radial extents designed to capture the nominally plane strain response prior to the arrival of boundary waves or other three-dimensional effects. Specifically, a rectangular mesh size identical to the first verification problem measuring 0.001 cm x 0.02 cm was used for each of these simulations which results in 400 cells through the thickness of both the impactor and target panel. The user-defined material used in these simulations were again assumed hydrodynamic (no strength component) and utilized the custom Sesame table equation of state described below in Section 5.3.3. The EOS parameters used to reference the user-defined Sesame table, which was given a material number of 9999, are provided below in Table 5-5.

EOS	SES
Material Option	"USER '
EOS	9999
FEOS	b9999

Table 5-5 EOS Parameters for Verification Test #2.

The CTH input file for the UD_1 test configuration is given in Appendix F for reference.

5.3.3. Analytical EOS Description

The user-defined Sesame EOS table used for this verification problem was developed from hypothetical analytical thermodynamic relationships between density, pressure, temperature, and energy. These hypothetical relationships were translated into the Sesame table format using the tools within BCAT [16]. Although the details of this Sesame table creating are beyond the scope of this V&V report, the basic procedure to develop the user-defined Sesame table was to first generate an EOS table in the CHEETAH [9] format and then utilize the built-in tools within BCAT to transform the CHEETAH formatted table into the required CTH format. An example for creating a user-defined Sesame table can be found in Appendix C of the BCAT manual [16].

The analytical relationships used to generate the user-defined Sesame table are given below in the equations below. It is noted again that these relationships are hypothetical relationships that were created for verification of the Sesame tables within CTH and do not represent any known material thermodynamic relationships. The initial relationship used to define the material energy as a function of temperature is given in Equation 30.

$$\text{Energy} = \frac{1}{v_0} C_v \left(T - T_{\text{room}}\right) C_1 \tag{30}$$

Where v_0 is the reference specific volume, C_v is the specific heat of the arbitrary user-defined material and C_1 is a material constant. For the hypothetical user-defined Sesame table generated for this verification problem, C_v was assumed to be a value of 390 cal/K/g and T_{room} was assumed to be 250 K.

The second relationship for the analytical user-defined Sesame table EOS, defines the pressure as a function of the energy and density states of the material and is given in Equation 31.

$$\text{Pressure} = \rho\, C_1\, \text{Energy} - C_2 \tag{31}$$

In Equation 31, ρ is the density state, and C_1 and C_2 are material constants. For the verification tests presented here these user-defined material constants have values of 7.3269E+06 (atm*cm^3)/(g*cal) and 328 atm, respectively.

5.3.4. Results

The resulting shock (Hugoniot) state in the user-defined material for each of the two symmetric impact conditions is given below in Table 5-6. The states for both the CTH simulations and the closed form analytical equations used to generate the Sesame table are presented. The values in the table show that the CTH simulations results using the user-defined Sesame table are nearly identical to the closed form equations. As with the previous verification problem, the density and temperature states are the known inputs into the analytical closed-form equations so they are defined to be in exact agreement with the CTH simulations. The largest error between the CTH simulations and the analytical equations for the dependent pressure and energy variables is 0.23% which is considered to be numerical round-off. Finally, it is noted that the energy values listed in Table 5-6 for the analytical solution are the sum of Equation 30 and the energy shift (1.161E+09 erg/g) that is calculated by CTH to avoid negative energies.

Test ID		Density (g/cm^3)	Temperature (eV)	Pressure ($dynes/cm^2$)	Energy (erg/g)
LEAD_1	CTH	2.21	0.131	1.880E+10	6.100E+09
	Analytical Solution	2.21	0.131	1.884E+10	6.114E+09
	% Error	0.0%	0.0%	0.21%	0.23%
LEAD_2	CTH	1.94	0.0324	1.33E+09	1.651E+09
	Analytical Solution	1.94	0.0324	1.33E+09	1.651E+09
	% Error	0.0%	0.0%	0.0%	0.0%

Table 5-6 Symmetric Impact Results Comparison for Verification Test #2.

6. VALIDATION TEST SUITE: JWL

6.1. JWL Validation Test #1: Cylinder Expansion Test

6.1.1. Description of the Test

The first validation test case considers the cylinder expansion tests performed by Lan et al. [17]. The cylinder expansion test configurations consisted of a 2.54 cm inside-diameter copper cylinder with a wall thickness of 0.26 cm, which is filled with selected high explosives. At the left end of the cylinder a plane wave lens was used to generate a planar detonation wave down the axis of the tube. As the planar detonation wave passes along the axis of the cylinder, a streak camera is used to measure the displacement history of the outer diameter of the cylinder. A schematic of the test configuration is shown in Figure 6-1. For this validation test suite, we consider four experimental configurations each with a different high explosive filling the cylinder. These four configurations were chosen as they provide validation of four different common explosives characterized for the JWL EOS within the CTH material library (VP_data). The four different high explosive configurations examined for this validation test were HMX, TNT, PBX-9404 and Nitromethane (NM).

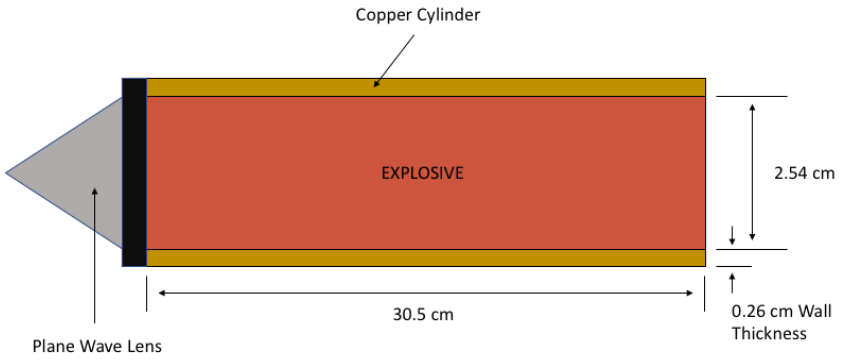

Figure 6-1 Schematic of the Expanding Cylinder Configuration.

6.1.2. Problem Setup and Parameters

The CTH simulations of this validation problem consisted of two-dimensional cylindrical (2DC) models with radial and axial extents that capture the entire cylindrical configuration and the surrounding void region. The copper material was modeled using the Mie-Grüneisen (MGR) EOS and the von-Mises elastic perfectly plastic (EPPVM) strength model [32]. The parameters for the Copper MGR EOS and EPPVM strength models are given in Table 6-1 and Table 6-2, respectively. For brevity, definitions of the model parameters listed in these tables are not provided. Instead, the reader is referred to the CTH user's manual [25] for a full definition.

EOS	MGR
EOS_Data ID	"COPPER"
ro	8.93 (g/cm^3)
C_s	3.94 (km/s)
S_1	1.489

Table 6-1 Copper EOS Parameters.

matep	EPPVM
VP_Data ID	"user"
yield	3.0e9 (dynes/cm^2)
poisson	0.27

Table 6-2 Copper Strength Parameters.

As detailed previously, cylinder expansion simulations were performed and compared against experimental test results for four different high explosives; HMX, TNT, PBX-9404 and Nitromethane (NM). Each of these high explosives were modeled using the JWL EOS with no strength model. The JWL materials parameters for each of these high explosives is provided in Table 6-3 through Table 6-6, respectively.

EOS	JWL
EOS_Data ID	"HMX"
R0	1.891 (g/cm^3)
AG	7.7830E+12 (dynes/cm^2)
BG	7.0710E+10 (dynes/cm^2)
R1	4.2
R2	1.0
WG	0.3
E0	1.2897345E+11 (dynes/cm^2)

Table 6-3 HMX JWL EOS Parameters.

EOS	JWL
EOS_Data ID	"TNT"
R0	1.630 (g/cm^3)
AG	3.7120E+12 (dynes/cm^2)
BG	3.2310E+10 (dynes/cm^2)
R1	4.15
R2	0.95
WG	0.3
E0	7.009056E+10 (dynes/cm^2)

Table 6-4 TNT JWL EOS Parameters.

EOS	JWL
EOS_Data ID	“PBX-9404-3”
R0	1.840 (g/cm^3)
AG	8.5240E+12 (dynes/cm^2)
BG	1.8020E+11 (dynes/cm^2)
R1	4.6
R2	1.3
WG	0.38
E0	1.0200E+11 (dynes/cm^2)

Table 6-5 PBX-9404 JWL EOS Parameters.

EOS	JWL
EOS_Data ID	“NM”
R0	1.128 (g/cm^3)
AG	2.0920E+12 (dynes/cm^2)
BG	5.6890E+10 (dynes/cm^2)
R1	4.4
R2	1.2
WG	0.3
E0	5.26666646E+10 (dynes/cm^2)

Table 6-6 Nitromethane (NM) JWL EOS Parameters.

The CTH input file for the expanding cylinder configuration using the HMX high explosive is given in Appendix G for reference.

6.1.3. Convergence Study

To ensure that convergence was achieved for the expanding cylinder simulations used in this validation problem suite, a mesh refinement study was performed. The convergence study was performed using the test configuration where HMX was the high explosive. Figure 6-2 shows the CTH predicted radial position versus time curves for the HMX test configuration for three different cell sizes (mesh densities). Specifically, the Level = -1 results are for a rectangular cell sizes of 0.04 cm x 0.1 cm which results in 6.5 cells through the thickness of the copper cylinder. The Level = 0 results are for a cell size of 0.02 cm x 0.05 cm and the Level = +1 results are for a cell size of 0.01 cm x 0.025 cm which results in 26 cells through the thickness of the copper cylinder. As can be seen from Figure 6-2, each of the three mesh density results show good agreement with nearly identical agreement observed between the Level = 0 and Level = +1 results. The Level = -1 results are slightly lower and hence considered not yet fully converged. Therefore, the Level = 0 results are considered to be sufficiently converged and are used for each of the subsequent CTH simulations of this validation test case.

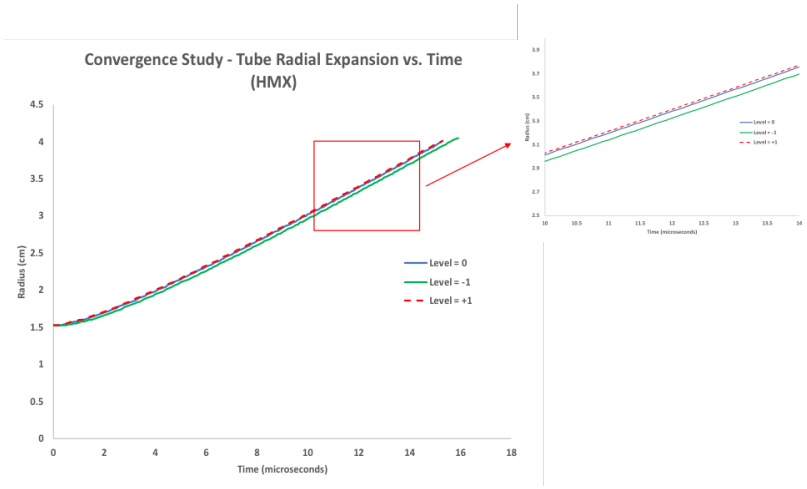

Figure 6-2 CTH Cylinder Expansion Convergence Study Results using the HMX HE.

6.1.4. Results

The experimentally measured radius of the cylinder along with the CTH predicted cylinder radius as a function of time are shown below in Figure 6-3 through Figure 6-6. Specifically, the experimental expansion profiles and the corresponding CTH simulations for HMX, TNT, PBX-9404, and NM are shown in Figure 6-3, Figure 6-4, Figure 6-5, and Figure 6-6, respectively. It is noted that the experimental radial expansion values were recorded from a streak camera during testing while the CTH simulations (black dashed lines) were determined from tracer points placed at the outer diameter of the copper tube.

Each of these figures show that the JWL EOS is producing radial expansion rates and values that correlate very well with the experimentally measured expansion. From these figures, one can also see that for the HMX, TNT, and PBX-9404, the CTH simulations slightly underpredict the radial expansion while the NM simulations are nearly identical to the measured experimental expansion. These differences are attributed to two aspects. First, Lan et al. [17] did not provide a specific location along the axis of the copper cylinder where they were recording the expansion. Therefore, the CTH simulations assumed a location 7 cm from the detonation plane which may or may not align exactly with the experimental measurements. Second, as pointed out by researchers [1] and [20], the cylinder motion is unstable at the early stages of expansion, so the instant of initial expansion from the testing is difficult to recognize.

Test ID	Correlation Coefficient R
HMX	0.9636
TNT	0.9644
PBX-9404	0.9671
NM	0.9614

Table 6-7 Correlation Coefficient for the Expanding Cylinder Simulations.

Table 6-7 provides a quantitative measure between the CTH simulation and the experimental test data for each of the four configurations using the Pearson's correlation coefficient (R) [23]. The coefficient values presented in Table 6-7 quantitatively demonstrate that all four simulation results are in good agreement with the experimental data (since each of the correlation coefficients (R) are greater than 0.9).

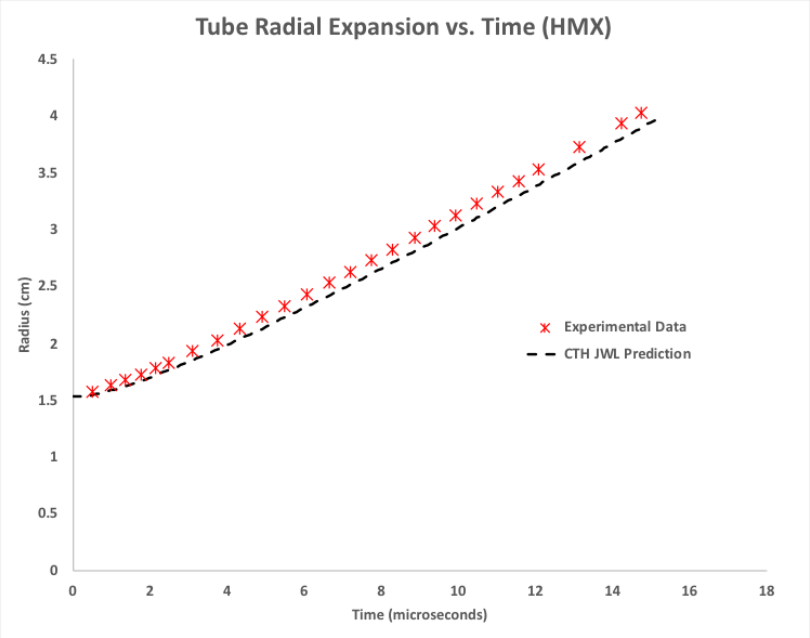

Figure 6-3 Comparison of the Cylinder Radial Expansion vs. Time for the HMX Configuration.

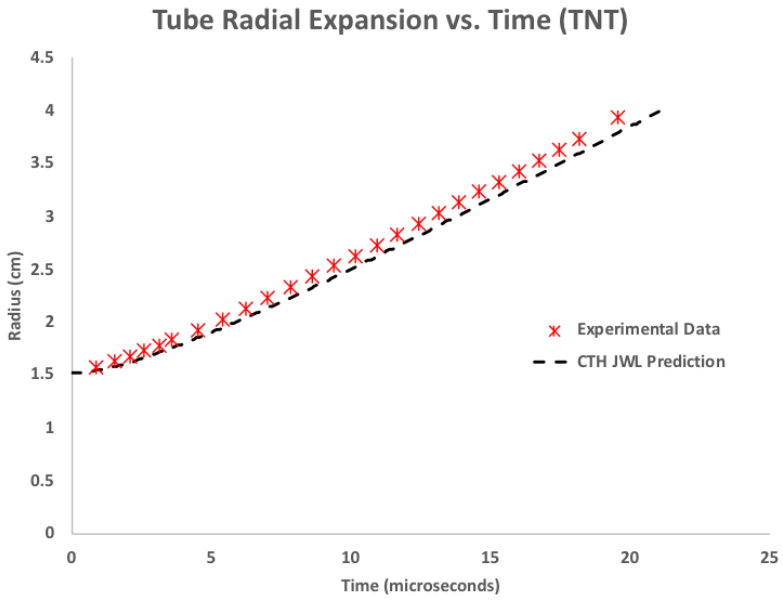

Figure 6-4 Comparison of the Cylinder Radial Expansion vs. Time for the TNT Configuration.

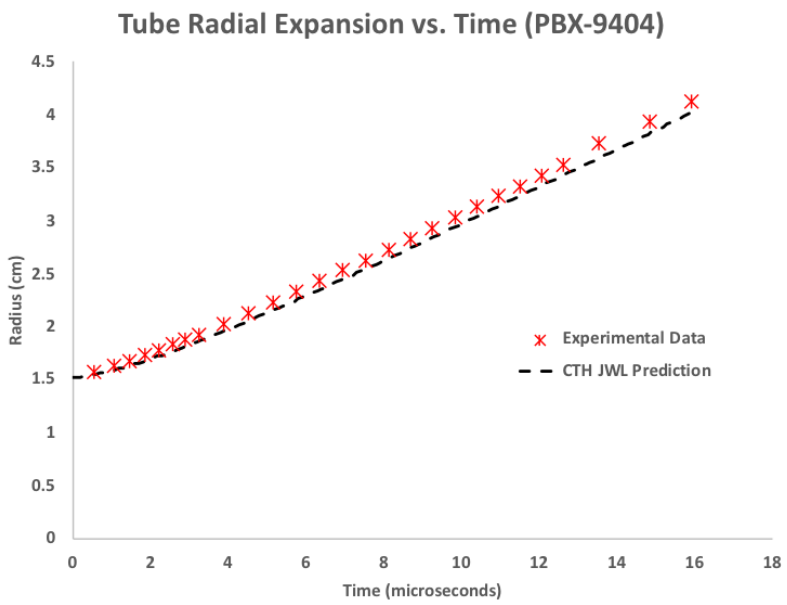

Figure 6-5 Comparison of the Cylinder Radial Expansion vs. Time for the PBX-9404 Configuration.

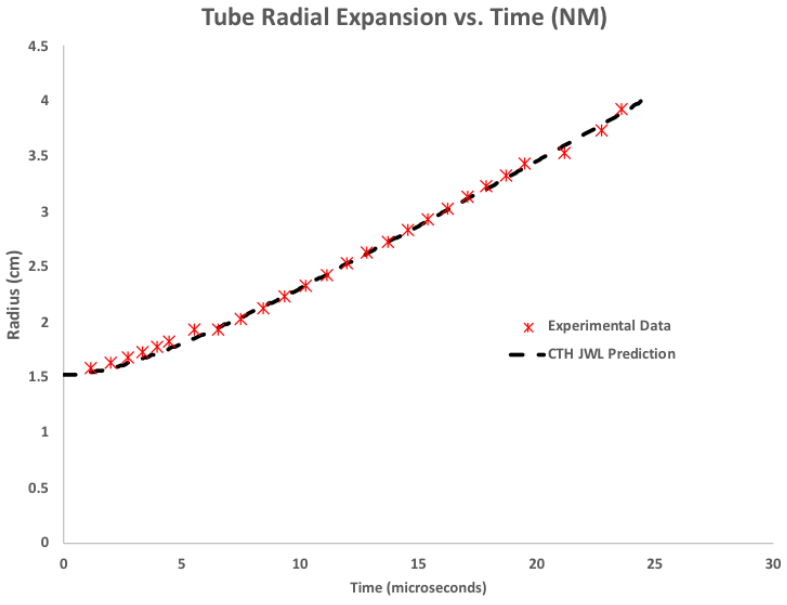

Figure 6-6 Comparison of the Cylinder Radial Expansion vs. Time for the NM Configuration.

6.2. JWL - Validation Test #2: Hemispherical Expansion

6.2.1. Description of the Test

The second validation test case considered is the hemispherical expansion tests performed by Lee et. al [19]. The hemispherical expansion test configurations are similar to the previous validation case, but rather than a cylinder, a 15.0 cm inner radius aluminum hemisphere with a wall thickness of 0.65 cm was used. The aluminum hemisphere was filled with selected high explosives and then set on top of a high explosive cylinder mate. For this configuration, the spherical detonation wave was initiated at the center of the hemisphere and caused the hemisphere to expand similar to the previous cylindrical expansion tests. Again, a streak camera was used to measure the displacement history of the outer diameter of the hemisphere. A schematic of the hemispherical expansion test configuration is shown in Figure 6-7. For this validation test suite, three different high explosives were studied. These three high explosives were chosen as they provide validation for different common explosives characterized for the JWL EOS within the CTH material library (VP_data). The three different high explosive materials used for this validation test were CompB-GradeA, PBX-9404, and LX-04-1.

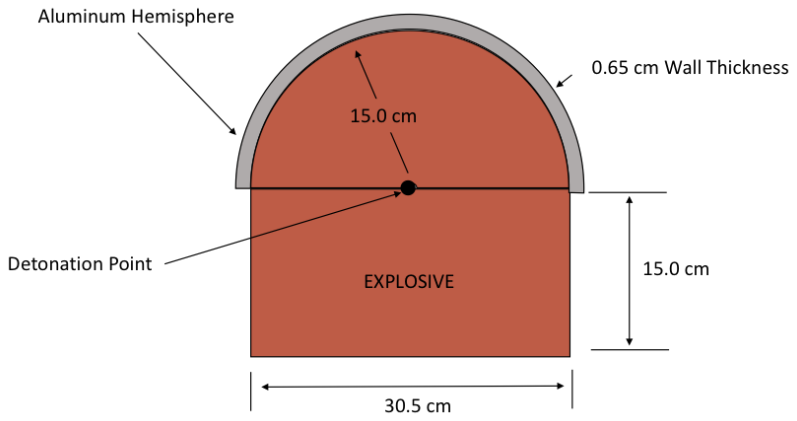

Figure 6-7 Schematic of the Expanding Cylinder Configuration.

6.2.2. Problem Setup and Parameters

The CTH simulations of this validation problem consisted of a two-dimensional cylindrical (2DC) model with radial extents that capture the entire hemispherical configuration and the surrounding void region. The aluminum material was modeled using the Mie-Grüneisen EOS and the Johnson-Cook (JO) strength model [12]. The material parameters for the aluminum EOS and strength model within the CTH simulations are given in Table 6-8 and Table 6-9, respectively. For brevity, definitions of the model parameters listed in these tables are not provided. Instead, the reader is referred to the CTH user's manual [25] for a full definition.

EOS	MGR
EOS_Data ID	“6061-T6_AL”
ro	2.703 (g/cm^3)
C_s	5.22 (km/s)
S_1	1.37

Table 6-8 Aluminum EOS Parameters.

matep	JO
Mat’l Name	“6061-T6_ALUMINUM”
AJO	3.2430E+09 (dynes/cm^2)
BJO	1.1385E+09 (dynes/cm^2)
CJO	0.002
MJO	1.34
NJO	0.42
TJO (Tmelt)	8.188042E-02 (eV)
POISSON	0.33

Table 6-9 Aluminum Strength Parameters.

As detailed previously, the hemispherical expansion simulations were performed and compared against experimental test results for three different high explosives; CompB-GradeA, PBX-9404, and LX-04-01. Each of these high explosives were modeled using the JWL EOS model with no strength model. The JWL materials parameters for each of these four high explosives are provided in Table 6-10 through Table 6-12.

EOS	JWL
EOS_Data ID	“COMPB_GRADEA”
R0	1.717 (g/cm^3)
AG	5.2420E+12 (dynes/cm^2)
BG	7.6780E+10 (dynes/cm^2)
R1	4.2
R2	1.1
WG	0.34
E0	8.5000E+10 (dynes/cm^2)

Table 6-10 CompB-GradeA JWL EOS Parameters.

EOS	JWL
EOS_Data ID	“PBX-9404-3”
R0	1.840 (g/cm^3)
AG	8.5240E+12 (dynes/cm^2)
BG	1.8020E+11 (dynes/cm^2)
R1	4.6
R2	1.3
WG	0.38
E0	1.0200E+11 (dynes/cm^2)

Table 6-11 PBX-9404 JWL EOS Parameters.

EOS	JWL
EOS_Data ID	“LX-04-1”
R0	1.865 (g/cm^3)
AG	8.3640E+12 (dynes/cm^2)
BG	1.2980E+11 (dynes/cm^2)
R1	4.62
R2	1.25
WG	0.42
E0	9.5000E+10 (dynes/cm^2)

Table 6-12 Nitromethane (NM) JWL EOS Parameters.

The CTH input file for the expanding cylinder configuration using the CompB-GradeA high explosive is given in Appendix H for reference.

6.2.3. Convergence Study

To ensure that convergence was achieved for the hemisphere expansion simulations, a mesh refinement study was also performed for this validation test. The test configuration where CompB-GradeA was the high explosive was chosen for this convergence study. Figure 6-8 shows the CTH predicted radial position versus time curves for the CompB-GradeA test configuration. Three different cell sizes (mesh densities) simulation results are shown in this figure. The Level = -1 results are for a square cell sizes of 0.1 cm x 0.1 cm which results in 6.5 cells through the thickness of the aluminum hemisphere. The Level = 0 results are for a cell size of 0.05 cm x 0.05 cm and the Level = +1 results are for a cell size of 0.025 cm x 0.025 cm which results in 13 and 26 cells through the thickness of the aluminum hemisphere, respectively. As can be seen from Figure 6-8 and the magnified inset of Figure 6-8, each of these mesh densities results in nearly identical agreement between the three levels of refinement. From the inset one can see that the Level = -1 results are slightly lower than the Level = 0 and Level = +1 results. Based on the results of this convergence study, the Level = 0 results are considered to be sufficiently converged and used for the each of the subsequent CTH simulations of this validation test case.

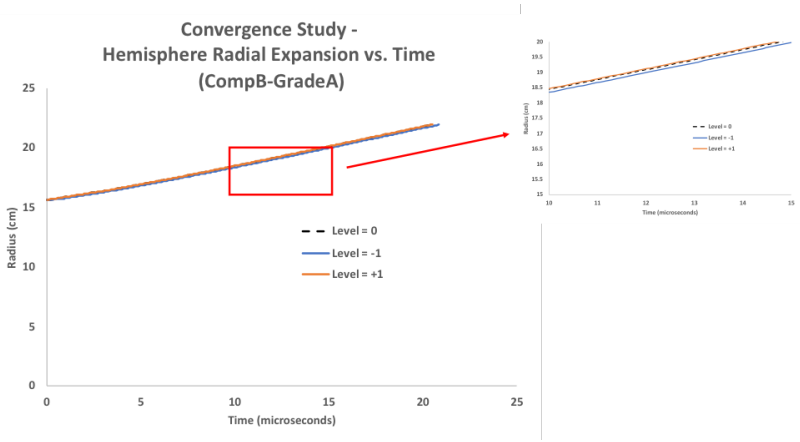

Figure 6-8 CTH Hemispherical Expansion Convergence Study Results using the CompB-GradeA HE.

6.2.4. Results

The experimentally measured radial deformation profile for each validation test along with the corresponding CTH simulations results is shown in Figure 6-9 through Figure 6-11. Specifically, Figure 6-9, Figure 6-10, and Figure 6-11 are shown for CompB-GradeA, PBX-9404, and LX-04-1, respectively. As mentioned previously, the experimental radial expansion values were recorded from a streak camera during testing while the CTH simulations (black dashed lines) were determined from tracer points placed at the outer diameter of the aluminum hemisphere.

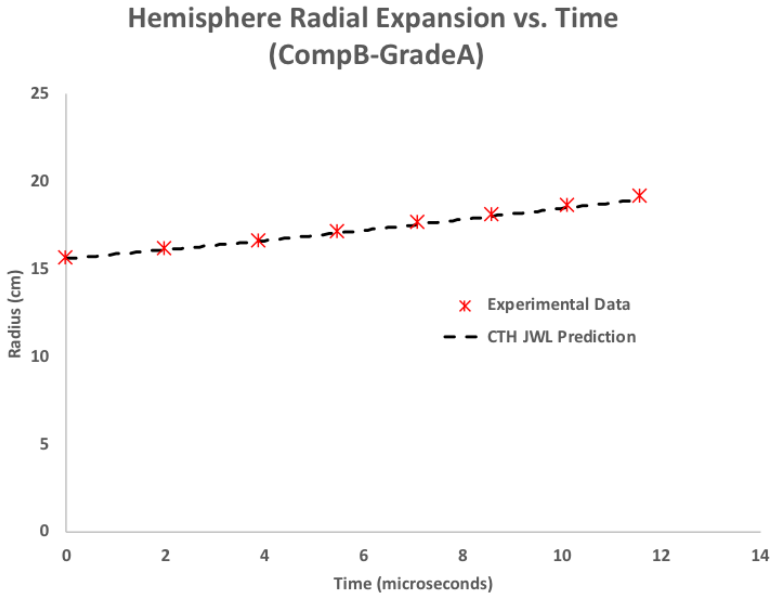

Figure 6-9 Comparison of the Hemispherical Radial Expansion vs. Time for the CompB-GradeA Configuration.

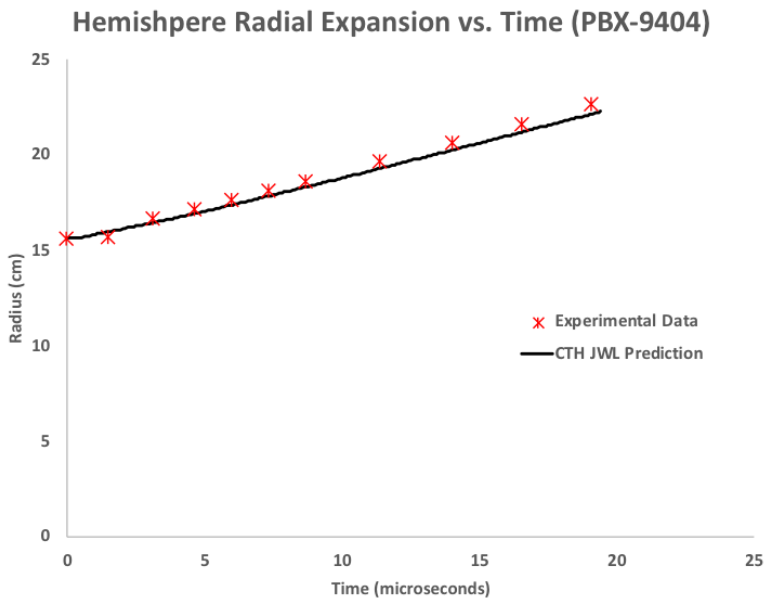

Figure 6-10 Comparison of the Hemispherical Radial Expansion vs. Time for the PBX-9404 Configuration.

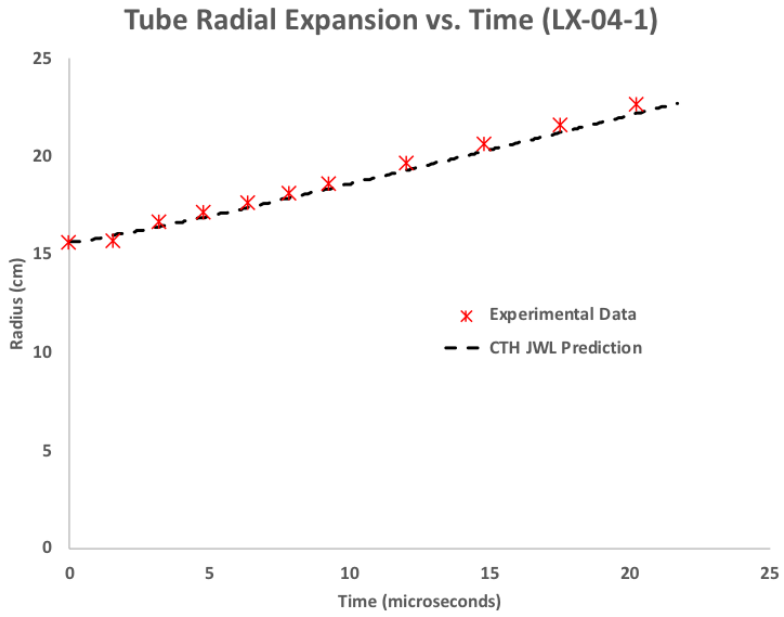

Figure 6-11 Comparison of the Hemispherical Radial Expansion vs. Time for the LX-04-1 Configuration.

From these figures, one can see that the JWL EOS is producing radial expansion results that correlate very well with the experimentally measured expansions. The PBX-9404 and LX-04-1 simulations slightly underpredict the radial expansion of the hemisphere during the later times, but the results are still in very good agreement.

Table 6-7 provides a quantitative measure between the CTH simulation and the experimental test data for each of the three configurations using the Pearson's correlation coefficient (R) [23]. The coefficient values presented in Table 6-7 quantitatively demonstrate that all four simulation results are in excellent agreement with the experimental data, based on each of the correlation coefficients (R) being greater than 0.9. In fact, the correlation coefficients for each of these three simulations are nearly equal to 1.

Test ID	Correlation Coefficient R
CompB-GradeA	0.9999
PBX-9404	0.9991
LX-04-1	0.9991

Table 6-13 Correlation Coefficient for the Hemispherical Expansion Tests.

7. VALIDATION TEST SUITE: SESAME

7.1. SESAME - Validation Test #1: On-Hugoniot and Off-Hugoniot Shock States of Aluminum, Copper, and Tantalum

7.1.1. Description of the Test

The first validation cases considered in this report consist of various flyer plate impact experiments performed by Nellis et al. [22]. The flyer plate configurations tested by Nellis et al. provide multiple levels of Sesame table validation as they consider combinations of aluminum, copper, and tantalum for the flyer, target, and anvil. These tests were also chosen as they probe both the on-Hugoniot and off-Hugoniot states caused by the initial shock and subsequent reshocks or release waves. A basic schematic of the experimental configuration of the test performed by Nellis et al. and simulated in CTH for these validation tests is shown in Figure 7-1.

For this report, we consider six of the twenty configurations tested by Nellis et al. These six configurations were chosen as they represent two conditions each where the target specimen was aluminum (AlTa5, TaAlPt2), copper (CuAl1, CuTa1) and tantalum (TaAl3, TaCu1). Details of the material layout, thickness, and impact velocity for each of the six configurations are provided in Table 7-1. It is noted that the thickness of the flyer plate is not provided and assumed to be much thicker than the target and anvil plate to avoid any free surface release during the time interval of interest.

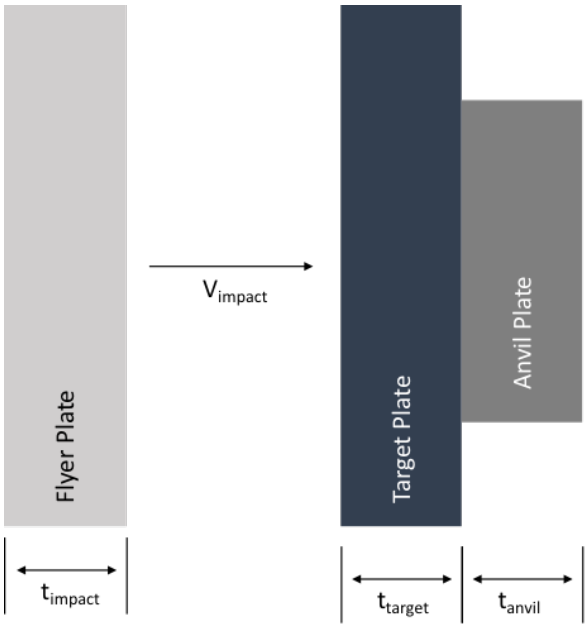

Figure 7-1 Schematic of Flyer Plate Impact Configuration for Validation Test #1 (Nellis et al. [22]).

Test ID	Flyer Velocity (km/s)	Flyer Plate Material	Target Plate Material	Target Plate Thickness (mm)	Anvil Plate Material	Anvil Plate Thickness (mm)
AlTa5	5.197	Al	Al	2.044	Ta	1.542
TaAlPt2	7.931	Ta	Al	1.499	Pt	0.967
CuAl1	6.649	Ta	Cu	1.962	Al	2.003
CuTa1	6.672	Ta	Cu	1.957	Ta	2.010
TaAl3	3.972	Ta	Ta	1.006	Al	1.994
TaCu1	6.638	Ta	Ta	0.974	Cu	2.005

Table 7-1 Selected Experimental Flyer Plate Configurations for Validation Test #1 (Nellis et al. [22]).

7.1.2. Problem Setup and Parameters

The CTH simulations for these flyer plate impact test consisted of two-dimensional (2DR) models with extents designed to capture the nominally plane strain response prior to the arrival of boundary waves or other three-dimensional effects. Specifically, the radial dimensions of the flyer and target plate were modeled as 3.0 cm while the anvil plate had a radius of 2.0 cm. A square mesh was used for the entire domain of the CTH simulation with a cell size of 0.01 mm. This cell size results in roughly 100 cells through the thinnest of any of the components in an attempt to ensure converged simulation results.

EOS	SES
Aluminum (Al)	“ALUMINUM”
Copper (Cu)	“COPPER”
Tantalum (Ta)	“TANTALUM”
Platinum (Pt)	"PLATINUM”

Table 7-2 EOS Models for Validation Test #1.

Material	Strength Model	ID
Aluminum (Al)	JO	“ALUMINUM”
Copper (Cu)	JO	“COPPER”
Tantalum (Ta)	JO	“TANTALUM”
Platinum (Pt)	ST	"PLATINUM”

Table 7-3 Strength Models for Validation Test #1.

Each of the materials used in the six test cases was modeled with the Sesame table EOS within CTH and the Johnson-Cook (JO) strength model [12]. The one exception to this was that the platinum used in test TaAlPt2 was modeled with a Steinberg strength model [28]. The parameters used in the CTH simulations for the Sesame EOS and strength models are given in Table 7-2 and Table 7-3, respectively. For brevity, definitions of the model parameters listed in these tables are not provided. Instead, the reader is referred to the CTH user’s manual [25] for a full definition.

The CTH input file for configuration AlTa5 is given in Appendix I for reference.

7.1.3. Results

Test ID		Pressure #1 (dynes/cm^2)	Particle Velocity #1 (cm/s)	Relative Volume #1	Pressure #2 (dynes/cm^2)	Particle Velocity #2 (cm/s)	Relative Volume #2
AlTa5	Exp	62.22E+10	2.598E+05	0.7069	113.9E+10	1.349E+05	0.6253
	CTH	62.09E+10	2.598E+05	0.7066	111.2E+10	1.333E+05	0.6188
	% Error	0.209%	0.000%	0.042%	2.371%	1.186%	1.040%
TaAlPt2	Exp	208.8E+10	5.849E+05	0.5575	444.0E+10	2.709E+05	0.4443
	CTH	206.1E+10	5.829E+05	0.5550	431.7E+10	2.694E+05	0.4370
	% Error	1.293%	0.342%	0.448%	2.770%	0.554%	1.643%
CuAl1	Exp	329.8E+10	3.82E+05	0.6047	175.5E+10	5.208E+05	-
	CTH	324.4E+10	3.77E+05	0.6077	168.6E+10	5.11E+05	0.7110
	% Error	1.637%	1.309%	0.496%	3.932%	1.882%	-
CuTa1	Exp	331.5E+10	3.831E+05	0.6042	425.8E+10	3.338E+05	0.5811
	CTH	326.1E+10	3.786E+05	0.6070	398.5E+10	3.297E+05	0.5773
	% Error	1.629%	1.175%	0.463%	6.411%	1.228%	0.654%
TaAl3	Exp	195.0E+10	1.986E+05	0.6627	77.13E+10	3.014E+05	-
	CTH	190.6E+10	1.986E+05	0.6556	75.82E+10	2.991E+05	0.8041
	% Error	2.256%	0.000%	1.071%	1.698%	0.763%	-
TaCu1	Exp	422.4E+10	3.319E+05	0.5651	336.5E+10	3.867E+05	-
	CTH	403.0E+10	3.315E+05	0.5448	323.4E+10	3.767E+05	0.5854
	% Error	4.593%	0.121%	3.592%	3.893%	2.586%	-

Table 7-4 Symmetric Impact Results Comparison for Validation Test #1.

Table 7-4 shows the experimentally measured pressure, particle velocity, and relative volume for each of the six test configurations from Nellis et al. [22] considered herein. Also included in this table are the corresponding CTH simulation results for pressure, particle velocity, and relative volume. This table also shows the results for two different states during the impact event. The first state, labeled #1, is the original or Hugoniot shock state in the target material. The second set of state parameters, labeled #2, is for either the re-shock or release of the target material. Specifically, tests AlTa5, TaAlPt2, and CuTa1 are re-shock conditions for state #2 and tests CuAl1, TaAl3, and TaCu1 are release conditions for state #2. The percent error between the experimentally measured shock state and the shock states predicted using CTH and the Sesame table EOS for each of these configurations is also shown in Table 7-4. The percentage error calculations show that the CTH simulations which use the Sesame table EOS model correlate very well with the experimentally measured values for all tests considered. In particular, the CTH simulations using the Sesame table EOS do a good job of capturing not only the shock response, but also the release or re-shock response as well. This serves to validate the model's ability to capture not only the on-Hugoniot shock conditions, but more importantly, the off-Hugoniot points of the release or re-shock. The largest error observed in any of the shock state quantities across the six test configurations was 6.411% with the average error being 1.615%.

7.2. SESAME - Validation Test #2: Flyer Plate Impact on Lithium Flouride (LiF)

7.2.1. Description of the Test

The second validation test case considered in this report is the flyer plate impact experiments performed on lithium fluoride (LiF) by Rigg et al. [24]. The experimental flyer plate configurations of Rigg et al. that are considered in this report are shown in the schematic of Figure 7-2. For these configurations, a nominally 1.3 mm thick tantalum flyer plate which is backed by a thick lexan sabot impacts a nominally 9 mm thick LiF target plate at various impact velocities. For this validation test suite, we consider the six experimental configurations from Rigg et al. [24] that are detailed below in Table 7-5. It is noted that these six configurations were chosen as they were the configuration for which Rigg et al. provided velocity profiles in their publication.

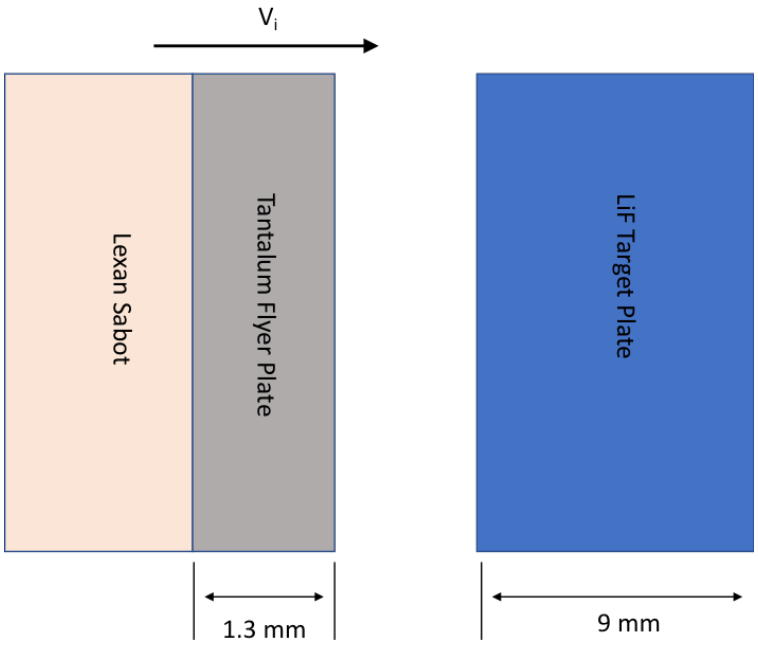

Figure 7-2 Schematic of the Flyer Plate Configuration for Validation Test #2 (Rigg et al. [24]).

Test ID	Flyer Velocity (km/s)
Shot 9	6.016
Shot 8	5.067
Shot 7	4.013
Shot 6	3.200
Shot 5	2.840
Shot 2	2.509

Table 7-5 Experimental Flyer Plate Configurations for Validation Test #2 (Rigg et al. [24]).

7.2.2. Problem Setup and Parameters

The CTH simulations for this validation test consisted of two-dimensional (2DR) models with extents designed to capture the nominally plane strain response prior to the arrival of boundary waves or other three-dimensional effects. Specifically, the radial dimensions of the flyer and target plate were modeled as 3.0 cm. A rectangular mesh was used for the entire domain of the CTH simulation with a cell size of 0.01 mm along the axis of impact and 0.2 mm in the radial direction. This cell size results in 130 cells through the thickness of the flyer plate and 900 cells through the thickness of the LIF target plate in an attempt to ensure converged simulation results.

Within the CTH models, the tantalum and LIF materials were both modeled using the Sesame table (SES) EOS model, while the lexan sabot was modeled using the Mie-Grüneisen (MGR) equation of state. The Johnson-Cook (JO) visco-plastic constitutive model [12] was used for the tantalum flyer plate and the Lexan sabot, while the Steinberg (ST) strength model [28] was used for the LIF target material. The Sesame EOS model inputs for the tantalum flyer plate and the LIF target plate are given below in Table 7-6, while the MGR EOS parameters for the Lexan sabot are given in Table 7-7. Finally, the strength parameters for all three of the materials are given in Table 7-8. For brevity, definitions of the model parameters listed in these tables are not provided. Instead, the reader is referred to the CTH user's manual [25] for a full definition.

Material	EOS	ID
Tantalum	SES	"TANTALUM"
Lithium Fluoride	SES	"LIF"

Table 7-6 Flyer and Target Plate SES EOS Models for Validation Test #2.

EOS	mgr
EOS_Data ID	"USER"
ro	1.196 (g/cc)
C_s	2.33 (km/s)
S_1	1.57
g0	0.61
C_v	1.39E+11 (erg/g/eV)

Table 7-7 Lexan Sabot EOS Parameters for Validation Test #2.

Material	Strength Model	ID
Lexan	JO	"LEXAN"
Tantalum	ST	"TANTALUM"
Lithium Fluoride	JO	"LIF"

Table 7-8 Strength Models for Validation Test #2.

The CTH input file for Shot #9 is given in Appendix J for reference.

7.2.3. Results

Figure 7-3 shows both the "corrected" experimentally measured particle velocity profiles for each of the six test configurations of Rigg et al. [24] and the corresponding velocity profiles for the CTH simulations which used the Sesame table entry for the tantalum and LiF materials. The experimental particle velocity results (solid lines) were each measured at the back face of the LIF target plate using a VISAR probe. The velocity profiles from the CTH simulations (dashed lines) are the calculated particle velocity at the target free surface. It is noted that both the experimental and simulation data have been shifted in this figure to show corresponding impact times that are incrementally shifted for the purpose of plotting. It is important to note here that the original velocity profiles presented in Rigg et al. [24] are for the "uncorrected" or apparent particle velocity traces. In order to correct for the refractive index of the LiF, Rigg et al. [24] determined the relationship given in Equation (32).

$$u_{\text{corrected}} = 0.7827 * u_{\text{apparent}}^{0.9902} \tag{32}$$

This "corrected" experimental particle velocity profile is what is plotted in Figure 7.

Figure 7-3 shows that the CTH predictions which use the Sesame Table (SES) EOS model correlate very well with the experimentally measured velocity profiles for each of these configurations. In particular, the Sesame EOS model does a good job of capturing not only the shock response, but the release response as well, validating the model's ability to capture the on-Hugoniot and off-Hugoniot conditions. being greater than 0.9.

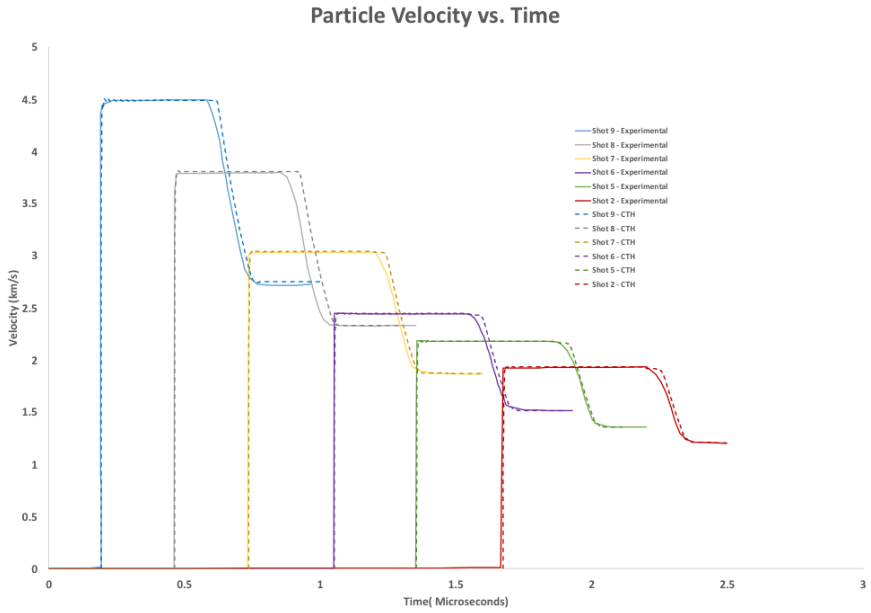

Figure 7-3 Comparison of "Corrected" Particle Velocity Histories for Validation Test #2 (Rigg et al. [24]).

There are a few minor discrepancies observed between the CTH simulations and the experimental data in Figure 7-3 during the release portion of the signals. These differences are in the timing of the release wave which is most likely a result of using the nominal thicknesses provided by Rigg

Test ID	Correlation Coefficient R
Shot 9	0.9954
Shot 8	0.9467
Shot 7	0.9966
Shot 6	0.9955
Shot 5	0.9984
Shot 2	0.9949

Table 7-9 Correlation Coefficient for the Validation Test #2.

et al. [24] rather than the exact thicknesses. These minor differences, especially in Shot 8, are also seen in the values of Table 7-9 which provide a quantitative measure between the CTH simulation and the experimental test data for each of the four configurations using the Pearson's correlation coefficient (R) [23]. Even with these minor differences, the coefficient values presented in Table 7-9 quantitatively demonstrate that all six simulation results are in good agreement with the experimental data, based on each of the correlation coefficients (R)

8. CONCLUSION

Establishing code credibility for CTH is essential in light of its importance to several different mission spaces, including NW work. The concerted effort of the past couple years to overhaul CTH's SQE and V&V processes has been aimed at addressing this need. The significant improvement in CTH's ratings in the most recent ASC appraisal [29] bear out the success of these efforts, but much remains to be done. The new V&V test suite assembled in FY19 [6] has been expanded in FY20 to cover more models and physics capabilities. V&V tests have been added for two commonly used equation of state models and two verification problems have been added from the Tri-Lab Test Suite and the Enhanced Tri-Lab Test Suite.

The first equation of state (EOS) model considered was the Jones-Wilkins-Lee (JWL) model in CTH. Both verification and validation test problems were added to the test suite. The verification problem is the one-dimensional Riemann shock tube problem using two different high explosives under different initial conditions. CTH results for both explosives are in nearly identical agreement with the analytical solution and provide good verification of the implementation of the JWL EOS model in CTH. The first validation problem is an expanding cylinder test where four different high explosives and their corresponding JWL EOS parameters were validated. Results of this validation test show excellent agreement between the experimental data and the simulation predictions. Finally, the last validation problem consisted of an expanding hemisphere using three different high explosives and their JWL EOS. Similar to the expanding cylinder validation tests, these CTH simulations were again in excellent agreement with the experimental results.

Verification and validation tests were also added for the Sesame Table (SES) EOS model in CTH. For the first verification test, comparisons are made between simple CTH symmetric flyer plate impact simulations using the Sesame table EOS and the BCAT code for multiple materials and induced shock states. For the second verification test, a simple user-defined analytical Sesame table was generated and used to verify the simulation results from the CTH implementation of the Sesame tables. Two validation test cases were also presented. The first of which compared the on-Hugoniot and off-Hugoniot conditions resulting from impact tests involving copper, aluminum, tantalum, and platinum. The CTH simulations for these tests all show excellent agreement with the experimental data. Finally, the second validation case compared the simulated particle velocity time history in a lithium fluoride (LiF) material using the Sesame table EOS against experimental data. Again, excellent agreement is observed between the CTH simulations which used the Sesame table EOS and the experimental data.

The Blake [2] verification problem, from the Tri-Lab Test Suite, was also added to the V&V test suite. The Blake problem, which mimics the scenario of an embedded explosive source, tests a code's ability to calculate elastic wave propagation in the absence of boundary reflections [4]. For the CTH simulation, the elastic material is modeled with the EPPVM strength model, with the yield strength set high enough to ensure that no plastic strain is accumulated. Simulation results showed good agreement with the analytic solution with convergence rates of roughly 2/3 for the entire region outside the cavity ($r > 11$ cm) and nearly first-order for the region 15 cm $< r <$ 85 cm. Similar codes exhibit convergence rates of roughly 1/2 for the region outside the cavity and 1 for the restricted region: 15 cm $< r <$ 85 cm.

The other verification problem added to the test suite in FY20 is the Mader problem, the linear-elastic analog to the Hunter problem from the Enhanced Tri-Lab Test Suite. The Mader problem, which models a detonation wave propagating through a slab of explosive, tests a code's ability to capture the Chapman-Jouget state at the detonation front and the rarefaction behind the burn front [4]. For the CTH simulation, both the unreacted explosive and the reaction products are modeled as γ-law gases and the detonation is modeled using the HEBURN (High Explosive Burn) model. The Mader problem has demonstrated a susceptibility to spurious oscillations behind the rarefaction wave and a lag in the position of the simulated detonation wave. Convergence rates for this problem are slightly less than half-order - lower than expected, a fact which should be explored further in order to determine the cause(s).

There are several test coverage gaps which have been prioritized for FY21. First, there is a lack of V&V tests for fracture models. This feature is commonly used, so adding testing for it is a high priority. Specifically, there are plans to add V&V tests for both the Johnson-Cook fracture (JFRAC) and Grady-Kipp fracture model in FY21. Likewise, there are plans to add validation tests of the Steinberg-Guinan-Lund (ST) plasticity model, a commonly exercised strength model. Adding verification tests for boundary conditions is another priority for FY21. Despite the fact that boundary conditions can greatly influence a simulation, currently there are few tests that explicitly test boundary conditions, making this a high priority. Continued evaluation of test coverage gaps and addressing those needs will allow us to build up a robust V&V test suite to ensure continued code quality and credibility for CTH.

REFERENCES

[1] W. BAILEY, R. BELCHER, D. CHILVERS, AND G. EDEN, *Explosive equation of state determination by the awre method*, 7th Symposium (International) on Detonation, (1981), pp. 304–311.

[2] F. BLAKE JR, *Spherical wave propagation in solid media*, The Journal of the Acoustical Society of America, 24 (1952), pp. 211–215.

[3] J. BROCK, J. KAMM, W. RIDER, S. BRANDON, C. WOODWARD, P. KNUPP, AND T. TRUCANO, *Verification test suite for physics simulation codes*, tech. rep., Lawrence Livermore National Lab.(LLNL), Livermore, CA (United States), 2006.

[4] S. W. DOEBLING, *Standardized definitions for code verification test problems*, tech. rep., Los Alamos National Lab.(LANL), Los Alamos, NM (United States), 2017.

[5] S. W. DOEBLING, J. L. BUDZIEN, J. M. FERGUSON, M. L. HARWELL, K. S. HICKMANN, D. M. ISRAEL, W. R. MAGROGAN III, R. SINGLETON JR, G. SRINIVASAN, J. W. WALTER JR, ET AL., *Code verification capabilities and assessments in support of asc v&v level 2 milestone# 6035*, tech. rep., Los Alamos National Lab.(LANL), Los Alamos, NM (United States), 2017.

[6] G. C. DUNCAN AND C. T. KEY, *Progress towards a new CTH code verification & validation test suite (SAND2019-12020)*, tech. rep., Sandia Technical Report, 2019.

[7] S. L. (EDITOR) AND J. J. (EDITOR), *SESAME: The los alamos national laboratory equation of state database, LA-UR-92-3407*, tech. rep., Los Alamos National Laboratory (LANL), Group T-1, Los Alamos, NM, 1992.

[8] W. FICKETT AND W. C. DAVIS, *Detonation*, University of California Press, Berkeley, CA, 1979.

[9] L. FRIED AND P. SOUERS, *CHEETAH: A next generation thermochemical code (UCRL-ID-117240)*, tech. rep., Lawrence Livermore National Laboratory (LLNL), Livermore, CA, 1994.

[10] E. HERTEL AND G. KERLEY, *CTH reference manual: The equation of state package (SAND98-0947)*, tech. rep., Sandia National Laboratories, Albuquerque, NM, 1998.

[11] W. M. HILBUN AND R. L. BELL, *Energy transport in a shock physics code (SAND2011-3890)*, tech. rep., Sandia Technical Report, 2011.

[12] G. JOHNSON AND W. COOK, *A constitutive model and data for metals subjected to large strains, high strain rates and high temperatures*, Proceeding of the Seventh International Symposium on Ballistics, The Hague, The Netherlands, (1983).

[13] H. JONES AND A. MILLER, *The detonation of solid explosives*, Proceedings of the Royal Society of London, A-194 (1948).

[14] J. R. KAMM, *Analysis of the blake and hunter problems with the sage code (LA-UR-08-06050)*, tech. rep., Los Alamos National Laboratory (LANL), Los Alamos, NM, 2008.

[15] J. R. KAMM, J. S. BROCK, S. T. BRANDON, D. L. COTRELL, B. JOHNSON, P. KNUPP, W. J. RIDER, T. G. TRUCANO, AND V. G. WEIRS, *Enhanced verification test suite for physics simulation codes*, tech. rep., Los Alamos National Laboratory (LANL), Los Alamos, NM, 2008.

[16] G. KERLEY AND C. . D. TEAM, *BCAT user's manual and input instructions, version 1.30*, tech. rep., Sandia National Laboratories, Albuquerque, NM, 2015.

[17] I. LAN AND J. S. S. HUNG, C. CHEN ND Y. NIU, *An improved simple method of deducing jwl parameters from cylinder expansion test*, Propellants, Explosives, Pyrotechnics, 18 (1993), pp. 18–24.

[18] B. LEE, E. TORO, C. CASTRO, AND N. NIKOFORAKIS, *Adaptive osher-type scheme for euler equations with highly nonlinear equations of state*, J. Comput. Phys., 246 (2013), pp. 165–182.

[19] E. LEE, H. HORNIG, AND J. KURY, *Adiabatic expansion of high explosive detonation products (UCRL-50422)*, tech. rep., Lawrence Radiation Laboratory, University of California, 1968.

[20] E. LEE, R. MCGUIRE, D. BREITHAUPT, N. PARKER, J. WALTON, M. FINGER, AND W. V. HOLLE, *UCRL-89846*, tech. rep., Lawrence Radiation Laboratory, University of California, 1983.

[21] J. M. MCGLAUN, S. THOMPSON, AND M. ELRICK, *CTH: a three-dimensional shock wave physics code*, International Journal of Impact Engineering, 10 (1990), pp. 351–360.

[22] W. NELLIS, A. MITCHELL, AND D. YOUNG, *Equation-of-state measurements for aluminum, copper and tantalum in the pressure range 80-440 gpa (0.8-4.4 mbar)*, Journal of Applied Physics, 93 (2003), pp. 304–310.

[23] K. PEARSON, *Notes on regression and inheritance in the case of two parents*, Proceedings of the Royal Society of London, 58 (1895), pp. 240–242.

[24] P. RIGG, M. KNUDSON, R. SCHARFF, AND R. HIXSON, *Determining the refractive index of shocked [100] lithium fluoride to the limit of transmissibility*, Journal of Applied Physics, 116 (2014).

[25] R. SCHMITT, A. BRUNDAGE, D. CRAWFORD, E. HARSTAD, K. RUGGIRELLO, S. SCHUMACHER, AND J. SIMMONS, *CTH user's manual and input instructions version 11.2*. unpublished, 2016.

[26] K.-M. SHYUE, *A fluid-mixture type algorithm for compressible multicomponent flow with mie-grüneissen equation of state*, J. Comput. Phys, 171 (2001), pp. 688–707.

[27] R. SINGLETON JR, D. M. ISRAEL, S. W. DOEBLING, C. N. WOODS, A. KAUL, J. W. WALTER JR, AND M. L. ROGERS, *Exactpack documentation (LA-UR-16-23260)*, tech. rep., Los Alamos National Laboratory (LANL), Los Alamos, NM, 2016.

[28] D. STEINBERG, S. COCHRAN, AND M. GUINAN, *A constitutive model for metals applicable at high strain rate*, Journal of Applied Physics, 51 (1980), p. 1498.

[29] A. A. TEAM, *FY2020 ASC appraisal results report*. available on request, 2020.

[30] F. TIMMES, B. FRYXELL, AND G. HRBEK, *Spatial-temporal convergence properties of the tri-lab verification test suite in 1d for code project a (LA-UR-06-6444)*, tech. rep., Los Alamos National Laboratory (LANL), Los Alamos, NM, 2006.

[31] F. X. TIMMES, G. GISLER, AND G. M. HRBEK, *Automated analyses of the tri-lab verification test suite on uniform and adaptive grids for code project a (LA-UR-05-6865)*, tech. rep., Los Alamos National Laboratory (LANL), Los Alamos, NM, 2005.

[32] R. VON MISES, *Mechanik der festen körper im plastisch deformablen zustand*, Göttin, Nachr. Math. Phys., 1 (1913), pp. 582–592.

[33] M. WILKINS, *The equation of state of pbx 9404 and lx04-01 (UCRL-7797)*, tech. rep., Lawrence Radiation Laboratory, University of California, 1964.

APPENDIX A. CTH INPUT FILE FOR BLAKE VERIFICATION TEST

```
*CTHid SPYPLT SPYHIS
**************************************************************************
*  CTH input deck for 1DS Blake problem calculation
*
*  The problem description that follows is taken from [1]:
*
*  The Blake verification problem [2] is based on the analytic solution to
*  the problem of a uniform infinite elastic medium with a spherical
*  cavity centered at the origin [3]. A time-dependent pressure is applied
*  to the inner boundary of the cavity, causing it to expand and a wave to
*  propagate through the elastic material. When the pressure in the cavity
*  is a simple step function, as is the case in the version of the problem
*  implemented here, the Blake problem approximates the scenario of
*  an embedded explosive source [4].
*
*  The Blake problem is one of the few dynamic strength of materials
*  problems that has a closed-form solution, and as such it is a traditional
*  hydrocode verification problem [3]. It tests small strain linear
*  elasticity [5]. Specifically, it tests the code's ability to simulate
*  wave propagation for outgoing, spherically divergent elastic
*  waves [4].
*
*  The problem is initialized as a stationary, unstressed isotropic
*  linear-elastic material, with the domain selected such that the elastic
*  wave front will not reach the edge of the domain before t_final [4].
*  At time t=0, a uniform pressure p_0 is applied to the inside of the
*  cavity wall. To ensure that no plastic strain is accumulated, the
*  elastic material is given an unattainably high yield strength [5].
*  The material filling the cavity is identical to the elastic medium,
*  except that it has zero strength.
*
*  Parameter values for this input deck match [4].
*  Problem parameter values are given below:
*
*  Parameters:
*  t_final = 1.6e-4 sec,
*  cavity_radius = 10cm
*  gamma = 1. + 1.0e-4,
*  rho_0 = 3.0 g/cc,
*  p_0 = 1e7 dynes/cm^2,
*  Shear modulus = 2.5e11,
*  Poisson's ratio = 0.25,
```

```
*  C_e = 5.0e5 cm/s
*
*  [1] G.C. Duncan-Reynolds and C.T. Key, FY20 Improvements to the New CTH
 ↪  Code Verification & Validation Test Suite, tech. rep., Sandia Technical
 ↪  Report, 2020.
*  [2] F. BLAKE JR, Spherical wave propagation in solid media, The Journal
 ↪  of the Acoustical Society of America, 24 (1952), pp. 211–215.
*  [3] S. W. DOEBLING, J. L. BUDZIEN, J. M. FERGUSON, M. L. HARWELL, K. S.
 ↪  HICKMANN, D. M. ISRAEL, W. R. MAGROGAN III, R. SINGLETON JR, G.
 ↪  SRINIVASAN, J. W. WALTER JR, Code verification capabilities and
 ↪  assessments in support of ASC V&V level 2 milestone# 6035, tech. rep.,
 ↪  Los Alamos National Lab.(LANL), Los Alamos, NM, 2017.
*  [4] S. W. DOEBLING, Standardized definitions for code verification test
 ↪  problems, tech. rep., Los Alamos National Lab.(LANL), Los Alamos, NM
 ↪  (United States), 2017.
*  [5] J. R. KAMM, Analysis of the Blake and Hunter problems with the Sage
 ↪  code (LA-UR-08-06050), tech. rep., Los Alamos National Laboratory
 ↪  (LANL), Los Alamos, NM, 2008.
*
**************************************************************************
*eor* cthin
**************************************************************************
*
Blake Problem
*
**************************************************************************
*
control
  mmp0
  tstop =  1.6e-4
endcontrol
*
*-------------------------------------------------------------------------
*
mesh
  block 1  geom=1ds    type=e
    x0  0.0
      x1  n=120  w=120.0 rat=1.0
    endx
  endb
endmesh
*
*-------------------------------------------------------------------------
*
spy
```

```
  Save("VOLM,P,M,PM,IE");

  define spyplt_main()
  {
    pprintf(" PLOT: Cycle=%d, Time=%e\n",CYCLE,TIME);

  }

  SaveHis("GLOBAL,P,DENS,IE,VX,J2P,XXSTRESS,YYSTRESS,ZZSTRESS,
   ↪  PSR,STS11,STN11,Q1");
  SaveTracer(ALL);
  HisTime(0,1e-10);

  define spyhis_main()
  {
    HisLoad(1,"hscth");
  }
endspy
*
*-------------------------------------------------------------------------
*
diatoms
  package 'Cavity/Source'
    material 2
    iteration 4
    dens = 3.0
    press = 1.0e7
    t = t3 *0.025
    insert box
      p1 0.0     p2  10.0
    endinsert
  endpackage
  package 'Perfectly Elastic Region'
    material 1
    iteration 4
    dens = 3.0
    *press = 0.0
    t = 0.025
    insert box
      p1 10.0     p2  1.e3
    endinsert
  endpackage
enddiatoms
*
*-------------------------------------------------------------------------
```

```
*
tracer
  add 0.0 to 100.00 n=200 fix=x
endt
*
*----------------------------------------------------------------------
*
deftable=3 name='table for cavity driving temperature'
  uvar='time'
  vvar='temperature'
  interpolation=linear
  uscale=1.e-4,0
*  time (1e-4 s)  cavity temperature (eV)
    0              0.025
    1.6            0.025
enddeftable
*
*----------------------------------------------------------------------
*
eos
*  material 1: Elastic medium
  mat1   mgrun   user G0=1.e-4  cv=1.0e12  r0=3.0  T0=0.025  cs=3.72678e5
   ↪  ce=5.0e5
*  material 2: Cavity/Source
  mat2   idgas   user gm1=1.e-4 r0=3.0 T0=0.025 cv=1.333333e12
endeos
*
*----------------------------------------------------------------------
*Poisson's ratio: nu=lambda/(2(lambda+mu)), lambda=First Lame Modulus
*mu=Shear Modulus
*lambda=2.5e+11, mu=2.5e+11, so nu=0.25
*
epdata
*  material 1: Elastic medium
matep = 1 , eppvm = user, yield = 1.e18, poisson = 0.25, csmin = 3.72678e5
* material 2: Cavity/Source (no strength)
lstrain
vpsave
endep
*
*----------------------------------------------------------------------
*
convct
  convection = 2
  interface = high
```

```
endc
*
*-------------------------------------------------------------------------
*
edit
  shortt
    tim = 0.0 , dt = 1.0
  ends

  longt
    tim = 0.0 , dt = 1.0
  endl

  plott
    tim =   0.,  dt = 10e-3
  endp
ende
*
*-------------------------------------------------------------------------
*
fracts
  pfrac1 =  -1.0e18
endf
*
*-------------------------------------------------------------------------
*
boundary
  bhy
    bxb = 0 , bxt = 1
  endh
endb
*
*************************************************************************
```

APPENDIX B. CTH INPUT FILE FOR JWL VERIFICATION TEST #1: RIEMANN SHOCK TUBE

```
clear*******************************************************************
*******************************************************************
* Problem Description:
*
* 1DR representation of an HMX shock tube (Riemann) problem
* Left State: Rho=1.7 Vel=0.0 Press=10.0 MBar
* Right State: Rho=1.0 Vel=0.0 Press=0.5 MBar
* The final states for comparison with the closed form solution are
* taken at 20 microseconds.
*
* Experimental Data Reference:
*
* Shyue, K.-M. "A Fluid-Mixture Type Algorithm for Compressible
* Multicomponent Flow with Mie- Gruneissen Equation of State", J.
* Comput. Phys 171:688-707 (2001)
*
*******************************************************************
*eor* cthin
*******************************************************************
*
1DR HMX Riemann Problem (Shock Tube)
*
*******************************************************************
*
*    CONTROL RECORDS
*
control
  mmp0
  tstop =  12.0e-6
  hashs = 1000000
endcontrol
*
*******************************************************************
*
*    FLAT MESH RECORDS
*
mesh
  block 1  geom=1dr    type=e
    x0  0.0
      x1  n=2000   dxf=0.01    w=100.0
    endx
```

```
    xact = 0.0,100.0
  endb
endmesh
*
%%%%%%%%%%%%%%%%%%%%% Spy %%%%%%%%%%%%%%%%%%%%%%%
%
spy
  Save("VOLM,P,M,EM,VOID,VX");
  SaveTime(0,1.25e-7);
  PlotTime(0,2.5e-7);
  ImageFormat(1024,768);
%
  define main()
    {
      pprintf(" PLOT: Cycle=%d, Time=%e\n",CYCLE,TIME);
      Image("Pres");
        Window(0,0,0.75,1);
        Label(sprintf("Materials at %0.2e s.",TIME));
        Plot1D("P",ON,ON,"Press");
      EndImage;
      Image("Dens");
        Window(0,0,0.75,1);
        Label(sprintf("Materials at %0.2e s.",TIME));
        Plot1D("DENS",ON,ON,"Dens");
      EndImage;
      Image("Velocity");
        Window(0,0,0.75,1);
        Label(sprintf("Materials at %0.2e s.",TIME));
        Plot1D("VX",ON,ON,"Vel");
      EndImage;
      Image("Energy");
        Window(0,0,0.75,1);
        Label(sprintf("Materials at %0.2e s.",TIME));
        Plot1D("EM+1",ON,ON,"Energy");
      EndImage;
    }
%
  SaveHis("GLOBAL,P,VX,EM,TK");
  SaveTracer(ALL);
  HisTime(0,5e-10);
%
  define spyhis_main()
  {
    HisLoad(1,"hscth");
%
```

```
  }
endspy
*
**********************************************************************
*
*    DIATOM MATERIAL INSERTION RECORDS
*
diatoms
  package 'gas #1'
    material 1
    iterations 5
    xvel 0.0
    pres = 1.0e13
    dens = 1.7
    insert box
      p1 0.     p2  50.0
    endinsert
  endpackage
  package 'gas #2'
    material 1
    iterations 5
    xvel 0.0
    pres = 5.0e11
    dens = 1.0
    insert box
      p1 50.     p2  100.0
    endinsert
  endpackage
enddiatoms
*
**********************************************************************
*
*      TRACER RECORDS
*
tracer
  add=4.0
  add=4.5
endt
*
**********************************************************************
*
*    EOS RECORDS
*
eos
  mat1   jwl TNT R0=1.84 WG=0.25 AG=8545e9 BG=205e9 R1=4.6 R2=1.35 E0=1.7e12
```

```
  mat2   jwl TNT R0=1.84 WG=0.25 AG=8545e9 BG=205e9 R1=4.6 R2=1.35 E0=1.7e12
endeos
*
**************************************************************************
*
*    CONVECTION RECORDS
*
convct
  convection = 1
  interface = high
endc
*
**************************************************************************
*
*    EDIT RECORDS
*
edit
  shortt
    tim = 0.0, dt = 1.0
  ends

  longt
    tim = 0.0, dt = 1.0
  endl
ende
*
**************************************************************************
*
*    FRACTURE RECORDS
*
fracts
  pfrac1 =  -1.0e15
  pfrac2 =  -1.0e15
endf
*
**************************************************************************
*
*    BOUNDARY CONDITION RECORDS
*
boundary
  bhy
    bxb = 0, bxt = 0
  endh
endb
*
```

****

APPENDIX C. CTH INPUT FILE FOR MADER VERIFICATION TEST

```
 *CTHid SPYPLT SPYHIS
************************************************************************
*  CTH input deck for 1DR Mader problem calculation
*
*  The problem description that follows is taken from [1]:
*
*  The Mader problem is based on the simplest detonation theory, as laid
*  out in Section 2A of Fickett and Davis [2]. It is characterized by a
*  one-dimensional steady detonation front, driven by a piston, followed
*  by a rarefaction wave. The chemical reaction is assumed to
*  instantaneously burn to completion so that the reaction products
*  emerge from the front at equilibrium [3]. From the moment of
*  initiation, the detonation wave travels at constant velocity,
*  generating a self-similar flow between it and the piston [2].
*
*  The problem setup is as follows. A piston-driven detonation wave
*  propagates through a 5 cm slab of high explosive (HE), which is modeled
*  as a gamma-law gas, with gamma=3, for both the unreacted explosive and
*  the reaction products. In order to use the HEBURN model, this is
*  implemented by using the JWL equation of state with the parameters AG
*  and BG set to 0, effectively reducing the JWL EOS to the Ideal Gas EOS.
*  For the Mader problem, the piston is assumed to be stationary. Because
*  of this, the head of the rarefaction stays at the detonation front and
*  the tail is halfway between the front and the piston [4]. The density of
*  the HE is taken to be 1.875 g/cm^3 and the temperature is 0.025 eV. The
*  Chapman-Jouget (CJ) detonation speed is 0.8 cm/us, so that the detonation
*  reaches the other edge of the HE (at x=0) in 6.25 us.
*
*  The Mader problem provides a test of how well a code captures the CJ
*  state at the detonation front and the rarefaction behind the front [5].
*
*
*  Parameter values for this input deck match [5].
*  Problem parameter values are given below:
*
*  Parameters:
*  t_final = 6.25e-6 sec,
*  gamma = 3,
*  D_cj = 0.8 cm/us
*  q = 4e10 erg/g
*  rho_0 = 1.875 g/cc,
*  u_0 = -v_piston = 0,
```

```
*  p_0 = 0.0 dyn/cm^2,
*
*  [1] G.C. Duncan-Reynolds and C.T. Key, FY20 Improvements to the New CTH
 ↪  Code Verification & Validation Test Suite, tech. rep., Sandia Technical
 ↪  Report, 2020.
*  [2] W. FICKETT AND W. C. DAVIS, Detonation, University of California
 ↪  Press, Berkeley, CA, 1979.
*  [3] R. SINGLETON JR, D. M. ISRAEL, S. W. DOEBLING, C. N. WOODS, A. KAUL,
 ↪  J. W. WALTER JR, AND M. L. ROGERS, Exactpack documentation
 ↪  (LA-UR-16-23260), tech. rep., Los Alamos National Laboratory (LANL), Los
 ↪  Alamos, NM, 2016.
*  [4] F. X. TIMMES, G. GISLER, AND G. M. HRBEK, Automated analyses of the
 ↪  Tri-Lab verification test suite on uniform and adaptive grids for code
 ↪  project A (LA-UR-05-6865), tech. rep., Los Alamos National Laboratory
 ↪  (LANL), Los Alamos, NM, 2005.
*  [5] S. W. DOEBLING, Standardized definitions for code verification test
 ↪  problems, tech. rep., Los Alamos National Lab.(LANL), Los Alamos, NM
 ↪  (United States), 2017.
*
*************************************************************************
*eor* cthin
*************************************************************************
*
Mader Problem
*
*************************************************************************
*
control
  mmp0
  tstop =  6.25e-6
endcontrol
*
*------------------------------------------------------------------------
*
mesh
  block 1  geom=1dr    type=e
    x0  0.0
      x1  n=100  w=5.0  rat=1.0  * dx=0.05
    endx
  endb
endmesh
*
*------------------------------------------------------------------------
*
spy
```

```
  Save("VOLM,P,M,PM,IE");

  define spyplt_main()
  {
    pprintf(" PLOT: Cycle=%d, Time=%e\n",CYCLE,TIME);

  }

  SaveHis("GLOBAL,P,DENS,IE,VX,VY,VZ");
  SaveTracer(ALL);
  HisTime(0,1e-9);

  define spyhis_main()
  {
    HisLoad(1,"hscth");
  }
endspy
*
*-------------------------------------------------------------------------
*
diatoms
  package 'Unreacted HE'
    material 1
    iteration 4
    dens = 1.875
    press = 1.0e6
    vel = 0.0 * v_piston = 0.0 cm/s
    insert box
      p1 0.00     p2  5.00
    endinsert
  endpackage
enddiatoms
*
*-------------------------------------------------------------------------
*
heburn
  material = 1
    detonation_velocity = 8.0e5
    q = 4.0e10
  dpoint = 5.0
  time = 0.0
  radius = 0.05
endheburn
*
*-------------------------------------------------------------------------
```

```
*
tracer
  add 0.00 to 5.0 n=500 fix=x
endt
*
*-----------------------------------------------------------------------
*
eos
  mat1  jwl  tnt  brn=1  r0=1.875  wg=2.0  ag=0.  bg=0.  * Use JWL in order
   ↪  to use heburn, but choose coefficients such that the HE is essentially
   ↪  a gamma-law ideal gas
  mat2 ses air
endeos
*
*-----------------------------------------------------------------------
*
convct
  convection = 1
  interface = high
endc
*
*-----------------------------------------------------------------------
*
edit
  shortt
    tim = 0.0 , dt = 1.0
  ends

  longt
    tim = 0.0 , dt = 1.0
  endl

  plott
    tim =   0.,  dt = 10e-9
  endp
ende
*
*-----------------------------------------------------------------------*
*
boundary
  bhy
     bxb = 1,  bxt = 0
  endh
endb
*
```

****

APPENDIX D. CTH INPUT FILE FOR SESAME VERIFICATION TEST #1: SYMMETRIC LEAD FLYER PLATE IMPACT

```
*CTHid SPYPLT SPYHIS
*eor*cthin
*
 2DR Symmetric Impact - SES Verification #1
* ***************************************************************
* Problem Description:
*
* 2DR representation of a symmetric flyer plate impact test on Lead.
* The flyer plate and target plate are each 0.4 cm thick and the
* impact velocity of the flyer plate is 0.5 km/s
*
*********************************************************************
*
*    CONTROL RECORDS
*
control
  tstop = 2.e-6
  tbad 1E30
  mmp0
  rdumpf = 86400.  *backup restart dump frequency, in seconds
endcontrol
*
*********************************************************************
*
*    FLAT MESH RECORDS
*
mesh
  block geometry=2dr
   x0=-3.01
    x1 dxf=0.001 dxl=0.001 w=3.01
   endx
   y0=0.0
    y1 dyf=0.02 dyl=0.02 w=0.5
   endy
   xact = -2. 0.
   yact = -15. 15.
  endb
endmesh
*
*********************************************************************
*
```

```
*    BOUNDARY CONDITION RECORDS
*
boundary
 bhydro
  bxbot 2 *allow mass to leave
  bxtop 2 *allow mass to leave
  bybot 3 *inflow-extrapolated
  bytop 3 *inflow-extrapolated
 endh
endb
*
*-------------------------------------------------------------
%%%%%%%%%%%%%%%%%%%%%%%% Spy %%%%%%%%%%%%%%%%%%%%%%%%%%%%
%
spy
% 256 Character Line Limit for Spy ...
  Save("VOID,M,VOLM,VX,VY,P,PM,DENS,T,CS,EM");
 SaveTime(0, 0.01e-6);
 PlotTime(0, 0.05e-6);
 ImageFormat(1024,768);
%
 SaveHis("VOID,M,VOLM,VX,VY,P,PM,DENS,T,CS,EM");
 SaveTracer(ALL);
 HisTime(0,0.4e-9);
%
 define main()
 {
   pprintf(" PLOT: Cycle=%d, Time=%e\n",CYCLE,TIME);
   MatColors(PALE_GREEN,LIGHT_BLUE,GRAY,ORANGE);
   MatNames("Impactor","LiF-Window","Target","TPX");
%
   XLimits(-3.01,0.00);
   YLimits(0.0,0.5);
%
   Image("MATS-",WHITE,BLACK);
    Window(0.,0.,0.85,1.);
    Label(sprintf("Mats, Time= %.2f~m~s",TIME*1.E6));
    Plot2DMats;
    DrawTracers(3);
   EndImage;
%
   Image("PRESSURE-",WHITE,BLACK);
    Window(0.,0.,0.85,1.);
    Label(sprintf("Pressure, Time= %.2f~m~s",TIME*1.E6));
    Plot2DMats;
```

```
    HotMap;
    Paint2DMats("P");
    DrawTracers(3);
   EndImage;
%
   Image("PRESS1D-",WHITE,BLACK);
    Window(0.,0.,0.85,1.);
    Label(sprintf("Presssure 1D, Time= %.2f~m~s",TIME*1.E6));
    VLimits(1e5,1e12);
    Fix1D(-2.0,0.25,1.01,0.25);
    Plot1D("P");
   EndImage;
%
   Image("DENS1D-",WHITE,BLACK);
    Window(0.,0.,0.85,1.);
    Label(sprintf("Density 1D, Time= %.2f~m~s",TIME*1.E6));
    VLimits(11.0,13.0);
    Fix1D(-2.0,0.25,1.01,0.25);
    Plot1D("DENS");
   EndImage;
%
   Image("TEMP1D-",WHITE,BLACK);
    Window(0.,0.,0.85,1.);
    Label(sprintf("Temperature 1D, Time= %.2f~m~s",TIME*1.E6));
    VLimits(0.025,0.032);
    Fix1D(-2.0,0.25,1.01,0.25);
    Plot1D("T");
   EndImage;
%
   Image("EnergyMat1-1D-",WHITE,BLACK);
    Window(0.,0.,0.85,1.);
    Label(sprintf("Energy 1D, Time= %.2f~m~s",TIME*1.E6));
    VLimits(1e9,3e9);
    Fix1D(-2.0,0.25,1.01,0.25);
    Plot1D("EM+1");
   EndImage;
%
   Image("EnergyMat2-1D-",WHITE,BLACK);
    Window(0.,0.,0.85,1.);
    Label(sprintf("Energy 1D, Time= %.2f~m~s",TIME*1.E6));
    VLimits(1e9,3e9);
    Fix1D(-2.0,0.25,1.01,0.25);
    Plot1D("EM+2");
   EndImage;
%
```

```
   XLimits(-3.01,0.00);
   YLimits(0.0,0.5);
%
   Image("ZOOM_PRESSURE-",WHITE,BLACK);
    Window(0.,0.,0.85,1.);
    Label(sprintf("Zoom Pressure, Time= %.2f~m~s",TIME*1.E6));
    Plot2DMats;
    HotMap;
    Paint2DMats("P");
    DrawTracers(3);
   EndImage;
 }
%
  define spyhis_main()
   {
    HisLoad(1,"hscth");
%
    % Output History Data
    HisOutCol(1,"VX.1","VX1.dat");
    HisOutCol(1,"VX.2","VX2.dat");
    HisOutCol(1,"P.1","P1.dat");
    HisOutCol(1,"P.2","P2.dat");
    HisOutCol(1,"DENS.1","DENS1.dat");
    HisOutCol(1,"DENS.2","DENS2.dat");
    HisOutCol(1,"T.1","T1.dat");
    HisOutCol(1,"T.2","T2.dat");
    HisOutCol(1,"EM+1.1","EM1.dat");
    HisOutCol(1,"EM+2.2","EM2.dat");
   }
endspy
*
**********************************************************************
*
*    DIATOM MATERIAL INSERTION RECORDS
*
diatom
 *Aluminum: Assume Impact Occurs at x=0
 set %vi=0.5e5          *cm/s, impact velocity
 set %ti=0.40          *cm, impactor thickness
 set %di=3.0             *cm, impactor diameter
 *
 set %t=0.40          *cm, target thickness
 set %d=3.0           *cm, target diameter
 *
 set %dx0=0.001    *cell size (cm)
```

```
 *
 package 'Projectile'
  material 1
  vel=%vi,0.0
  insert box
   p1 -2.0,0.0
   p2 {-2.0+%ti},{%di}
  endinsert
 endpackage
 *
 package 'Target-Int'
  material 2
  insert box
   p1 {-2.0+%ti},{0.0}
   p2 {-2.0+%ti+%t},{%di}
  endinsert
 endpackage
*
*************************************************************************
*
*      TRACER RECORDS
*
 tracer
  add {-2.0+%ti/2}, 0.25      *center projectile
  add {-2.0+%ti+%t/2}, 0.25   *center target
 endtracer
enddiatom
*
*************************************************************************
*
*    EOS RECORDS
*
eos
   mat1 ses LEAD     *projectile
   mat2 ses LEAD     *target
endeos
*
*************************************************************************
*
*    FRACTURE RECORDS
*
fracts
  pressure
  pfrac1=-1.0e20   *artificially large
  pfrac2=-1.0e20   *artificially large
```

```
  pfmix  -1e30
  pfvoid -1e30
endf
*
*****************************************************************************
*
*    CONVECTION RECORDS
*
convct
  convect=1
  interface=smyra
endc
*
*****************************************************************************
*
*    EDIT RECORDS
*
edit
  shortt
    tim=0.  dt=1e-6
  ends
  longt
    tim=0.  dt=10000.
  endl
endedit
*
*****************************************************************************
```

APPENDIX E. BCAT INPUT FILE FOR SESAME VERIFICATION TEST #1: SYMMETRIC LEAD FLYER PLATE IMPACT

```
BCAT Input File (lead_eos.in):
eos
 mat1 ses LEAD
endeos


BCAT Output File:
                     THE BCAT CODE, VERSION 1.30, 03/19/15
               SANDIA NATIONAL LABORATORIES, ALBUQUERQUE, NM 87185

 PROBLEM: LEAD_1  DATE: 2/3/2020

 OPTION?
 set eos
 ENTER NAME OF CTH INPUT FILE.
 lead_eos.in

 ------------------------------------------------------
 Opening /Users/ctkey/cth/develop/cth_votd_8_29_2019/source/data/EOS_data
 ------------------------------------------------------

 EOS MODEL FOR MATERIAL 1--SES, LEAD
    UI(  1)= EOS    =  3.21000000E+03
    UI(  2)= SR     =  1.00000000E+00
    UI(  3)= R0     =  1.13464470E+01
    UI(  4)= T0     =  2.56798095E-02
    UI(  5)= RMIN   =  9.07715759E+00
    UI(  6)= ZNUC   =  8.20000000E+01
    UI(  7)= ATWT   =  2.07199997E+02
    UI(  8)= RP     =  1.13464470E+01
    UI(  9)= PS     =  0.00000000E+00
    UI( 10)= PE     =  0.00000000E+00
    UI( 11)= CE     =  0.00000000E+00
    UI( 12)= NSUB   =  0.00000000E+00
    UI( 13)= ESFT   =  3.65038258E+08
    UI( 14)= TYP    =  1.00000000E+00
    UI( 15)= RO     =  0.00000000E+00
    UI( 16)= TO     =  0.00000000E+00
    UI( 17)= CLIP   =  0.00000000E+00
    UI( 18)= PWR    =  2.00000000E+00
```

```
MAT 1,  MODEL=   2
Reference density  11.34645 (g/cc)
OPTION?
eos mat1
  RHO(G/CC)          T(K)           P(GPA)          E(MJ/KG)       S(MJ/KGK)
   ↪  CS(KM/S)
ENTER DENSITY (G/CC) AND TEMPERATURE (K)
12.6883 419.64
1.2688300E+01   4.1964001E+02   6.7065854E+00   6.7505457E-02
 ↪  0.0000000E+00   2.4434803E+00

OPTION?
exit
 *** ERROR - NO SUCH OPTION
OPTION?
Quit
```

APPENDIX F. CTH INPUT FILE FOR SESAME VERIFICATION TEST #2: SYMMETRIC USER DEFINED MATERIAL FLYER PLATE IMPACT

```
*CTHid SPYPLT SPYHIS
*eor*cthin
*
 2DR Symmetric Impact - SES Verification #2
* ************************************************************
* Problem Description:
*
* 2DR representation of a symmetric flyer plate impact test on a user
* defined Sesame table material.
*
* The flyer plate and target plate are each 0.4 cm thick and the
* impact velocity of the flyer plate is 0.5 km/s
*
*********************************************************************
*
*    CONTROL RECORDS
*
control
  tstop = 2.e-6
  tbad 1E30
  mmp0
  rdumpf = 86400.  *backup restart dump frequency, in seconds
endcontrol
*
*********************************************************************
*
*    FLAT MESH RECORDS
*
mesh
  block geometry=2dr
   x0=-3.01   *
    x1 dxf=0.001 dxl=0.001 w=3.01
   endx
   y0=0.0
    y1 dyf=0.02 dyl=0.02 w=0.5
   endy
   xact = -2. 0.
   yact = -15. 15.
  endb
endmesh
```

```
*
**********************************************************************
*
*    BOUNDARY CONDITION RECORDS
*
boundary
 bhydro
  bxbot 2 *allow mass to leave
  bxtop 2 *allow mass to leave
  bybot 3 *inflow-extrapolated
  bytop 3 *inflow-extrapolated
 endh
endb
*
*-----------------------------------------------
%%%%%%%%%%%%%%%%%%%% Spy %%%%%%%%%%%%%%%%%%%%
%
spy
% 256 Character Line Limit for Spy ...
  Save("VOID,M,VOLM,VX,VY,P,PM,DENS,T,CS,EM");
 SaveTime(0, 0.01e-6);
 PlotTime(0, 0.05e-6);
 ImageFormat(1024,768);
%
 SaveHis("VOID,M,VOLM,VX,VY,P,PM,DENS,T,CS,EM");
 SaveTracer(ALL);
 HisTime(0,0.4e-9);
%
 define main()
 {
   pprintf(" PLOT: Cycle=%d, Time=%e\n",CYCLE,TIME);
   MatColors(PALE_GREEN,LIGHT_BLUE,GRAY,ORANGE);
   MatNames("Impactor","LiF-Window","Target","TPX");
%
   XLimits(-3.01,0.00);
   YLimits(0.0,0.5);
%
   Image("MATS-",WHITE,BLACK);
    Window(0.,0.,0.85,1.);
    Label(sprintf("Mats, Time= %.2f~m~s",TIME*1.E6));
    Plot2DMats;
    DrawTracers(3);
   EndImage;
%
   Image("PRESSURE-",WHITE,BLACK);
```

```
    Window(0.,0.,0.85,1.);
    Label(sprintf("Pressure, Time= %.2f~m~s",TIME*1.E6));
    Plot2DMats;
    HotMap;
    Paint2DMats("P");
    DrawTracers(3);
   EndImage;
%
   Image("PRESS1D-",WHITE,BLACK);
    Window(0.,0.,0.85,1.);
    Label(sprintf("Presssure 1D, Time= %.2f~m~s",TIME*1.E6));
 %   VLimits(1e5,1e12);
    Fix1D(-2.0,0.25,1.01,0.25);
    Plot1D("P",,ON);
   EndImage;

   Image("DENS1D-",WHITE,BLACK);
    Window(0.,0.,0.85,1.);
    Label(sprintf("Density 1D, Time= %.2f~m~s",TIME*1.E6));
    Fix1D(-2.0,0.25,1.01,0.25);
    Plot1D("DENS",,ON);
   EndImage;
%
   Image("TEMP1D-",WHITE,BLACK);
    Window(0.,0.,0.85,1.);
    Label(sprintf("Temperature 1D, Time= %.2f~m~s",TIME*1.E6));
    Fix1D(-2.0,0.25,1.01,0.25);
    Plot1D("T",,ON);
   EndImage;
%
   Image("EnergyMat1-1D-",WHITE,BLACK);
    Window(0.,0.,0.85,1.);
    Label(sprintf("Energy 1D, Time= %.2f~m~s",TIME*1.E6));
    Fix1D(-2.0,0.25,1.01,0.25);
    Plot1D("EM+1",,ON);
   EndImage;
%
   Image("EnergyMat2-1D-",WHITE,BLACK);
    Window(0.,0.,0.85,1.);
    Label(sprintf("Energy 1D, Time= %.2f~m~s",TIME*1.E6));
    Fix1D(-2.0,0.25,1.01,0.25);
    Plot1D("EM+2",,ON);
   EndImage;
%
   XLimits(-3.01,0.00);
```

```
   YLimits(0.0,0.5);
%
   Image("ZOOM_PRESSURE-",WHITE,BLACK);
    Window(0.,0.,0.85,1.);
    Label(sprintf("Zoom Pressure, Time= %.2f~m~s",TIME*1.E6));
    Plot2DMats;
    HotMap;
    Paint2DMats("P");
    DrawTracers(3);
   EndImage;
%
 }
  define spyhis_main()
   {
    HisLoad(1,"hscth");
%
    % Output History Data
    HisOutCol(1,"VX.1","VX1.dat");
    HisOutCol(1,"VX.2","VX2.dat");
    HisOutCol(1,"P.1","P1.dat");
    HisOutCol(1,"P.2","P2.dat");
    HisOutCol(1,"DENS.1","DENS1.dat");
    HisOutCol(1,"DENS.2","DENS2.dat");
    HisOutCol(1,"T.1","T1.dat");
    HisOutCol(1,"T.2","T2.dat");
    HisOutCol(1,"EM+1.1","EM1.dat");
    HisOutCol(1,"EM+2.2","EM2.dat");
   }
endspy
*
**********************************************************************
*
*    DIATOM MATERIAL INSERTION RECORDS
*
diatom
 *Aluminum: Assume Impact Occurs at x=0
 set %vi=2.0e5          *cm/s, impact velocity
 set %ti=0.40          *cm, impactor thickness
 set %di=3.0             *cm, impactor diameter
 *
 set %t=0.40          *cm, target thickness
 set %d=3.0           *cm, target diameter
 *
 set %dx0=0.001    *cell size (cm)
 *
```

```
 package 'Projectile'
  material 1
  vel=%vi,0.0
  insert box
   p1 -2.0,0.0
   p2 {-2.0+%ti},{%di}
  endinsert
 endpackage
 *
 package 'Target-Int'
  material 2
  insert box
   p1 {-2.0+%ti},{0.0}
   p2 {-2.0+%ti+%t},{%di}
  endinsert
 endpackage
*
*************************************************************************
*
*      TRACER RECORDS
*
 tracer
  add {-2.0+%ti/2}, 0.25      *center projectile
  add {-2.0+%ti+%t/2}, 0.25   *center target
 endtracer
enddiatom
*
*************************************************************************
*
*    EOS RECORDS
*
eos
   mat1 SES USER EOS=9999 FEOS='b9999'     *projectile
   mat2 SES USER EOS=9999 FEOS='b9999'    *target
endeos
*
*************************************************************************
*
*    FRACTURE RECORDS
*
fracts
  pressure
  pfrac1=-1.0e20   *artificially large
  pfrac2=-1.0e20   *artificially large
  pfmix  -1e30
```

```
  pfvoid -1e30
endf
*
*****************************************************************************
*
*    CONVECTION RECORDS
*
convct
  convect=1
  interface=smyra
endc
*
*****************************************************************************
*
*    EDIT RECORDS
*
edit
  shortt
    tim=0.  dt=1e-6
  ends
  longt
    tim=0.  dt=10000.
  endl
endedit
*
*****************************************************************************
```

APPENDIX G. CTH INPUT FILE FOR JWL VALIDATION TEST #1: CYLINDER EXPANSION (HMX)

```
clear*****************************************************************
*****************************************************************
* Problem Description:
*
* CTH Calculation of a Cylinder Expansion Test using HMX as the HE
*
* 2DC Simulation of a 2.54 cm diameter x 30.5cm long cylinder of HMX
* explosive encased in a copper thin walled tube (0.26 cm thick).
*
* The HEBURN option is used to generate a plane wave at the left end
* of the HMX and the (radial) expansion is then measured at various
* points along the outer diameter of the copper tube as a function
* a time.
*
*Experimental Data Reference:
*
* Lan, I., S. Hung, C. Chen, Y. Niu, J. Shiuan, "An Improved Simple
* Method of Deducing JWL Parameters from Cylinder Expansion Test",
* Propellants, Explosives, Pyrotechnics, Vol. 18, pp. 18-24. 1993.
*
*****************************************************************
*
*eor* cthin
*
*****************************************************************
*
HMX Cylinder Expansion Test - JWL EOS, HEBurn Option
*
*****************************************************************************
*
*    CONTROL RECORDS
*
control
  mmp3
  tstop = 40.0e-6
  ntbad = 100000
  rdumpf = 3600.
endc
*
*****************************************************************
*
```

```
*     SPY RECORDS
spy
  PlotTime(0.0, 1.e-6);
  SaveTime(0.0, 1.e-6);
  Save("M,VOLM,VX,VY,P");
  ImageFormat(1024,768);
  define main()
    {
      pprintf(" PLOT: Cycle=%d, Time=%e\n",CYCLE,TIME);
      Image("Mats");
        Window(0,0,0.75,1);
        MatColors(PERU,RED);
        Label(sprintf("Materials at %0.2e s.",TIME));
        Plot2DMats;
        MatNames("Copper","HNS1");
        DrawMatLegend("",0.75,0.2,0.99,0.9);
      EndImage;
      Image("Pressure");
        Window(0,0,0.75,1);
        MatColors(PERU,TAN);
        Label(sprintf("Pressure at %0.2e s.",TIME));
        Plot2DMats;
        Paint2DMat(2,"P");
        Draw2DMatContour;
        %ColorMapRange(1e9,1e12,LOG_MAP);
        ColorMapRange(1e9,1e11,LOG_MAP);
        ColorMapClipping(ON,OFF);
        DrawColorMap("(dyn/cm^2^)",0.75,0.4,0.9,0.9);
      EndImage;
    }
  HisTime(0,1.e-7);
  SaveTracer(ALL);
  SaveHis("GLOBAL,POSITION,P,VX,VY,DENS");
  define spyhis_main()
    {
      HisLoad(1,"hscth");
%
      HisImageName("Tracer1_Velocity_vs_Displacement");
      Label("Cylinder Test: HNS Tracer 1");
      AutoScale(1,"XPOS.1","VX.1");
      Plot("VX.1","XPOS.1");
%
      HisOut(1,"Tracer Velocity vs Position.data","XPOS.1","VX.1");
      HisOutCol(1,"XPOS.1","XPOS1.txt");
    }
```

```
endspy
*
**************************************************************************
*
*    CONVECTION RECORDS
*
convct
  interface = smyra
  nofragment = 1
  nofragment = 2
endc
*
**************************************************************************
*
*    FLAT MESH RECORDS
*
mesh
  block 1 geom=2DC type=E
    x0=0.0
      xl w=4.0 dxf=0.02 dxl=0.02
    endx
*
    y0=-1.3
      y1 w=36.3 dyf=0.05 dyl=0.05
    endy
*
    xact 0.0 1.5
    yact -1.3 0.0
*
  endb
*
endm
*
**************************************************************************
*
*    DIATOM MATERIAL INSERTION RECORDS
*
diatom
*
    package 'Booster'
      material 2
      insert box
        p1 = 0.0, -15.0
        p2 = 1.27 0.0
      endi
```

```
    endp
    package 'HE'
      material 2
      insert box
        p1 = 0.0, -15.0
        p2 = 1.27, 30.5
      endi
    endp
    package 'Copper Case'
      material 1
      insert box
        p1 = 1.27, -15.0
        p2 = 1.53, 30.5
      endi
    endp
    tracer
      add 1.53,7.0 to 1.53,9.0 n=3 fixed=y
      add 0.08,7.0 to 0.08,9.0 n=3
    endtracer
enddiatom
*
*************************************************************************
*
*    EOS RECORDS
*
eos
* Copper - Mie-Gruneisen
  mat1 mgrun copper
* HNS 1 Explosive JWL Model, r0=1.65g/cc
  mat2 jwl HMX
endeos
*
*************************************************************************
*
*    HEBURN RECORDS
*
heburn
  mat 2 d 9.110E+05
  dl 0.0, -1.3 to 1.5, -1.3 r 100.0 time 0.0
endh
*
*************************************************************************
*
*    EP RECORDS
*
```

```
epdata
  matep 1 eppvm user yield 3.0e9 poisson 0.27
  mix 3
endep
*
**********************************************************************
*
*    BOUNDARY CONDITION RECORDS
*
boundary
  bhy
    bxb=0, bxt=2
    byb=2, byt=2
  endh
endb
*
**********************************************************************
*
*    MINDT/MAXDT RECORDS
*
mindt
  time=0, dt=1.0e-11
endmindt
maxdt
  time=0, dt=0.01
endmaxdt
*
**********************************************************************
*
*    FRACTURE RECORDS
*
fracts
  pressure
  pfrac1 -0.3e10
  pfrac2 -5.0e6
  pfmix -0.3e10
  pfvoid -0.3e10
endf
*
**********************************************************************
*
*    EDIT RECORDS
*
edit
  shortt
```

```
    time=0.0 dt=5.0e-4
  ends
  longt
    time=0.0 dt=5.0e-4
  endl
ende
```

APPENDIX H. CTH INPUT FILE FOR JWL VALIDATION TEST #2: HEMISPHERE EXPANSION COMPB-GRADEA

```
clear*************************************************************
*****************************************************************
* Problem Description:
*
* CTH Calculation of a Hemipsherical Expansion Test using CompB-GradeA
* as the HE
*
* 2DC Simulation of a 30.5 cm diameter hemisphere of CompB-GradeA
* explosive covered with a thin walled aluminum hemisphere
* (0.65 cm thick).  The hemisphere of CompB-GradeA then sits on top
* of a 30.5 cm diameter x 15.0 cm tall cyclinder of CompB-GradeA HE.
*
* The HEBURN option is used to generate a detonation point at the
* center of the hemisphere and the (radial) expansion is then measured
* at various points along the outer diameter of the aluminum
* hemisphere as a function of time.
*
*Experimental Data Reference:
*
* Lee, E.L., H.C. Hornig, and J.W. Kury, "Adiabatic Expansion of High
* Explosive Detonation Products", Lawrence Radiation Laboratory,
* University of California, UCRL-50422, May 2, 1968.
*
*****************************************************************
*
*eor* cthin
*
*********************************************************************
*
CompB-GradeA Hemisphere Expansion Test - JWL EOS, HEBurn Option
*
*********************************************************************
*
*    CONTROL RECORDS
*
control
  mmp3
  tstop = 40.0e-6
  ntbad = 100000
  rdumpf = 3600.
endc
```

```
*
*********************************************************************
*
*     SPY RECORDS
spy
  PlotTime(0.0, 1.e-6);
  SaveTime(0.0, 1.e-6);
  Save("M,VOLM,VX,VY,P");
  ImageFormat(1024,768);
  define main()
    {
      pprintf(" PLOT: Cycle=%d, Time=%e\n",CYCLE,TIME);
      Image("Mats");
        Window(0,0,0.75,1);
        MatColors(PERU,RED);
        Label(sprintf("Materials at %0.2e s.",TIME));
        Plot2DMats;
        MatNames("Copper","HNS1");
        DrawMatLegend("",0.75,0.2,0.99,0.9);
      EndImage;
      Image("Pressure");
        Window(0,0,0.75,1);
        MatColors(PERU,TAN);
        Label(sprintf("Pressure at %0.2e s.",TIME));
        Plot2DMats;
        Paint2DMat(2,"P");
        Draw2DMatContour;
        %ColorMapRange(1e9,1e12,LOG_MAP);
        ColorMapRange(1e9,1e11,LOG_MAP);
        ColorMapClipping(ON,OFF);
        DrawColorMap("(dyn/cm^2^)",0.75,0.4,0.9,0.9);
      EndImage;
    }
  HisTime(0,1.e-7);
  SaveTracer(ALL);
  SaveHis("GLOBAL,POSITION,P,VX,VY,DENS");
  define spyhis_main()
    {
      HisLoad(1,"hscth");
%
      HisOutCol(1,"YPOS.1","YPOS1.txt");
    }
endspy
*
*********************************************************************
```

```
*
*    CONVECTION RECORDS
*
convct
  interface = smyra
  nofragment = 1
  nofragment = 2
endc
*
*************************************************************************
*
*    FLAT MESH RECORDS
*
mesh
  block 1 geom=2DC type=E
    x0=0.0
      xl w=20.0 dxf=0.05 dxl=0.05
    endx
*
    y0=-1.0
      y1 w=40.0 dyf=0.05 dyl=0.05
    endy
*
    xact 0.0 1.5
    yact -1.3 0.0
*
  endb
*
endm
*
*************************************************************************
*
*    DIATOM MATERIAL INSERTION RECORDS
*
diatom
*
    package 'HE'
      material 2
      insert box
        p1 = 0.0, 0.0
        p2 = 15.25, 15.0
      endi
      insert circle
       center=0.0, 15.0
       radius= 15.0
```

```
      endi
    endp
    package 'Copper Case'
      material 1
      insert circle
        center = 0.0, 15.0
        radius = 15.65
        rinner = 15.0
      endi
      delete box
        p1 = 15.0, 0.0
        p2 = 60, 15.0
      endd
      delete box
        p1 = 0.0, -10.0
        p2 = 20, 0.0
      endd
    endp
    tracer
      add 0.0, 30.65
    endtracer
enddiatom
*
************************************************************************
*
*    EOS RECORDS
*
eos
* Copper - Mie-Gruneisen
  mat1 mgrun 6061-T6_AL
* HNS 1 Explosive JWL Model, r0=1.65g/cc
  mat2 jwl COMPB_GRADEA
endeos
*
************************************************************************
*
*    HEBURN RECORDS
*
heburn
  mat 2 d 7.980E+05
  dp 0.0, 15.0 r 100.0 time 0.0
endh
*
************************************************************************
*
```

```
*    EP RECORDS
*
epdata
  matep 1 JO 6061-T6_ALUMINUM
  mix 3
endep
*
*************************************************************************
*
*    BOUNDARY CONDITION RECORDS
*
boundary
  bhy
    bxb=0, bxt=2
    byb=2, byt=2
  endh
endb
*
*************************************************************************
*
*    MINDT/MAXDT RECORDS
*
mindt
  time=0, dt=1.0e-11
endmindt
maxdt
  time=0, dt=0.01
endmaxdt
*
*************************************************************************
*
*    FRACTURE RECORDS
*
fracts
  pressure
  pfrac1 -0.3e10
  pfrac2 -5.0e6
  pfmix -0.3e10
  pfvoid -0.3e10
endf
*
*************************************************************************
*
*    EDIT RECORDS
*
```

```
edit
  shortt
    time=0.0 dt=5.0e-4
  ends
  longt
    time=0.0 dt=5.0e-4
  endl
ende
```

APPENDIX I. CTH INPUT FILE FOR SESAME VALIDATION TEST #1: CONFIGURATION ALTA5

```
*CTHid SPYPLT SPYHIS
*eor*cthin
*
 AlTa5 - Nellis et al. - SES Validation #1
* ************************************************************
* Problem Description:
*
* 2DR representation of an Aluminum flyer plate impact test on an
* aluminum target plate that is backed by a Tantalum anvil.
*
* This input deck is for Shot AlTa5 where the aluminum flyer plate
* velocity is 5.197 km/s, the target plate is 2.044 mm thick and the
* anvil backing plate is 1.542 mm thick.
*
* Experimental Data Reference:
*
* Nellis, W.J., A.C. Mitchell and D.A. Young. 2003.
* "Equation-of-state measurements for aluminum, copper and tantalum
* in the pressure range 80-440 GPa (0.8-4.4 Mbar)," Journal of Applied
* Physics, Vol. 93, No. 1, pp 304-310.
*
************************************************************************
*
*    CONTROL RECORDS
*
control
  tstop = 2.e-6
  tbad 1E30
  *print
  mmp0
  rdumpf = 86400.  *backup restart dump frequency, in seconds
endcontrol
*
************************************************************************
*
*    FLAT MESH RECORDS
*
mesh
  block geometry=2dr
   x0=-8.01
    x1 dxf=0.001 dxl=0.001 w=11.01
```

```
   endx
   y0=0.0
    y1 dyf=0.02 dyl=0.02 w=0.5
   endy
   xact = -2. 0.
   yact = -15. 15.
  endb
endmesh
*
**********************************************************************
*
*    BOUNDARY CONDITION RECORDS
*
boundary
 bhydro
  bxbot 2 *allow mass to leave
  bxtop 2 *allow mass to leave
  bybot 3 *inflow-extrapolated
  bytop 3 *inflow-extrapolated
 endh
endb
*
*---------------------------------------------------------------------
*
spy
% 256 Character Line Limit for Spy ...
  Save("VOID,M,VOLM,VX,VY,CVMAG,P,PM,DENS,TK,XXDEV,XYDEV,YYDEV,XZDEV,
   ↪  YZDEV,ZZDEV,PSR,YLD,Q2,Q3,Q4");
 SaveTime(0, 0.01e-6);
 PlotTime(0, 0.02e-6);
 ImageFormat(1024,768);
%
 SaveHis("GLOBAL,VOID,M,VOLM,VX,VY,P,TK,DENS,POSITION,XXSTRESS,YYSTRESS,
  ↪  ZZSTRESS,XXDEV,XYDEV,YYDEV,XZDEV,YZDEV,ZZDEV");
 SaveTracer(ALL);
 HisTime(0,0.4e-9);
%
 define main()
 {
   pprintf(" PLOT: Cycle=%d, Time=%e\n",CYCLE,TIME);
   MatColors(PALE_GREEN,LIGHT_BLUE,GRAY,ORANGE);
   MatNames("Impactor","LiF-Window","Target","TPX");
%
   XLimits(-4.01,3.0);
   YLimits(0.0,0.5);
```

```
%
   Image("MATS-",WHITE,BLACK);
    Window(0.,0.,0.85,1.);
    Label(sprintf("Mats, Time= %.2f~m~s",TIME*1.E6));
    Plot2DMats;
    DrawTracers(3);
   EndImage;
%
   Image("PRESSURE-",WHITE,BLACK);
    Window(0.,0.,0.85,1.);
    Label(sprintf("Pressure, Time= %.2f~m~s",TIME*1.E6));
    VLimits(1e5,2e12);
    Fix1D(-2.0,0.25,1.01,0.25);
    Plot1D("P",ON);
   EndImage;
%
   Image("VELOCITY-",WHITE,BLACK);
    Window(0.,0.,0.85,1.);
    Label(sprintf("Presssure 1D, Time= %.2f~m~s",TIME*1.E6));
    VLimits(1e5,5e5);
    Fix1D(-2.0,0.25,1.01,0.25);
    Plot1D("VX",ON);
   EndImage;
%
   Image("DENSITY",WHITE,BLACK);
    Window(0.,0.,0.85,1.);
    Label(sprintf("Presssure 1D, Time= %.2f~m~s",TIME*1.E6));
    VLimits(1.0,22.0);
    Fix1D(-2.0,0.25,1.01,0.25);
    Plot1D("DENS",ON);
   EndImage;
%
   XLimits(-2.01,0.0);
   YLimits(0.0,0.5);
%
   Image("ZOOM_PRESSURE-",WHITE,BLACK);
    Window(0.,0.,0.85,1.);
    Label(sprintf("Zoom Pressure, Time= %.2f~m~s",TIME*1.E6));
    Plot2DMats;
    HotMap;
    Paint2DMats("P");
    DrawTracers(3);
   EndImage;
 }
  define spyhis_main()
```

```
   {
    HisLoad(1,"hscth");
%
    % Output History Data
    HisOutCol(1,"VX.1","VX1.dat");
    HisOutCol(1,"P.1","P1.dat");
    HisOutCol(1,"DENS.1","DENS1.dat");
%
    HisImageName("Sample_VelHist-");
      ULimits(0,3.0E-6);
      %VLimits(-0.1e5,1.0e5);
      HisLegend(ON);
      Label("Target/Window Interface Velocity (y=0.25)");
      LegendName("Interface");
      Set1DLineProperties(1.0,1,SOLID,BLUE);
      TPlot("VX.1",1,ON);
      LegendName("+2dx");
      Set1DLineProperties(1.0,1,SOLID,RED);
      TDraw("VX.2",1,ON);
      LegendName("-2dx");
      Set1DLineProperties(1.0,1,SOLID,GREEN);
      TDraw("VX.3",1,ON);
      LegendName("+5dx");
      Set1DLineProperties(1.0,1,MDASH,CYAN);
      TDraw("VX.4",1,ON);
      LegendName("-5dx");
%
    HisImageName("Anvil_VelHist-");
      ULimits(0,3.0E-6);
      %VLimits(-0.1e5,1.0e5);
      HisLegend(ON);
      Label("Target/Window Interface Velocity (y=0.25)");
      LegendName("Interface");
      Set1DLineProperties(1.0,1,SOLID,BLUE);
      TPlot("VX.5",1,ON);
      LegendName("+2dx");
      Set1DLineProperties(1.0,1,SOLID,RED);
      TDraw("VX.6",1,ON);
      LegendName("-2dx");
      Set1DLineProperties(1.0,1,SOLID,GREEN);
      TDraw("VX.7",1,ON);
      LegendName("+5dx");
      Set1DLineProperties(1.0,1,MDASH,CYAN);
      TDraw("VX.8",1,ON);
      LegendName("-5dx");
```

```
%
    HisImageName("Sample_DensHist-");
      ULimits(0,3.0E-6);
      %VLimits(-0.1e5,1.0e5);
      HisLegend(ON);
      Label("Target/Window Interface Velocity (y=0.25)");
      LegendName("Interface");
      Set1DLineProperties(1.0,1,SOLID,BLUE);
      TPlot("DENS.1",1,ON);
      LegendName("+2dx");
      Set1DLineProperties(1.0,1,SOLID,RED);
      TDraw("DENS.2",1,ON);
      LegendName("-2dx");
      Set1DLineProperties(1.0,1,SOLID,GREEN);
      TDraw("DENS.3",1,ON);
      LegendName("+5dx");
      Set1DLineProperties(1.0,1,MDASH,CYAN);
      TDraw("DENS.4",1,ON);
      LegendName("-5dx");
%
    HisImageName("Anvil_DensHist-");
      ULimits(0,3.0E-6);
      %VLimits(-0.1e5,1.0e5);
      HisLegend(ON);
      Label("Target/Window Interface Velocity (y=0.25)");
      LegendName("Interface");
      Set1DLineProperties(1.0,1,SOLID,BLUE);
      TPlot("DENS.5",1,ON);
      LegendName("+2dx");
      Set1DLineProperties(1.0,1,SOLID,RED);
      TDraw("DENS.6",1,ON);
      LegendName("-2dx");
      Set1DLineProperties(1.0,1,SOLID,GREEN);
      TDraw("DENS.7",1,ON);
      LegendName("+5dx");
      Set1DLineProperties(1.0,1,MDASH,CYAN);
      TDraw("DENS.8",1,ON);
      LegendName("-5dx");
%
    HisImageName("Sample_PresHist-");
      ULimits(0,3.0E-6);
      %VLimits(-0.1e5,1.0e5);
      HisLegend(ON);
      Label("Target/Window Interface Velocity (y=0.25)");
      LegendName("Interface");
```

```
      Set1DLineProperties(1.0,1,SOLID,BLUE);
      TPlot("P.1",1,ON);
      LegendName("+2dx");
      Set1DLineProperties(1.0,1,SOLID,RED);
      TDraw("P.2",1,ON);
      LegendName("-2dx");
      Set1DLineProperties(1.0,1,SOLID,GREEN);
      TDraw("P.3",1,ON);
      LegendName("+5dx");
      Set1DLineProperties(1.0,1,MDASH,CYAN);
      TDraw("P.4",1,ON);
      LegendName("-5dx");
%
    HisImageName("Anvil_PresHist-");
      ULimits(0,3.0E-6);
      %VLimits(-0.1e5,1.0e5);
      HisLegend(ON);
      Label("Target/Window Interface Velocity (y=0.25)");
      LegendName("Interface");
      Set1DLineProperties(1.0,1,SOLID,BLUE);
      TPlot("P.5",1,ON);
      LegendName("+2dx");
      Set1DLineProperties(1.0,1,SOLID,RED);
      TDraw("P.6",1,ON);
      LegendName("-2dx");
      Set1DLineProperties(1.0,1,SOLID,GREEN);
      TDraw("P.7",1,ON);
      LegendName("+5dx");
      Set1DLineProperties(1.0,1,MDASH,CYAN);
      TDraw("P.8",1,ON);
      LegendName("-5dx");
   }
endspy
*
**********************************************************************
*
*    DIATOM MATERIAL INSERTION RECORDS
*
diatom
 *Aluminum: Assume Impact Occurs at x=0
 set %vi=5.197e5          *cm/s, impact velocity
 set %ti=1.00          *cm, impactor thickness
 set %di=3.0             *cm, impactor diameter
 *
 set %t=0.2044          *cm, target thickness
```

```
 set %d=3.0           *cm, target diameter
 *
 set %ta=0.1542          *cm, anvil thickness
 set %da=2.0           *cm, anvil diameter
 *
 set %dx0=0.001    *cell size (cm)
 *
 package 'Impactor'
  material 1
  vel=%vi,0.0
  insert box
   p1 -2.0,0.0
   p2 {-2.0+%ti},{%di}
  endinsert
 endpackage
 *
 package 'Specimen'
  material 2
  insert box
   p1 {-2.0+%ti},{0.0}
   p2 {-2.0+%ti+%t},{%di}
  endinsert
 endpackage
 *
 package 'Anvil'
  material 3
  insert box
   p1 {-2.0+%ti+%t},{0.0}
   p2 {-2.0+%ti+%t+%ta},{%da}
  endinsert
 endpackage
*
*************************************************************************
*
*      TRACER RECORDS
*
 tracer
  add {-2.0+%ti+%t/2}, 0.25      *sample center
  add {-2.0+%ti+%t}, 0.25  *sample backface
  add {-2.0+%ti+%t-2*%dx0}, 0.25  *2 cells in sample
  add {-2.0+%ti+%t-4*%dx0}, 0.25  *4 cells in sample
  add {-2.0+%ti+%t+%ta/2}, 0.25  *Anvil center
  add {-2.0+%ti+%t+%ta/2}, 0.25  *Anvil backface
  add {-2.0+%ti+%t+%ta/2-2*%dx0}, 0.25  *2 cells in Anvil
  add {-2.0+%ti+%t+%ta/2-4*%dx0}, 0.25  *4 cells in Anvil
```

```
 endtracer
enddiatom
*
**********************************************************************
*
*    EOS RECORDS
*
eos
   mat1 SES ALUMINUM     *Impactor
   mat2 SES ALUMINUM     *Specimen
   mat3 SES TANTALUM     *Anvil
endeos
*
**********************************************************************
*
*    EPDATA RECORDS
*
epdata
  vpsave
  mix=3
  matep 1 JO ALUMINUM
  matep 2 JO ALUMINUM
  matep 3 JO TANTALUM
endep
*
**********************************************************************
*
*    FRACTURE RECORDS
*
fracts
  pressure
  pfrac1=-1.0e20
  pfrac2=-0.36e10
  pfrac3=-1.0e20
  pfmix  -1e30
  pfvoid -1e30
endf
*
**********************************************************************
*
*    CONVECTION RECORDS
*
convct
  convect=1
  interface=smyra
```

```
endc
*
**********************************************************************
*
*    EDIT RECORDS
*
edit
  shortt
    tim=0.  dt=1e-6
  ends
  longt
    tim=0.  dt=10000.
  endl
endedit
*
**********************************************************************
```

APPENDIX J. CTH INPUT FILE FOR SESAME VALIDATION TEST #2: SHOT #9 CONFIGURATION

```
*CTHid SPYPLT SPYHIS
*eor*cthin
*
 Shot #9 - Rigg et al. - SES Validation #2
* ************************************************************
* Problem Description:
*
* 2DR representation of a flyer plate impact test on a LIF sample.
* This input deck is for Shot #9 which
* consists of a 1.3mm thick tantalum flyer backed by a thick lexan
* sabot.  The flyer configuration is impacting a 9 mm thick LIF target
* plate at 6.016 km/s
*
* Experimental Data Reference:
*
* Rigg, P.A., M.D. Knudson, R.J. Scharff and R.S. Hixson. 2014.
* "Determining the refractive index of shocked [100] lithium fluoride
* to the limit of transmissibility," Journal of Applied Physics,
* Vol. 116.
*
*********************************************************************
*
*    CONTROL RECORDS
*
control
  tstop = 2.e-6
  tbad 1E30
  *print
  mmp0
  rdumpf = 86400.  *backup restart dump frequency, in seconds
endcontrol
*
*********************************************************************
*
*    FLAT MESH RECORDS
*
mesh
  block geometry=2dr
   x0=-4.01   *
    x1 dxf=0.001 dxl=0.001 w=7.01  *xmax=3
   endx
```

```
   y0=0.0
    y1 dyf=0.02 dyl=0.02 w=0.5
   endy
   xact = -2. 0.
   yact = -15. 15.
  endb
endmesh
*
************************************************************************
*
*    BOUNDARY CONDITION RECORDS
*
boundary
 bhydro
  bxbot 2 *allow mass to leave
  bxtop 2 *allow mass to leave
  bybot 3 *inflow-extrapolated
  bytop 3 *inflow-extrapolated
 endh
endb
*
*-----------------------------------------------------------------------
*
spy
% 256 Character Line Limit for Spy ...
 Save("VOID,M,VOLM,VX,VY,CVMAG,P,PM,DENS,TK,XXDEV,XYDEV,YYDEV,XZDEV,
  ↪  YZDEV,ZZDEV,PSR,YLD,Q2,Q3,Q4");
 SaveTime(0, 0.01e-6);
 PlotTime(0, 0.02e-6);
 ImageFormat(1024,768);
%
 SaveHis("GLOBAL,VOID,M,VOLM,VX,VY,P,TK,DENS,POSITION,XXSTRESS,YYSTRESS,
  ↪  ZZSTRESS,XXDEV,XYDEV,YYDEV,XZDEV,YZDEV,ZZDEV");
 SaveTracer(ALL);
 HisTime(0,0.4e-9);
%
 define main()
 {
   pprintf(" PLOT: Cycle=%d, Time=%e\n",CYCLE,TIME);
   MatColors(PALE_GREEN,LIGHT_BLUE,GRAY,ORANGE);
   MatNames("Impactor","LiF-Window","Target","TPX");
%
   XLimits(-4.01,3.0);
   YLimits(0.0,0.5);
%
```

```
   Image("MATS-",WHITE,BLACK);
    Window(0.,0.,0.85,1.);
    Label(sprintf("Mats, Time= %.2f~m~s",TIME*1.E6));
    Plot2DMats;
    DrawTracers(3);
   EndImage;
%
   Image("PRESSURE-",WHITE,BLACK);
    Window(0.,0.,0.85,1.);
    Label(sprintf("Pressure, Time= %.2f~m~s",TIME*1.E6));
    Plot2DMats;
    HotMap;
    Paint2DMats("P");
    DrawTracers(3);
   EndImage;
%
   Image("PRESS1D-",WHITE,BLACK);
    Window(0.,0.,0.85,1.);
    Label(sprintf("Presssure 1D, Time= %.2f~m~s",TIME*1.E6));
    VLimits(1e5,1e12);
    Fix1D(-2.0,0.25,1.01,0.25);
    Plot1D("P");
   EndImage;
%
   Image("VELX-",WHITE,BLACK);
    Window(0.,0.,0.85,1.);
    Label(sprintf("Velocity 1D, Time= %.2f~m~s",TIME*1.E6));
    VLimits(1e5,1e12);
    Fix1D(-2.0,0.25,1.01,0.25);
    Plot1D("VX");
   EndImage;
%
   XLimits(-2.01,0.0);
   YLimits(0.0,0.5);
%
   Image("ZOOM_PRESSURE-",WHITE,BLACK);
    Window(0.,0.,0.85,1.);
    Label(sprintf("Zoom Pressure, Time= %.2f~m~s",TIME*1.E6));
    Plot2DMats;
    HotMap;
    Paint2DMats("P");
    DrawTracers(3);
   EndImage;
%
 }
```

```
  define spyhis_main()
   {
    HisLoad(1,"hscth");
%
    % Output History Data
    HisOutCol(1,"VX.1","VX1.dat");
    HisOutCol(1,"VX.2","VX2.dat");
    HisOutCol(1,"VX.3","VX3.dat");
%
    HisImageName("VelHist-");
      ULimits(0,3.0E-6);
      VLimits(0.0,6.0e5);
      HisLegend(ON);
      Label("Target/Window Interface Velocity (y=0.25)");
      LegendName("Interface");
      Set1DLineProperties(1.0,1,SOLID,BLUE);
      TPlot("VX.1",1,ON);
      LegendName("+2dx");
      Set1DLineProperties(1.0,1,SOLID,RED);
      TDraw("VX.2",1,ON);
      LegendName("-2dx");
      Set1DLineProperties(1.0,1,SOLID,GREEN);
      TDraw("VX.3",1,ON);
      LegendName("+5dx");
      Set1DLineProperties(1.0,1,MDASH,CYAN);
      TDraw("VX.4",1,ON);
      LegendName("-5dx");
      Set1DLineProperties(1.0,1,MDASH,MAGENTA);
      TDraw("VX.5",1,ON);
%
    HisImageName("VelImpHist-");
      ULimits(0,3.0E-6);
      %VLimits(-0.1e5,1.0e5);
      HisLegend(ON);
      Label("Impact Interface Velocity (y=0.25)");
      LegendName("Interface");
      Set1DLineProperties(1.0,1,SOLID,BLUE);
      TPlot("VX.6",1,ON);
   }
endspy
*
**********************************************************************
*
*    DIATOM MATERIAL INSERTION RECORDS
*
```

```
diatom
 *Aluminum: Assume Impact Occurs at x=0
 set %vi=6.016e5          *cm/s, impact velocity
 set %ti=0.13         *cm, impactor thickness
 set %di=3.0             *cm, impactor diameter
 *
 set %t=0.9          *cm, target thickness
 set %d=3.0           *cm, target diameter
 *
 set %dx0=0.0005    *cell size (cm)
 *
 package 'Lexan Sabot'
  material 3
  vel=%vi,0.0
  insert box
   p1 -4.0,0.0
   p2 {-2.0},{%di}
  endinsert
 endpackage
*
 package 'Projectile'
  material 1
  vel=%vi,0.0
  insert box
   p1 -2.0,0.0
   p2 {-2.0+%ti},{%di}
  endinsert
 endpackage
 *
 package 'Target-Int'
  material 2
  insert box
   p1 {-2.0+%ti},{0.0}
   p2 {-2.0+%ti+%t},{%d}
  endinsert
 endpackage
*
*************************************************************************
*
*      TRACER RECORDS
*
 tracer
  add {-2.0+%ti}, 0.25          *at interface
  add {-2.0+%ti+2*%dx0}, 0.25  *2 cells in Target window
  add {-2.0+%ti-2*%dx0}, 0.25  *2 cells in Flyer target
```

```
  add {-2.0+%ti+5*%dx0}, 0.25  *5 cells in Target window
  add {-2.0+%ti-5*%dx0}, 0.25  *5 cells in Flyer target
  *
  add {-2.0+%ti}, 0.25          *at impact interface
  add {-2.0+%ti+%t/2}, 0.25      *sample center
 endtracer
enddiatom
*
**********************************************************************
*
*    EOS RECORDS
*
eos
   mat1 SES TANTALUM     *projectile
   mat2 SES LIF
   mat3 mgr user ro=1.196 cs=2.33e5 s1=1.57 g0=0.61 cv=1.39e11  * Lexan=PC
endeos
*
**********************************************************************
*
*    EPDATA RECORDS
*
epdata
  vpsave
  mix=3
   *Flyer
   matep 1 jo TANTALUM
   * LiF
   matep 2 st LIF
   matep 3 jo LEXAN tmelt=1.e10 *      *mulboy PC
endep
*
**********************************************************************
*
*    FRACTURE RECORDS
*
fracts
  pressure
  pfrac1=-1.0e20
  pfrac2=-1.0e20
  pfmix  -1e30
  pfvoid -1e30
endf
*
**********************************************************************
```

```
*
*    CONVECTION RECORDS
*
convct
  convect=1
  interface=smyra
endc
*************************************************************************
*
*    EDIT RECORDS
*
edit
  shortt
    tim=0.  dt=1e-6
  ends
  longt
    tim=0.  dt=10000.
  endl
endedit
*
*************************************************************************
```

DISTRIBUTION

Hardcopy—Internal

Number of Copies	Name	Org.	Mailstop
1	Duncan-Reynolds, Gabrielle C	1555	0840
1	Key, Christopher T	1555	0840
1	Mish, Kyran D	1555	0845

Email—Internal [redacted]

Name	Org.	Sandia Email Address
Witkowski, Walter R	1540	wrwitko@sandia.gov
Eckert, Aubrey C	1544	acecker@sandia.gov
Klenke, Scott E	1550	seklenk@sandia.gov
Cox, James V	1555	jvcox@sandia.gov
Duncan-Reynolds, Gabrielle C	1555	gcmille@sandia.gov
Key, Christopher T	1555	ctkey@sandia.gov
Mish, Kyran D	1555	kdmish@sandia.gov
Technical Library	1911	sanddocs@sandia.gov

Sandia National Laboratories

Sandia National Laboratories is a multimission laboratory managed and operated by National Technology & Engineering Solutions of Sandia LLC, a wholly owned subsidiary of Honeywell International Inc., for the U.S. Department of Energy's National Nuclear Security Administration under contract DE-NA0003525.